1. Report No.	2. Government Accession No.	3. Recipient's Catalog No.
FHWA/TX-12/0-6037-2		

4. Title and Subtitle	5. Report Date
SUBBASE AND SUBGRADE PERFORMANCE INVESTIGATION AND DESIGN GUIDELINES FOR CONCRETE PAVEMENT	February 2010 Published: March 2012
	6. Performing Organization Code

7. Author(s)	8. Performing Organization Report No.
Youn su Jung, Dan G. Zollinger, Byoung Hooi Cho, Moon Won, and Andrew J. Wimsatt	Report 0-6037-2

9. Performing Organization Name and Address	10. Work Unit No. (TRAIS)
Texas Transportation Institute The Texas A&M University System College Station, Texas 77843-3135	11. Contract or Grant No. Project 0-6037

12. Sponsoring Agency Name and Address	13. Type of Report and Period Covered
Texas Department of Transportation Research and Technology Implementation Office P.O. Box 5080 Austin, Texas 78763-5080	Technical Report: September 2007 − September 2009
	14. Sponsoring Agency Code

15. Supplementary Notes

Project performed in cooperation with the Texas Department of Transportation and the Federal Highway Administration.
Project Title: Alternatives to Asphalt Concrete Pavement Subbases for Concrete Pavement
URL: http://tti.tamu.edu/documents/0-6037-2.pdf

16. Abstract

The main issue associated with this research is if cheaper alternatives can be configured for subbase construction. Subbase layers have certain functions that need to be fulfilled in order to assure adequate pavement performance. One key aspect is resistance to erosion, and assessment of each of these functions relative to different alternatives is key to understanding the capability of different alternatives to perform adequately. In this respect, this project was poised to examine the design assumptions associated with each alternative and provide design recommendations accordingly to include test methods and material specifications.

This report describes some of the work accomplished by summarizing data on subbase performance and testing relative to concrete pavement subbase and subgrade erosion but mainly addresses guidelines for concrete pavement subbase design. Findings from field investigations are discussed to identify factors associated with erosion. An approach to mechanistically consider the erosion process was introduced and review of current design procedures was conducted to reveal how they address erosion. This review was extended to include erosion models described in the literature as a means to shed light on the relationship between measurable material properties and performance.

Additionally, past and current design procedures relative to erosion were reviewed in terms of test methods, erosion models, and their utility to characterize subbase materials with respect to erosion resistance. With this information, a new test configuration was devised that uses a rapid tri-axial test and a Hamburg wheel-tracking device for evaluating erodibility with respect to the subbase type and degree of stabilization (cement content). Test devices, procedures, and results are explained and summarized for application in mechanistic design processes. A proposed erosion model was validated by comparing erosion predictions to erosion results. Several computer program analyses were conducted to assess the design and performance implications of different subbases alternatives. Guidelines are provided to promote economical and sustainable design of concrete pavement subbases.

17. Key Words	18. Distribution Statement
Subbase Material, Erosion, Field Performance, Concrete Pavement, k-value, GPR, FWD, DCP, Static Plate Load Test	No restrictions. This document is available to the public through NTIS: National Technical Information Service Alexandria, Virginia 22312 http://www.ntis.gov

19. Security Classif.(of this report)	20. Security Classif.(of this page)	21. No. of Pages	22. Price
Unclassified	Unclassified	170	

SUBBASE AND SUBGRADE PERFORMANCE INVESTIGATION AND DESIGN GUIDELINES FOR CONCRETE PAVEMENT

by

Youn su Jung
Post Doctoral Research Associate
Texas Transportation Institute

Dan G. Zollinger
Program Manager
Texas Transportation Institute

Byoung Hooi Cho
Graduate Research Assistant
Center for Transportation Research

Moon Won
Associate Professor
Texas Tech University

and

Andrew J. Wimsatt
Division Head
Texas Transportation Institute

Report 0-6037-2
Project 0-6037
Project Title: Alternatives to Asphalt Concrete Pavement Subbases for Concrete Pavement

Performed in cooperation with the
Texas Department of Transportation
and the
Federal Highway Administration

February 2010
Published: March 2012

TEXAS TRANSPORTATION INSTITUTE
The Texas A&M University System
College Station, Texas 77843-3135

DISCLAIMER

The contents of this report reflect the views of the authors, who are responsible for the facts and the accuracy of the data presented herein. The contents do not necessarily reflect the official view or policies of the Federal Highway Administration (FHWA) or the Texas Department of Transportation (TxDOT). This report does not constitute a standard, specification, or regulation. This report is not intended for construction, bidding, or permit purposes. The United States Government and the State of Texas do not endorse products or manufacturers. Trade or manufacturers' names appear herein solely because they were considered essential to the object of this report. The engineer in charge of the project was Andrew J. Wimsatt, Texas P.E., #72270.

ACKNOWLEDGMENTS

This project was conducted in cooperation with TxDOT and FHWA. The authors wish to express their appreciation of the personnel of the Federal Highway Administration and the Texas Department of Transportation for their support throughout this project, as well as of the project coordinator, David Head (El Paso District Director of Construction); the project director, Ralph Browne (Fort Worth District North Tarrant County Area Engineer); and members of the Project Monitoring Committee: Buddy (Jere) Williams, Darrell Anglin, Doug Beer, Eric Ingamells, Hua Chen, and David Head.

TABLE OF CONTENTS

Page

List of Figures ix
List of Tables xii

Chapter 1 Introduction 1
Field Investigations 3
Alternative Subbase Materials 9
Conclusions 12

Chapter 2 Literature Review 13
Previous Laboratory Test Methods for Erosion 13
Previous Erosion Models 14
Current Design Guidelines for Base/Subbase 16
TxDOT Pavement Design Guide 16
1993 AASHTO Design Guide 19
PCA Design Method 22
NCHRP Design Guide 25
Summary and Discussions 29

Chapter 3 Subbase Erosion 33
New Method of Erosion Testing 34
Erosion Testing 35
Sample Preparation 37
Erosion Test Results Using RATT Device 38
Test for Maximum Aggregate Size Selection 40
Erosion Test Using HWTD 41
Erosion Model Development 46

Chapter 4 Subbase Performance Factors 55
Evaluation of Subbase Friction, Stiffness, and Erosion 56
Subbase Friction 56

Subbase Support Stiffness 64
Erodibility Effects 78
Conclusions 80
Chapter 5 Guidelines for the Design of Concrete Pavement Subbase 81
Subbase Performance Considerations 81
Subbase Design Flowchart 82
Material Factors 84
Design Factors 88
Sustainability Factors 91
Base/Subbase Design Example Using the Design Guide Sheet 94
Chapter 6 Summary and Conclusions 107
References 111
Appendix A: Supplemental Analysis of Response of PCC Slabs 115
Appendix B: Erosion Test Procedure Using Hamburg Wheel-Tracking Device 135
Appendix C: Modifications of Specifications 143

LIST OF FIGURES

Page

Figure 1 Chart for Estimating Modulus of Subgrade Reaction (*15*).....20
Figure 2 Correction of Effective Modulus of Subgrade Reaction due to Loss of Foundation Contact (*16*). 21
Figure 3 Approximate Interrelationships of Soil Classifications and Bearing Values (*16*). 23
Figure 4 Schematic of Erosion Test Using RaTT Device.....35
Figure 5 Erosion Test Using Hamburg Wheel-Tracking Device.....36
Figure 6 Aggregate Size Distributions of RaTT Erosion Test Samples. 38
Figure 7 Weight Loss versus Various Levels of Shear Stress during RaTT Testing. 39
Figure 8 Weight Loss versus Various Number of Loading by RaTT.....40
Figure 9 Aggregate Size Distributions of Erosion Test Samples. 41
Figure 10 Erosion versus Number of Loading by HWTD Test.....41
Figure 11 Erosion versus Change of Cement Percentage by RaTT.....42
Figure 12 Erosion Depth Changes of HWTD Erosion Test due to Cement Percentage Modification.....42
Figure 13 Maximum Erosion Depth at Joint Location versus Number of Load by HWTD Test.....44
Figure 14 Mean Erosion Depth of 11 Measuring Spots versus Number of Load by HWTD Test.....45
Figure 15 Slab Configuration of Erosion Modeling. 46
Figure 16 Log Plot to Acquire a and ρ from HWTD Test.....51
Figure 17 Erosion Model Fitting to HWTD Test Results.....52
Figure 18 Model Fitted Erosion versus Measured Erosion from HWTD Test.....53
Figure 19 Concept of Friction Stiffness.....57
Figure 20 Analysis of Frictional Effects: Crack Width and Spacing.....58
Figure 21 Analysis of Frictional Effects: Steel Stress and Punchout. 59
Figure 22 Mean Crack Spacing Analysis of Frictional Effects. 61
Figure 23 Crack Width Analysis of Frictional Effects. 61

Figure 24 LTE Analysis of Frictional Effects. 62
Figure 25 Punchout Analysis of Frictional Effects. 63
Figure 26 IRI Analysis of Frictional Effects. 63
Figure 27 Tensile Stress Pattern in Slabs (*23*). 66
Figure 28 Coefficients for Maximum Stress in Curled Slab (*22*). 67
Figure 29 Temperature Loading Conditions. 69
Figure 30 Output Values. 69
Figure 31 Modulus of Subgrade Reaction Effects under Nighttime Temperature Condition. 70
Figure 32 Modulus of Subgrade Reaction Effects under Daytime Temperature Condition. 70
Figure 33 Modulus of Subgrade Reaction Effects under Temperature and Vehicle Loads. 71
Figure 34 Curling Stresses. 73
Figure 35 Relationship between the Effective k-value and the Bradbury C Factor. 74
Figure 36 Analysis of Modulus of Subgrade Reaction Effects: Crack Width and Spacing. 75
Figure 37 Analysis of Modulus of Subgrade Reaction Effects: Steel Stress and Punchout. 76
Figure 38 Punchout Analysis of Modulus of Subgrade Reaction Effects. 77
Figure 39 IRI Analysis of Modulus of Subgrade Reaction Effects. 77
Figure 40 Effect of Base Erodibility on Predicted Faulting at JPCP (*19*). 79
Figure 41 Decision Flowchart for Subbase Design of Concrete Pavement. 83
Figure 42 Deflection-Based Subbase Thickness and Modulus Design Chart. 91
Figure 43 Screen shot of Base/Subbase Design Guide Sheet for Concrete Pavement. 97
Figure 44 Erosion Potential versus Material Type and Stabilization Level. 102
Figure 45 Erosion Potential versus Load Transfer Devices. 103
Figure 46 Erosion Potential versus Drainage and Joint Seal Maintenances. 105
Figure 47 Finite Element Configuration. 117
Figure 48 Temperature Gradients for Analysis Input. 119
Figure 49 Stress Distributions at Daytime Temperature Condition. 120
Figure 50 Stress at Slab Center on Daytime Temperature Gradient Condition. 121
Figure 51 Stress Distributions at Slab Center along Slab Depth on Daytime Condition. 122
Figure 52 Stress Distributions at Nighttime Temperature Condition. 123
Figure 53 Stress at Slab Center on Nighttime Temperature Gradient Condition. 124

Figure 54 Stress Distributions at Slab Center along Slab Depth on Nighttime Condition. 125
Figure 55 Daytime Relative Vertical Movements between Slab Center and Edge. 126
Figure 56 Nighttime Relative Vertical Movements between Slab Center and Edge. 127
Figure 57 Stresses due to Wheel Loading.....128
Figure 58 Modified FE Model. 129
Figure 59 Temperature Gradients for Analysis Input. 129
Figure 60 Stress Distributions at Daytime and Nighttime Temperature Conditions. 131
Figure 61 Effects of Subbase Thickness at Daytime. 132
Figure 62 Effects of Subbase Thickness at Nighttime. 133
Figure 63 Configuration of High-Density Polyethylene Molds. 139
Figure 64 Configuration of Jointed Concrete Capping Blocks.....139

LIST OF TABLES

Page

Table 1 Subbase Type and Performance of Highways in Texas. 4

Table 2 Performance of Field Test Sections US 75 and US 81/287 in Texas. 6

Table 3 Performance of Field Test Sections US 81/287 and FM 364 in Texas....7

Table 4 Performance of Field Test Sections IH 10 and IH 635 in Texas. 8

Table 5 Features of Candidate Alternative Subbase Types. 10

Table 6 Performance Comparisons of Candidate Alternative Subbase Types (*2*, *3*)....10

Table 7 Strength Requirements (*14*). 17

Table 8 Recommended Material Design Modulus Values (*13*)....18

Table 9 Typical Ranges of LS Factors for Various Types of Materials (*15*). 20

Table 10 Subgrade Soil Types and Approximate *k*-Values (*16*). 24

Table 11 Design *k*-Values for Untreated and Cement-Treated Subbases (*16*). 24

Table 12 Level 2 Recommendations for Assessing Erosion Potential of Base Material (*17*, *19*). 25

Table 13 Recommendations for Base Type to Prevent Significant Erosion (*17*). 28

Table 14 Summary of Erosion Test Methods. 29

Table 15 Summary of Erosion Models. 30

Table 16 Summary of Subbase Design Guides....31

Table 17 Mechanical Erosive Forces and Strength Factors. 33

Table 18 Sieves for Aggregate Size Analysis. 38

Table 19 Results of Paired T-test Statistic on Measured and Modeled Erosion. 54

Table 20 Input Values. 56

Table 21 Frictional Stiffness Values. 57
Table 22 Value Range of Frictional Coefficient. 60
Table 23 Geometry Input Values. 68
Table 24 Erodibility Classification. 78
Table 25 Subbase Design Considerations. 84
Table 26 Subbase Erosion Resistance Criteria in Design Factors. 88
Table 27 Erosion Rate Adjustment Factor by Equivalent Erosion Ratio. 91
Table 28 Erosion Rate Adjustment Factor by Load Transfer Systems. 92
Table 29 Erosion Rate Adjustment Factor Based on Annual Wet Days and Joint Seal Maintenance Condition. 94
Table 30 Input Factors of Design Guide Sheet − General. 95
Table 31 Input Factors of Design Guide Sheet − Traffic 98
Table 32 Input Factors of Design Guide Sheet - Base, Subbase, and Subgrade 99
Table 33 Erodibility of Stabilized Base/Subbase Materials Using HWTD Test. 101
Table 34 Typical Friction Coefficient of Stabilized Base/Subbase Materials. 102
Table 35 Drainage Quality Based on the Time of Water Removing from Pavement. 104
Table 36 Output Factors of Design Guide Sheet. 105
Table 37 Concrete Property. 118
Table 38 Subbase Property. 118
Table 39 Analysis Cases. 119
Table 40 Input Values. 130
Table 41 Input Variables and Values. 131

CHAPTER 1
INTRODUCTION

A subbase layer under a concrete pavement may be bonded or unbonded to the concrete slab. The term bonded refers to some form of chemically induced adhesion or cohesion between the layers while unbonded covers a wide range of frictionally restrained interlayer conditions between the slab and the subbase that can vary between unbonded to fully bonded.

Subbase layers perform many important roles in a concrete pavement system such as providing:

- a stable construction platform,
- uniform and consistent support,
- erosion resistance,
- drainage, and
- a gradual vertical transition in layer moduli.

The first function of a subbase layer is to provide a stable construction platform. For instance, construction traffic can pass over a cement-treated base (CTB) when a compressive strength of approximately 350 psi is achieved (normally 2 days after placement), while protecting the natural subgrade from damage due to construction or other related traffic. Consequently, the natural default function of a subbase layer beyond any relevant construction issues is to provide uniform and consistent support.

The role of uniform and consistent support cannot be overstated in the performance of long-lasting concrete pavement systems; good performing concrete pavements can co-exist with a wide range of support strength, but variation from the slab center to the edge or corner area or differences in support between segments of continuously reinforced concrete (CRC) pavement, for instance, cannot be tolerated to any great extent, which is why erosion is and has been a key factor in performance. Erosion potential is greatest where sufficient slab action under load has taken place creating a loosened layer of subbase material along the interface, in conjunction with upward curling and warping along edge and corner areas debonding the slab from the subbase and allowing moisture to saturate the interface. These circumstances enable the slab to “pump” any water that may be trapped under the applied wheel loads along the slab/subbase interface.

This action, combined with the viscous nature of water, creates a shearing stress that carries or transports eroded subbase material, further disrupting the continuity of the slab support.

Another interesting function of a subbase layer is to facilitate drainability, which may have different meanings depending on whether moisture is able to permeate the subbase layer or be completely repelled due to its stabilized nature. Most concrete pavement types will manifest some evidence of pumping if water is present along the interface between the slab and the subbase or subgrade as a key factor for transport to occur. Any means to remove or to minimize the presence of moisture on the interface is considered effective drainage; however, the means to do that may vary depending on the nature of the drainability of the pavement system.

Subbase materials stiff enough to resist erosive forces under the action of pumping may not require the removal of moisture within the subbase layer but need only enough unobstructed cross slope to allow the removal of water from the interface. Unfortunately, most CTB subbases are not sufficiently erosion resistant or permeable to allow for a timely removal of water from the interface to avoid erosion damage unless they are fully bonded to the slab. The use of an asphalt interlayer certainly improves the erosion resistance of CTB under unbonded conditions but the main reason for using such materials has been to reduce the frictional resistance between the slab and the subbase to ensure, for instance, the proper development of the crack pattern in CRC pavements. The use of an asphalt interlayer has served important purposes as far as CRC pavement design and performance to reduce friction stress, reduce potential for reflection of block cracking, and reduce variability of yield during paving. The use of open-graded, stabilized layers has been a consideration on some projects but interlocking between the two layers can be a cause of concern. Also, drainable, stabilized layers have had constructability and stability issues. The Dallas District, for instance, changed the subbase on the North Central Expressway (US 75) project from an open-graded asphalt stabilized subbase to a regular dense-graded base because the open-graded base was found to be difficult to construct and unstable under construction traffic.

Functions to provide increased slab support and to provide a gradual vertical transition in layer moduli may tend to counter the effects of each other but nonetheless refer to some key considerations in the design of a subbase layer. Subbase layers certainly can add structural capacity to a concrete pavement but the contribution in this regard is generally small in light of the inherent load spreading capability of the slab. Consequently, this function is not an absolute

necessity and can be sacrificed to some extent. Perhaps a more important feature is provision of a gradual change in layer stiffness from the slab to the top of the subgrade layer. Abrupt changes in this regard can lead to undesirable shear concentrations along the corners and pavement edges; enhancing the potential for poor support conditions to evolve over time and loading cycles. Stiff subbases also tend to magnify the environmentally induced load stresses in the slab and inadvertently shorten the cracking fatigue life of the pavement system. Again, the use of a graduated layer stiffness support system may help to reduce these types of stresses and prolong the fatigue life of the slab by reducing the curling and warping-related stresses.

FIELD INVESTIGATIONS

Table 1 shows the performance of non-asphalt treated subbase of selected pavement sections in Texas. Untreated base and lime-treated subgrade have not performed well under both CRC and jointed concrete (JC) pavement. These sections were subject to pumping damage through the displacement of fines causing voiding of the subbase layer. However, sections constructed in the 1950s involving a seal-coated flexible base have performed well; these sections were also constructed on elevated ground, which apparently facilitates good surface drainage and maintains unsaturated conditions in the subgrade. The presence of the seal coat may have helped to reduce moisture intrusion into the base while minimizing the friction between a slab and the flex base.

Preserving the integrity of a subgrade soil support is an important design consideration when selecting subbase type, stiffness, and thickness. Generally, flexible base materials (even though permeable) have not performed well, particularly over moisture saturated subgrades while most cement stabilized bases (CSB) protect the subgrade well enough due to their high resistance to deflection and erosion.

Some CSBs in Texas placed without a bond breaker have performed well under both jointed and CRC pavements and various traffic levels since CSB is highly resistant to erosion. However, sections statewide with weakly constructed CSBs built during the 1950s and 1960s have shown premature failures—possibly due to the low cement content of these bases.

Table 1 Subbase Type and Performance of Highways in Texas.

Poorly Performing Subbases	Well Performing Subbases
Statewide – 8 inch CRC pavement over weak CSB (1950s–1960s)	**IH 30 in Fort Worth** – 8 inch CRC pavement over seal coat and flexible base, built in the late 1950s (overlaid with 2 inch Asphalt Concrete Pavement [ACP], still in place)
IH 35E near Waxahachie – 8 inch CRC pavement over flexible base, built in the 1960s	**IH 10 in El Paso** – 8 inch CRC pavement built directly over CSB
US 75 near Sherman – 10 inch concrete pavement contraction design (CPCD) over flexible base, built in the early 1980s	**IH 10 in Houston** – 8 inch CRC pavement over CSB
IH 35W N. of Fort Worth – 8 inch CRC pavement over lime-treated subgrade, built in the 1960s	**Beaumont District** – CPCD over CSB
Various roadways in Atlanta and Childress – 13 inch CPCD (no dowels) over natural subgrade (usually sandy)	**IH 45 in Houston** – 8 inch jointed reinforced concrete (JRC) pavement over Oyster Shell Base (1945)

One benefit of the field investigation carried out in this study was the identification of factors associated with the erosion process. Sample sections were investigated using a number of techniques including visual survey, nondestructive test using falling weight deflectometer (FWD) and the ground penetrating radar (GPR), as well as dynamic cone penetrometer (DCP) and coring (*1*).

Untreated aggregate base under jointed concrete on US 75 in the Sherman area showed poor performance, possibly due to saturated subgrade conditions and poor drainage. The modulus of the new base materials used in the patched areas was about twice the modulus of the original base in the unrepaired sections. An Asphalt Concrete (AC) base on a lime-treated subgrade on US 81/287 in Wise County has performed reasonably well except in areas where the subbase and subgrade were eroded. The bond condition, particularly between CRC and an AC base layer, was generally good but erosion at the slab/AC layer and the AC layer/lime-treated subgrade interfaces diminished the structural integrity of the pavement.

The cement stabilized oyster shell base on FM 364 in the Beaumont area showed some erosion at the interface with the portland cement concrete (PCC) near the joint. No erosion was noted away from the joint as indicated by the good contact between the concrete slab and the

base. Distressed areas on the frontage road along IH 10 in Beaumont consisted of severe map cracking, spalling, and pumping due to placement of a CRC pavement over a soft silty and sandy subgrade. Some patched areas had settled and experienced corner breaks due to low load transfer efficiency (LTE) and poor support. Most of the damage appeared to be due to a weak subgrade and an insufficient slab thickness for the applied loads.

The key distress types of CRC pavement over CTB on IH 635 in the Dallas area were related to the condition of the full-depth patches and the widened longitudinal joints; nonetheless, the overall condition of the pavement appeared to be very good. The patches in the pavement were most likely repairs of either full or partial punchouts that were possibly a result of erosion and loss of support immediately below the slab. Summarized evaluations of selected sections are discussed from Table 2 to Table 4.

In conclusion, well maintained joint seals seem to be effective in blocking surface water from intruding the pavement section and help to reduce hydraulic pumping action. Causes for early joint-related pavement failure could be due to insufficient stiffness of the joints associated with degraded base support. Accordingly, routine monitoring and timely sealing of joints and cracks should cost effectively extend pavement service life.

Table 2 Performance of Field Test Sections US 75 and US 81/287 in Texas.

Test Section	US 75 – Sherman District	US 81/287 – Wise County Sections 1 and 2
Pavement Type	10 inch (15 ft joint spacing) JC pavement built in 1983	8 inch CRC pavement on northbound near Decatur constructed in 1971
Subbase Type	6 inch unbound aggregate base	4 inch AC base
Subgrade Type	Weathered soil subgrade	6 inch lime-treated subgrade, sandy soil
Traffic	Average daily traffic (ADT) = 43,000 Total = 25 million equivalent single axle load (ESAL)s	ADT = 23,000 (23% truck) Total = 35 million ESALs
Distress Type	Faulting, pumping	Pumping, faulting, patching
Cause of Distress	Joint sealing deterioration, weak subbase, erosion	Wide crack widths, wide and no longitudinal joint sealing
GPR Analysis Results	Most sections showed voided and eroded areas. Patched sections showed no erosion but slabs adjacent to the patched areas did indicate voided areas	GPR images showed significant amounts of wet or eroded areas in the lime-treated subgrade layer; however, little erosion on the AC base layer was detected
FWD Analysis Results	Patched sections had low LTE and effective thickness due to the lack of aggregate interlock along the joints and consequently potential problem locations for future repair	Section with wetter subgrade conditions showed a greater mean deflection. Some cracks have a relatively low LTE and may hold a higher possibility of erosion in the future at those locations
DCP Analysis Results	Patched areas showed a base modulus to be about twice the base modulus of the unrepaired sections caused discontinuous base support	Section 1 had the lowest elastic modulus, perhaps due to the wet subgrade conditions as noted by the GPR images
Coring Analysis Results	The evidence of separation due to erosion and pumping action were apparent	Some erosion at the interface between AC and subgrade was detected

Table 3 Performance of Field Test Sections US 81/287 and FM 364 in Texas.

Test Section	US 81/287 – Wise County Section 3	FM 364 – Beaumont Area
Pavement Type	12 inch CRC pavement with 3 ft extended lane width as part of the shoulder constructed in 1985	10 inch (15 ft joint spacing) JC pavement constructed in 1985
Subbase Type	2 inch AC base 2 inch AC subbase	6 inch cement stabilized oyster shell base
Subgrade Type	6 inch lime-treated subgrade, sandy soil	Natural soil subgrade
Traffic	ADT = 23,000 (23% truck) Total = 35 million ESALs	ADT = 21,000 (2.5% truck) Total = 2.5 million ESALs
Distress Type	No major distress	Transverse cracks near the joints
Cause of Distress	Thick PCC, extended lane width, good longitudinal joint seal	Late saw-cutting
GPR Analysis Results	Low level of moisture at the interface between two AC base layers and a moderate level of moisture on the subgrade layer, no significant erosion was identified	High chance of water was presented at the interface of the slab and base layer as well as an indication of erosion-related damage
FWD Analysis Results	Low deflection and high effective thickness	Most joints show good LTEs and low deflections except eroded area
DCP Analysis Results	Modulus was in the low end of the range of typical values since the untreated natural subgrade material was a low modulus material	Calculated modulus was in the normal range of subgrade material moduli
Coring Analysis Results	Manifest erosion on the AC subbase layer; debonding and the erosion between two AC layers diminishes the structural integrity of the pavement	Damage at the interface between base and subgrade was limited to the vicinity of the joint. The bottom of each layer indicated a debonded condition

Table 4 Performance of Field Test Sections IH 10 and IH 635 in Texas.

Test Section	IH 10 – Beaumont Area	IH 635 – Dallas Area
Pavement Type	6 inch CRC pavement constructed in 1963	8 inch CRC pavement with a concrete shoulder opened to traffic in 1967
Subbase Type	No subbase	4 inch cement stabilized base
Subgrade Type	Silty and sandy subgrade	Sandy and clay subgrade
Traffic	ADT = 100 (3.2% truck) Total = 130,000 ESALs	ADT = 200,000 (12% truck)
Distress Type	Severe map cracking with spalling and pumping	Spalled cracks and patches, widened longitudinal joints
Cause of Distress	No joint sealing, subgrade erosion and saturation to 12 inch depth	Erosion and loss of support immediately below the slab
GPR Analysis Results	High degree of moisture and voiding under the slab; some peaks of dielectric constant (DC) values occurring at the beginning and end of the full depth repair (FDR) patches	Some moisture areas under the concrete slab but no significant sign of erosion was identified. Dielectric constant (DC) values of overall sections represented a low level of moisture on the base layer
FWD Analysis Results	Low effective thickness in combination with high deflection was found at the FDR patch joints, indicating weakened subgrade conditions at those locations	Good LTEs but there were a few areas where low values of effective thickness exist indicating the integrity of this pavement is beginning to diminish
DCP Analysis Results	The subgrade was very weak; All tested locations showed very high penetration ratios through the top 12 inches. Backcalculated moduli were around 2.5 to 3 ksi	Good subgrade conditions. The pavement support is not presently an issue but could soon become serious if maintenance activities are terminated or diminished
Coring Analysis Results	All cores showed eroded conditions and, of course, no bonding between the concrete and the subgrade. There was no base layer	Erosion was found only at areas where the condition of the longitudinal construction joint was not well maintained and moisture had penetrated the pavement

ALTERNATIVE SUBBASE MATERIALS

Over the last 40 years, subbases have consisted or cycled between dense, open-graded, bound, and unbound materials; different varieties of cement-treated bases (both asphalt and portland), lean concrete bases, and CTB with AC bond breaker layer have been utilized. Lean concrete subbases, although highly erosion resistant, have been perhaps far too stiff for conventional jointed concrete pavements but less stiff than CTBs, which have not been erosion resistant enough unless combined with an interlayer. Nonetheless, some level of stabilization seems to be the most popular trend as of late, but subbases with high friction properties have been found to be problematic (unless fully bonded) relative to the formation of well-distributed cracking patterns.

A list of alternative subbase types and materials was developed based on evaluation of field performance and discussion with the project monitoring committee. Accordingly, cement-treated bases are at the top of the list as they are performing well in many instances. Recyclable materials (recycled asphalt and recycled concrete) also show promise and were the focus of laboratory testing carried out in this project.

The features of an ideal subbase layer might consist of sufficient strength having at moderate level of friction, some potential to bond to the slab, sufficient erosion resistance, and a conforming but uniform support. A subbase layer should be adequately flexible to minimize curling and warping-related stress but free of any tendencies to block crack and reflect into the concrete slab. Additionally, a medium level of frictional restraint (while avoiding any interlocking with the slab) is desired to minimize the shear stress between the concrete and the base layer.

With these suggested features, a variety of candidate subbase types are listed in Table 5 and can be evaluated in terms of the desirable features of an ideal subbase layer. Each alternative subbase material in the list is evaluated relative to the performance factors listed in the heading of Table 6 (*2*, *3*).

Table 5 Features of Candidate Alternative Subbase Types.

Type	Stabilizer Agent or Interlayer	Aggregate Type	Combination Features	TxDOT Specification Items
Cement-Treated Base	Cement	Limestone or gravel	Cement + flex base	Item 275
Reclaimed Asphalt Pavement (RAP) Base	Cement and RAP	Crushed asphalt and limestone/ gravel	Cement + RAP > 50% subbase	Item 305, 275
Recycled Concrete Base	Cement	Crushed concrete	Cement + 100% crushed concrete	Item 251, 275
Lime-Fly Ash Treated Base	Lime or fly ash	Limestone or gravel	Lime and/or fly ash + flex base	Item 260, 265
Thin AC on Treated Subgrade	Lime or cement depending on soil type	Subgrade material	2 inch AC base over treated subgrade (usually 8 inches minimum)	Item 330, 275
Recycled Asphalt/AC Bond Breaker	RAP asphalt	Limestone or gravel	RAP > 30% bond breaker over CTB	Item 305, 275
Emulsion Bond Breaker	Emulsion	Limestone or gravel	Emulsion bond breaker over CTB	Item 300, 275

Table 6 Performance Comparisons of Candidate Alternative Subbase Types (*2*, *3*).

Type	Stabilizer Content	Coefficient of Friction (when natural subgrade = 1)	Elastic Modulus, ksi (*2*)	Erosion Ratio, g/min (*3*)	Relative Cost to 4 inch AC Bond Breaker
Cement-Treated Base	3% cement	10	1,000 ~ 2,000	30	Low
RAP Base	2–4% cement	6	350 ~ 1,000	57	Low
Recycled Concrete Base	4% cement	15	450 ~ 1,500	12	Low
Lime-Fly Ash Treated Base	1:3 lime/fly ash	10	20 ~ 70	350	Low
Thin AC on Treated Subgrade	cement or lime	6	350 ~ 1,000	AC:10, CTS*: 132	Medium
Recycled Asphalt /AC Bond Breaker	4.4% asphalt concrete	6	350 ~ 1,000	AC:10, CTB**: 30	Medium
Emulsion Bond Breaker	3% cement	3	CTB**: 1,000 ~ 2,000	Emulsion: N/A CTB**: 30	Medium

*CTS – Cement-Treated Subgrade **CTB – Cement-Treated Base

TxDOT subbase design practice calls for either a 6 inch CTB with a 1 inch AC bond breaker or a 4 inch AC subbase layer over a treated subgrade. Using a reduced thickness or a high RAP content AC layer may yield possibilities to reduce cost. Using a spray-on emulsion (asphalt, resin, or wax-based emulsions) may have certain advantages (if chemical bonding is not excessive), particularly from a construction perspective; but this option would be limited to stiff concrete subbases in order to ensure non-erodibility. The purpose of the emulsion would be to reduce the interlayer friction to acceptable levels but must be applied only if a certain amount of bond is achieved.

Considering these characteristics in light of the objective of identifying alternative subbase types and materials, CTB, RAP, and the subbase materials using recycled concrete are selected as some of the most feasible candidate alternative subbase combinations.

A bond breaker has been used over the years to separate the action of the reinforcing steel in the concrete layer form those in the base layer to facilitate suitable cracking pattern development in CRC pavement. Therefore, some measures are required (such as using an asphalt concrete bond breaker with only limited bonding capability) to prevent strong bonding between a stabilized base layer and the concrete slab. Such a layer is highly resistant to erosive actions. Providing separation of this nature avoids adjustment of the steel content to compensate for the reduced amount of cracking due to bonding between the base and the slab.

RAP is removed and/or reprocessed asphalt materials and aggregates for pavement reconstruction. Full-depth reclamation consists of a mix of the original base material and the deteriorated asphalt pavement with the addition of cement to create a new stabilized base material. Recycling costs are typically less than the removal and replacement of the old pavement, and performance has been satisfactory relative to the original subbase (*4*, *5*).

Recycled concrete pavement has become an important candidate as an alternative subbase material due to less erosion potential with reasonably good durability as well as being economically and environmentally feasible. Lab testing should be useful to evaluate erodibility and stiffness versus various cement contents. Previous research recommended only 1.5 percent cement content as optimal for stabilizing based on unconfined compressive strength, durability, and moisture susceptibility testing (*6*). Such low cement content may be the result of the residual cementitious material on the surface of the crushed concrete.

CONCLUSIONS

The performance of subbases in Texas was investigated using a number of techniques including visual survey and nondestructive testing. Generally, untreated subbases have not performed well, particularly over moisture sensitive subgrades; most CSBs over sound subgrades have performed well due to reduced deflection. Well maintained joint seals seem to be effective in blocking surface water from intruding the pavement section and limiting hydraulic pumping action. Causes of early pavement failures in many instances were traced to insufficient stiffness of the associated joints due to degraded base support. Accordingly, routine monitoring and timely resealing of joints and cracks could cost effectively extend the life of good performing pavements.

The features of an ideal subbase layer might consist of sufficient strength having a moderate level of friction but with sufficient resistance to erosion while providing a conforming but uniform support of the slab. Use of exceptionally stiff subbase layer should be avoided in order to minimize curling and warping-related stress. Additionally, a medium level of subbase frictional restraint is desired to facilitate structural stiffness of the pavement section but at the same time limit the shear stress between the concrete and the base layer, particularly at early ages. Considering these characteristics will allow for the successful selection of alternative subbase types and materials consisting of combinations of CSB, RAP, and the use of recycled concrete.

CHAPTER 2
LITERATURE REVIEW

In this chapter, as background relative to the development of design guidelines, previous test methods and erosion models as to their utility to characterize subbase materials in terms of erosion resistance are briefly reviewed as well as past and current subbase design guides pertaining to erosion.

PREVIOUS LABORATORY TEST METHODS FOR EROSION

Many erosion tests were developed in the 1970s and 1980s using various testing devices but none of those tests have been selected as a standardized form of testing. Some of the more prominent test methods are described relative to their utility to characterize subbase and subgrade materials for erosion resistance.

Phu and Ray tested the erodibility of various materials using a rotational brush test (*3*). A 100 mm (4 inches) diameter brush with ten thousand 45 mm (1.8 inches) long bristles was used to erode samples by rotating at 840 rpm under 1 kg (2.2 lb) mass. This test used in France is fairly simple and it provides a quantitative measure of degree of erodibility of stabilized materials. The erosion index (IE) is defined as the ratio of the weight loss by the rotational brush test to the weight loss of a reference material (granular material stabilized with 3.5 percent cement). One unit of IE is the rate of the weight loss of 26 g/min (0.05 lb/min) and a lower IE means better erosion resistance. A table of the erodibility for various material types and stabilizer ratios was suggested as a design guide for erosion. Since this method takes six weeks to complete 12 wet-dry cycles, the utility of applying this method to design is limited. Although a common issue with all erosion tests, base materials consisting of large-sized aggregates that loosen and dislodge during testing tend to create inaccurate weight loss rates.

Van Wijk developed two test methods using a rotational shear device and a jetting device to measure erosion under a jet of pressurized water (*7*). Cohesive materials are tested using the rotational shear device, while non-cohesive materials are tested using the jetting device. The concept is based on surface erosion occurring when water-induced shear stress is higher than the shear strength of the test material. The rotational shear device creates erosion by applying a shear stress to the surface of a cohesive specimen by exceeding the shear strength of the test

material. The jetting device creates a mass loss in non-cohesive samples over time under the effect of a pressurized jet of water applied at an angle of approximately 20 degrees to the upper surface of the sample. Shear stress determinations on the surface are calculated based on the assumption of stress being applied uniformly over a designated area even though the surface area changes with time as well as the pressure distribution. Weight loss could be overestimated by the loss of aggregate-sized particles, which may not take place in the field.

de Beer developed the rolling wheel erosion test device that applies the movement of a wheel over a friction pad (neoprene covering) to serve as the source of erosion of the test sample (*8*). Fines are produced on the surface of the test sample by direct contact between the friction pad and the test sample; submerging the test sample during testing allows water to wash out generated fines similar as would take place under the slab pumping action. The erosion index is the measure of erosion and defined as the average depth of erosion after 5,000 wheel load applications. This test attempts to simulate field conditions since it addresses mechanical abrasive and hydraulic erosion together. However, pumping action caused by the flexible membrane in this test may not be similar to the pumping action under a rigid pavement. The expansion of the neoprene pad tends to distribute shear stress across the sample non-uniformly, which may not represent how voiding of the base material under a concrete slab due to erosion occurs.

PREVIOUS EROSION MODELS

Many empirical erosion models have been proposed based on field performance data. The presence of water, the erodibility of a subbase material, the rate of water ejection, the amount of deflection, and the number of loads are factors that influence erosion but previous design procedures scarcely address these factors.

Rauhut et al. proposed a pumping model based on nonlinear regression analysis of the Concrete Pavement Evaluation System (COPES) database as a function of many comprehensive factors such as precipitation, drainage, subbase type (degree of stabilization), subgrade type (soil type), load transfer, slab thickness, freezing index, Thornthwaite moisture index, and traffic (*9*).

Markow and Brademeyer proposed a model based on the American Association of State Highway Officials (AASHO) road test data relating slab thickness to ESAL and subbase

drainage conditions through a pumping index (*10*). The model is simple but does not consider many important factors. The pumping index indicates the potential of erosion that increases with a cumulative number of ESALs and diminishing drainage conditions but decreases quickly with an increase in slab thickness. A drainage adjustment factor is considered based on subbase permeability.

Larralde proposed another model again based on the AASHO road test data relating erosion to the amounts of deformation energy imposed by the application of load; again through a pumping index parameter (*11*). The deformation energy was computed using finite element modeling and the pumping index is normalized to eliminate the effect of slab length and reinforcement. The model does not consider many important factors related to erosion.

Van Wijk included factors derived from field data to make improvements to the Larralde model by predicting the volume of eroded material as a function of the deformation energy produced by traffic (*7*). The effect of many factors on pumping such as subbase and subgrade type, drainage, load transfer, and climate conditions are considered in this model. Since this model is empirical in nature, its application is limited to the variable ranges included in the database.

Jeong and Zollinger developed a mechanistic-empirical model using the water-induced shear stresses model by Van Wijk (*7, 12*). Key factors such as vehicle load and speed, load transfer, number of applications, and climatic conditions are included in the model's prediction of erosion. The accuracy and inclusion of environmental factors in the model depend upon calibration to field performance.

CURRENT DESIGN GUIDELINES FOR BASE/SUBBASE

The design guides published by the Texas Department of Transportation (TxDOT), American Association of State Highway and Transportation Officials (AASHTO), National Cooperative Highway Research Program (NCHRP) 1-37 A: Mechanistic-Empirical Pavement Design Guide (MEPDG) and Portland Cement Association (PCA) were reviewed relative to design of the subbase based on material type and the erosion mechanism.

TxDOT Pavement Design Guide

TxDOT's *Pavement Design Guide* (*13*) approved the 1993 AASHTO *Guide for Design of Pavement Structures* for rigid pavement design. This design guide suggests using one of the following two types of base layer combinations and a k-value of 300 psi/inch in the rigid pavement design procedure:

- 4 inches of ACP or asphalt stabilized base (ASB) or
- a minimum 1 inch asphalt concrete bond breaker over 6 inches of a cement stabilized base.

TxDOT aims to prevent pumping by using non-erosive stabilized bases in accordance with Table 7, which shows the strength requirements for the three classes of cement-treated base:

> Bases that are properly designed and constructed using TxDOT specifications and test methods should provide adequate long-term support. Where long-term moisture susceptibility of ACP is a concern, using a plan note to increase the target laboratory density (and thus total asphalt content) may be beneficial. To ensure long-term strength and stability of cement stabilized layers, sufficient cement must be used in the mixture. Item 276, Cement Treatment (Plant-Mixed) currently designates three classes of cement-treated flexible base, based on 7-day unconfined compressive strength. Classes L and M are intended for use with flexible pavements. Class N, which has a minimum strength as shown on the plans, is intended for use with rigid pavements. There are several approaches to selecting an appropriate strength (and thus indirectly cement content):

- successful long-term experience with similar materials,
- laboratory testing using 100 percent of the retained strength of a conditioned specimen to determine if the design cement content and strength are acceptable, and
- laboratory testing using the tube suction test to determine if the design cement content and strength are acceptable.

A bond breaker should always be used between concrete pavement and cement stabilized base.

Table 7 Strength Requirements (*14*).

Class	7-Day Unconfined Compressive Strength, Min. psi
L	300
M	175
N	As shown on the plans

To achieve economical design, it needs to develop various subbase type and thickness guidelines over different treated subgrades (i.e., can possibly use 2 inch ACP if 8 inch lime-treated subgrade [LTS] has adequate stiffness and durability). Table 8 is a partial listing of typical design moduli by material type for new materials in the TxDOT design guide.

Table 8 Recommended Material Design Modulus Values (*13*).

Material Type	2004 Specification	Design Modulus	Poisson's Ratio
Asphalt Treatment (Base)	Item 292	250–400 ksi	0.35
Emulsified Asphalt Treatment (Base)	Item 314, various OTU special specs	50–100 ksi	0.35
Flexible Base	Item 247	If historic data not available, modulus should be from 3–5 times the subgrade modulus or use FPS default. Typical range 40–70 ksi.	0.35
Lime Stabilized Base	Item 260, 263	60–75 ksi	0.30–0.35
Cement Stabilized Base	Item 275, 276	80–150 ksi	0.25–0.30
Fly Ash or Lime Fly Ash Stabilized Base	Item 265	60–75 ksi	0.30
Lime or Cement Stabilized Subgrade	Item 260, 275	30–45 ksi	0.30
Emulsified Asphalt Treatment (Subgrade)	Item 314, various OTU special specs	15–25 ksi	0.35
Subgrade	(Existing)	Priority should be to use the project-specific back-calculated subgrade modulus. Defaults by county are available in the FPS design program. Typical range is 8–20 ksi.	0.40–0.45

1993 AASHTO Design Guide

The AASHTO design guide (*15*) suggests the sub-layer material property of concrete pavement is the composite modulus subgrade reaction determined from Figure 1. The composite modulus of subgrade reaction is estimated based on a subbase thickness and subbase elastic modulus with a road soil resilient modulus. However, this method is criticized by Huang (*2*) as follows:

> The chart was developed by using the same method as for a homogeneous half space, except that the 30 inch plate is applied on a two-layer system. Therefore, the *k* -values obtained from the chart are too large and do not represent what actually occurs in the field.

The 1993 design guide also considers potential loss of support (LS) due to foundation erosion by effectively reducing the modulus of subgrade reaction in the design procedure relative to four different contact conditions (i.e., with LS = 0, 1, 2, and 3). The best case is LS = 0, where the slab and foundation are assumed to be in full contact, while the worst case is LS = 3, where an area of slab is assumed not to be in contact with the subgrade, thus warranting reduced values of k-value over the non-contact area.

In Table 9, the possible ranges of LS factors for different types of subbase materials are provided to adjust the effective modulus of subgrade reaction, as shown in Figure 2. The subjective nature of determining the LS value based on the wide range of possibilities for each material type inherently reduces the sensitivity of the design process to the erosion mechanism leading to inconsistency and limiting applicability of the design procedure.

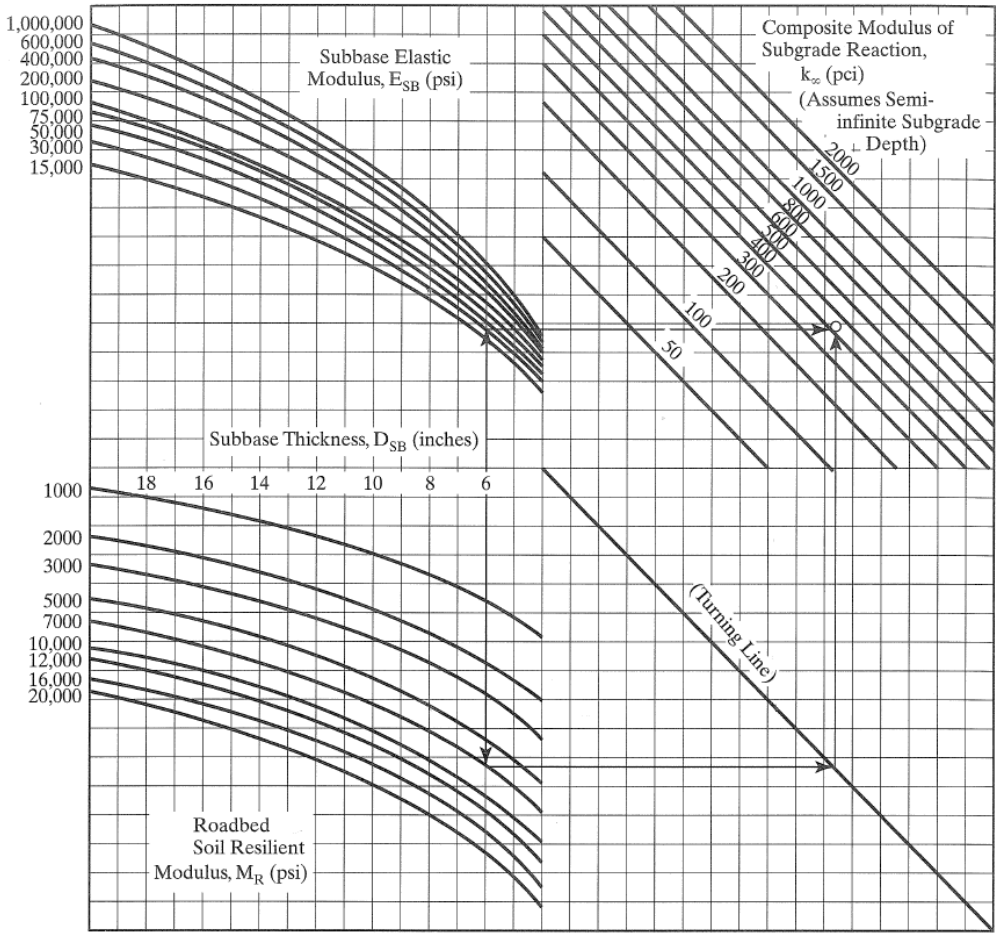

Figure 1 Chart for Estimating Modulus of Subgrade Reaction (*15*).

Table 9 Typical Ranges of LS Factors for Various Types of Materials (*15*).

Type of Material	Loss of Support
Cement-treated granular base (E = $1x10^6$ to 2×10^6 psi)	0.0 to 1.0
Cement aggregate mixtures (E = 500,000 to 1×10^6 psi)	0.0 to 1.0
Asphalt-treated bases (E = 350,000 to 1×10^6 psi)	0.0 to 1.0
Bituminous-stabilized mixture (E = 40,000 to 300,000 psi)	0.0 to 1.0
Lime-stabilized materials (E = 20,000 to 70,000 psi)	1.0 to 3.0
Unbound granular materials (E = 15,000 to 45,000 psi)	1.0 to 3.0
Fine-grained or natural subgrade materials (E = 3,000 to 40,000 psi)	2.0 to 3.0

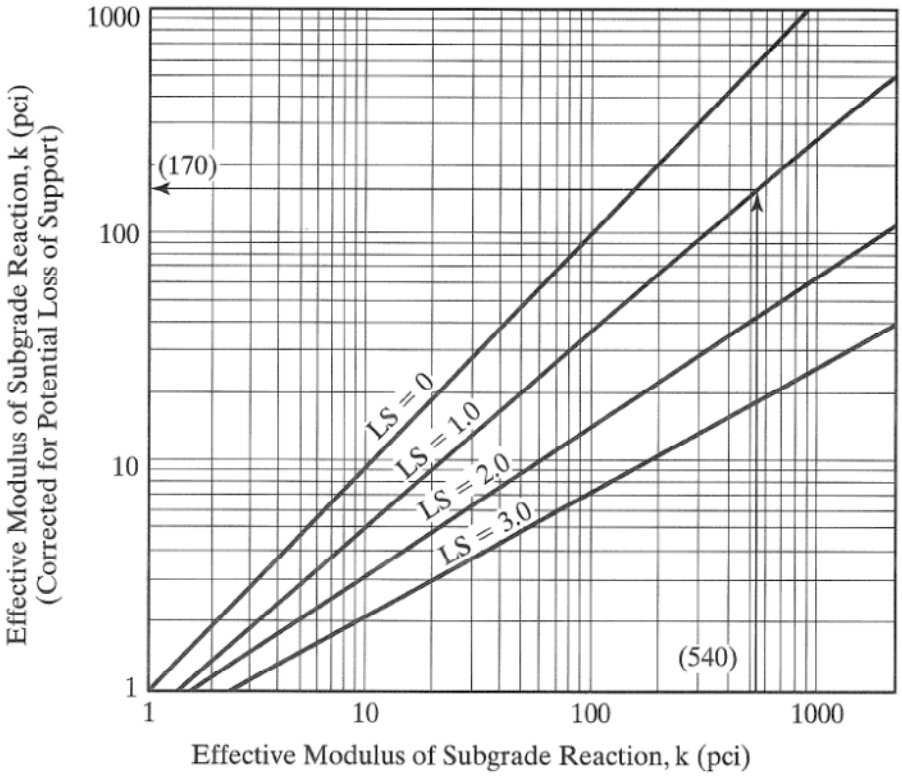

Figure 2 Correction of Effective Modulus of Subgrade Reaction due to Loss of Foundation Contact (*16*).

However, load transfer and drainage coefficients are also indirectly related with erosion; a lower deflection caused by better load transfer would reduce shear stress at the interface between the slab and base/subgrade and in the vicinity of a joint or crack, as well as minimize the time water is present on the interface due to better drainage; both situations should decrease the potential for pumping. Therefore, these factors affecting erosion can be considered in the design.

PCA Design Method

The subbase erosion in the PCA procedure (*16*) is related to pavement deflection (at the slab corner) due to axle loading. Equations 1 and 2 were developed based on the results of the AASHO Road Test for allowable load repetitions and erosion damage:

$$\log N = 14.524 - 6.777(C_1 P - 9.0)^{0.103} \quad (1)$$

$$\text{Percent erosion damage} = 100 \sum_{i=1}^{m} \frac{C_2 n_i}{N_i} \quad (2)$$

where:

N = allowable number of load repetitions based on a pressure of a PSI of 3.0

C_1 = adjustment factor (1 for untreated subbase, 0.9 for stabilized subbase)

P = rate of work or power = $268.7 \frac{p^2}{hk^{0.73}}$

p = pressure on the foundation under the slab corner in psi, $p = kw$

k = modulus of subgrade reaction in psi/inch

w = corner deflection, inch

h = thickness of slab, inch

m = total number of load groups

C_2 = 0.06 for pavement without concrete shoulder, 0.94 for pavements with tied concrete shoulder

n_i = predicted number of repetitions for ith load group

N_i = allowable number of repetitions for ith load group

Separate sets of tables and charts are used for doweled and aggregate interlock joints with or without concrete shoulders. Since the erosion criterion was developed primarily from the results of the AASHO Road Test using a specific type of subbase (that was incidentally highly erodible), the application of the model is limited to a single subbase type. Nonetheless, this procedure represents a significant advancement in the mechanistic analysis of pavement support condition in design.

Figure 3 shows approximate k-value that could be used for design purpose based on soil classification or other test methods. Table 10 also suggests a simple guide for approximate range of k-value based on subgrade soil types, but the vagueness associated with this classification reduces its sensitivity to the erosion mechanism.

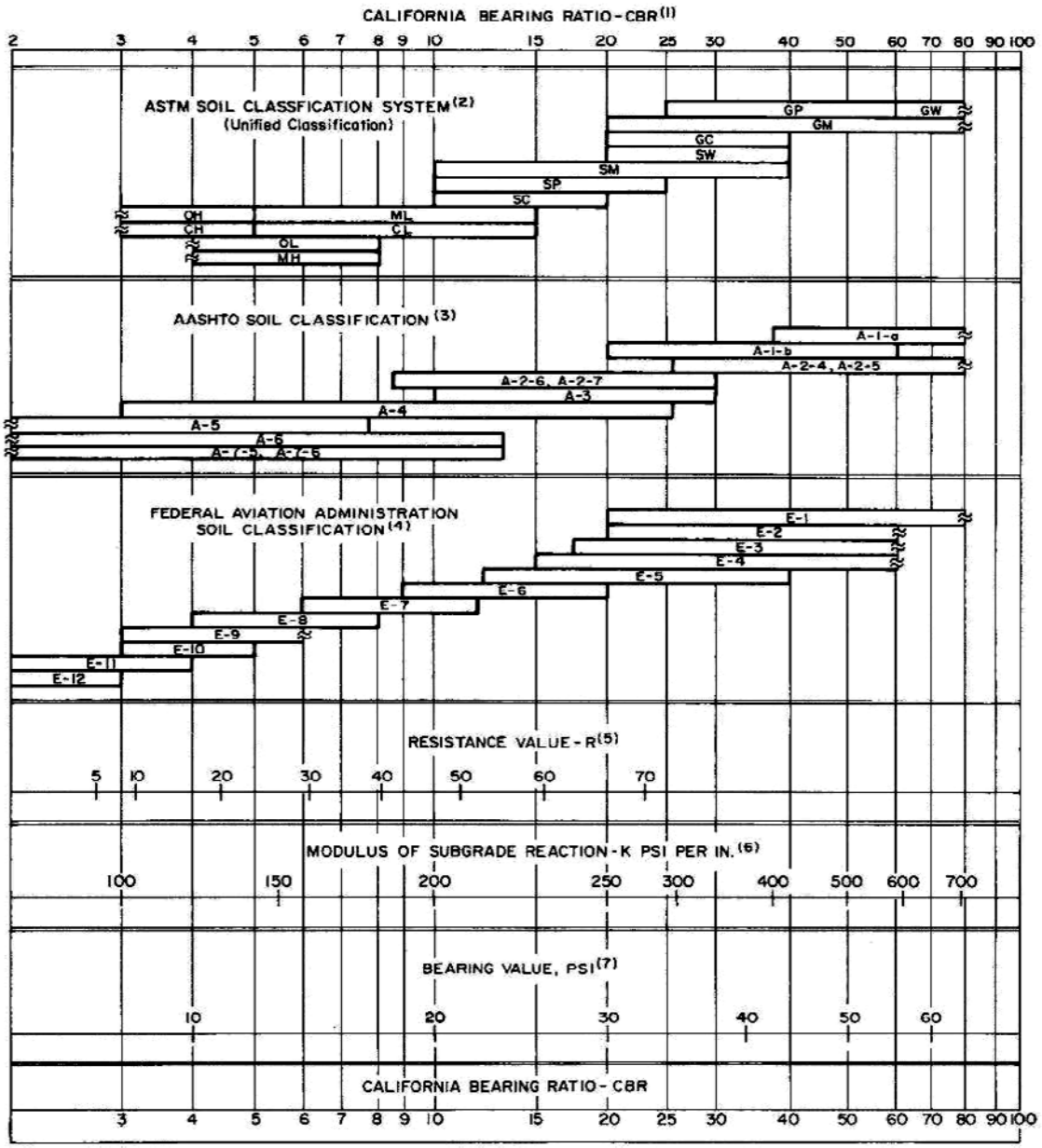

Figure 3 Approximate Interrelationships of Soil Classifications and Bearing Values (*16*).

Table 10 Subgrade Soil Types and Approximate *k*-Values (*16*).

Type of Soil	Support	k-values Range, pci
Fine-grained soils in which silt and clay-size particles predominate	Low	75–120
Sand and sand-gravel mixtures with moderate amounts of silt and clay	Medium	130–170
Sand and sand-gravel mixtures relatively free of plastic fines	High	180–220
Cement-treated subbases	Very high	250–400

Table 11 shows adjustment of k-value for subbases that could be construed for determining an effective or composite k-value. It is well accepted that cement-treated subbases significantly increase the effective k-value over a subgrade k-value or that caused by use of untreated subbases, but only in regard to curling and warping behavior. As mentioned early in the AASHTO design guide, the analysis using a 30 inch plate test on a two-layer system may result in a high k-value, which may not represent actual foundation behavior.

Table 11 Design *k*-Values for Untreated and Cement-Treated Subbases (*16*).

Subgrade k-value, pci	Untreated Subbase k-value, pci				Cement-treated Subbase k-value, pci			
	4 inches	6 inches	9 inches	12 inches	4 inches	6 inches	8 inches	10 inches
50	65	75	85	110	170	230	310	390
100	130	140	160	190	280	400	520	640
200	220	230	270	320	470	640	830	-

NCHRP Design Guide

The NCHRP 1-37A MEPDG (*17, 18, 19*) categorizes three different design input levels. Level 1 classification is site-specific material inputs obtained through direct testing or methods of measurements that may not be fully developed at this time. Level 2 classification uses correlations to establish or determine the required inputs, as shown in Table 12. Level 3 classification is based on material type description as in other design guides.

Table 12 Level 2 Recommendations for Assessing Erosion Potential of Base Material (*17*, *19*).

Erodibility Class	Material Description and Testing
1	(a) Lean concrete with approximately 8 percent cement; or with long-term compressive strength >2,500 psi (>2,000 psi at 28 days) and a granular subbase layer or a stabilized soil layer, or a geotextile fabric is placed between the treated base and subgrade, otherwise Class 2. (b) Hot-mixed asphalt concrete with 6 percent asphalt cement that passes appropriate stripping tests and aggregate tests and a granular subbase layer or a stabilized soil layer, otherwise Class 2.
2	(a) Cement-treated granular material with 5 percent cement manufactured in plant, or long-term compressive strength 2,000 to 2,500 psi (1,500 to 2,000 psi at 28 days) and a granular subbase layer or a stabilized soil layer, or a geotextile fabric is placed between the treated base and subgrade, otherwise Class 3. (b) Asphalt-treated granular material with 4 percent asphalt cement that passes appropriate stripping test and a granular subbase layer or a treated soil layer or a geotextile fabric is placed between the treated base and subgrade, otherwise Class 3.
3	(a) Cement-treated granular material with 3.5 percent cement manufactured in plant, or with long-term compressive strength 1,000 to 2,000 psi (750 to 1,500 psi at 28 days). (b) Asphalt-treated granular material with 3 percent asphalt cement that passes appropriate stripping test.
4	Unbound crushed granular material having dense gradation and high quality aggregates.
5	Untreated soils (PCC slab placed on prepared/compacted subgrade).

The MEPDG addresses erosion through modeling faulting distress (Equations 3 and 4). Classes of erodibility are formulated based on a modification of Permanent International Association of Road Congresses (PIARC) specifications relative to material type and stabilizer percent. Five levels of erosion resistance listed in Table 12 distinguish between material types based on stabilizer type and content (asphalt or portland cement) as well as long-term compressive strength (later than 28 days). Prediction of erodibility is closely associated with the material compressive strength. Each class of erosion is assumed to offer five times the resistance to erosion than the next class (i.e., Class 1 materials are five times more erosion resistant than Class 2 and so on).

However, field performance of lower strength subbase material has been good perhaps because of low friction interface bases. For instance, a 2 inch AC overlaid 8 inch thick CRC pavement of IH 30 in Fort Worth constructed in the 1950s over a seal-coated flexible base has been performing well for 50 years. Little guidance is provided addressing the degree of friction that should exist between the concrete and an underlying base layer or its contribution to erosion of the interface via load-induced shear stress. Moreover, PIARC uses the classification based on brush test results (previously noted) under dry conditions, which yields conservation results compared to erosion action under saturated conditions.

$$FAULTMAX_i = FAULTMAX_0 + C_7 * \sum_{j=1}^{m} DE_j * Log(1 + C_5 * 5.0^{EROD})^{C_6} \quad (3)$$

$$FAULTMAX_0 = C_{12} * \delta_{curling} * \left[Log(1 + C_5 * 5.0^{EROD}) * Log(\frac{P_{200} * WetDays}{P_s}) \right]^{C_6} \quad (4)$$

where:

$FAULTMAX_i$	=	maximum mean transverse joint faulting for month i, in
$FAULTMAX_0$	=	initial maximum mean transverse joint faulting, in
DE_i	=	differential deformation energy accumulated during month i
$EROD$	=	base/subbase erodibility factor
C_{12}	=	$C_1 + C_2 * FR^{0.25}$
C_i	=	calibration constants

FR	=	base freezing index defined as percentage of time the top base temperature is below freezing (32°F) temperature
$\delta_{curling}$	=	maximum mean monthly slab corner upward deflection PCC due to temperature curling and moisture warping
P_s	=	overburden on subgrade, lb
$P200$	=	percent subgrade material passing No. 200 sieve
$WetDays$	=	average annual number of wet days (greater than 0.1 inch rainfall)

Table 12 also can be used to estimate erosion width in CRC pavement and incorporated into the punchout prediction model. An empirical model for expected erosion width (Equation 5) is developed from expert opinion since no model, procedure, or field data are available for developing relationships between the erosion class, precipitation, and eroded area.

$$e = -7.4 + 0.342\,P_{200} + 1.557\,BEROD + 0.234\,PRECIP \quad (5)$$

where:

e	=	maximum width of eroded base/subbase measured inward from the slab edge during 20 years, inch (if $e < 0$, set $e = 0$)
P_{200}	=	percent subgrade soil (layer beneath treated base course) passing the No. 200 sieve
$BEROD$	=	base material erosion class (1, 2, 3, or 4)
$PRECIP$	=	mean annual precipitation, in

The NCHRP 2002 design guide provides general recommendations for subbase class selection for all concrete pavement types based on load transfer efficiency and traffic level but there is little guidance for other details such as the determination of layer thickness. A high volume lane requires high joint load transfer with an erosion-resistant base, as shown in Table 13. Therefore, MEPDG design recommendations can only be generally applied for material type and stabilization level.

Table 13 Recommendations for Base Type to Prevent Significant Erosion (*17*).

Design Lane Initial ADTT	JPCP		CRCP
	Nondoweled	Doweled	
>2,500	n/a – nondoweled design not recommended	Class 1	Class 1
1,500–2,500	n/a – nondoweled design not recommended	Class 1	Class 1
800–1,500	n/a – nondoweled design not recommended	Class 2, 3, or 4	Class 1
200–800	Class 2 or 3	Class 3 or 4	Class 2
<200	Class 4 or 5	Class 4 or 5	Class 3

SUMMARY AND DISCUSSIONS

The review of existing erosion test methods is summarized in Table 14. Key points such as generating erodibility index values, assessment of the strengths and weaknesses of testing approach including its relevance to field conditions are provided.

Table 14 Summary of Erosion Test Methods.

Test Method	Features	Strengths	Weaknesses
Rotational shear device	Stabilized test samples are eroded by application of hydraulic shear stress. The critical shear stress serves as an index of erosion resistance	Easy to control shear stress	Overestimation of weight loss by coarse aggregates loss
Jetting device	Pressurized water at an angle to the upper surface of unstabilized samples generating weight loss over time	-	Shear stress is not uniform and difficult to evaluate. Overestimation of weight loss by coarse aggregates loss
Brush test device	Rotational brush abrasions generate fines. An erosion index, IE is defined as the ratio of the weight loss to that of a reference material	Easy to setup. Test method considers durability under wet and dry cycles. Relative erodibility of each material is determined using an erosion index, IE	Test times are long and weight losses are overestimated due to displacement of coarse aggregates particles
Rolling wheel erosion test device	Wheel movements occur over a friction pad placed over a sample of the subbase material induces erosion. Average erosion depth is measured after 5,000 wheel load applications	Simulation of field conditions for flexible pavement structures	Voiding of the subbase under concrete slab cannot be considered

Table 15 is similar to Table 14 except it addresses the review of previous erosion models. The mechanistic model by Jeong and Zollinger (*12*) was found to be suitable for improvement based on its capability for calibration to the test results from the new lab test developed in this project (to be discussed in Chapter 3) and to available field.

Table 15 Summary of Erosion Models.

Erosion Model	Features	Strengths	Weaknesses
Rauhut model	Empirical model using COPES data	Includes many key erosion related factors	Key factors are overly generalized
Markow model	Empirical model using AASHO data: traffic, slab thickness, drainage	Considers detailed drainage conditions	Key subbase material properties are ignored
Larralde model	Empirical model using AASHO data: traffic, slab thickness	Normalized pumping index to eliminate the effect of slab length and reinforcement	Many key erosion related factors are missing from the model
Van Wijk model	Combination of Rauhut and Larralde models	Considers various erosion related factors and four types of climates	Key factors are overly generalized
PCA model	Mechanistic-empirical model using AASHO data	Significant advancement in the mechanistic analysis of faulting	Application of the model is limited to subbase types used in AASHO test
Jeong and Zollinger model	Mechanistic model using theoretical hydraulic shear stress	Predict erosion depth based on a feasible distress mechanism	Calibration required through lab tests and field performance data

According to the review of previous subbase design guides in Table 16, NCHRP 1-37A MEPDG presented some of the most comprehensive guidance with erodibility classes that was determined based on the dry condition brush and strength test results. However, erosion occurs mostly under saturated conditions, therefore, advanced guidance would establish criteria for subbase erosion based on wet condition test results for specific site materials. Moreover, all design factors in AASHTO and PCA design guides are void of specific material properties.

Table 16 Summary of Subbase Design Guides.

Design Guide	Features	Strengths	Weaknesses
TxDOT	Select one from two types of stabilized subbase and require minimum 7-day compressive strength	Historical performance and erosion resistance	Costly designs may be the result
1993 AASHTO	Based on a composite modulus of subgrade reaction that is adjusted for the loss of support due to the foundation erosion	Accounting structural degradation of support due to erosion using the LS factor	k-value obtained from the chart is over estimated and LS is insensitive to various stabilized materials
PCA	Provide erosion factor as a function of the slab thickness, composite k-value, dowel, and shoulder type	Consider erosion analysis in design procedures as the most critical distress in rigid pavement performance	Require more detail discrimination for different stabilization levels
NCHRP 1-37A MEPDG	Classified erodibility of subbase materials are utilized in JCP faulting prediction model as well as erosion under CRCP	Employed the erodibility class based on the type and level of stabilization along with compressive strength	Erodibility class is determined based on dry brush test results and strength even though erosion occurs mostly under saturated conditions

CHAPTER 3
SUBBASE EROSION

The slab deterioration process due to subbase erosion process can be classified simply into four steps: 1) back and forth abrasion or shearing action under load creating a layer of unbound, loosened material at the interface, 2) saturation, liquefaction and suspension of the loosened material, and 3) hydraulic transport of the suspended solids creating a void, and 4) accelerated slab deterioration due to the lack of support. After breaking of the interfacial bonding between the concrete slab and the subbase, the erosion process begins by either mechanical and/or hydraulic shearing of the subbase material. A low permeability subbase layer could reduce erosive action but when erosion starts, the permeability of the loosened material will be high enough to contribute to liquefaction and transportation. Table 17 shows a summary of items related to the erosion process.

Table 17 Mechanical Erosive Forces and Strength Factors.

Erosive Enablers	Erosive Resistors
Abrasion: Due to mechanical shear and hydraulic stress on interface between two layers or two aggregate particles due to friction.	**Interfacial Bonding:** The presence of interfacial bonding between two layers inhibits layer separation and promotes composite layer behavior that results in less deflection.
Liquefaction: Becomes saturated and subject to excessive pore water pressure and suction induced by traffic.	**Shear Strength:** The material characteristic that resists mechanical and hydraulic induced shear.
Hydraulic Transport: Movement of fine materials by pumping action and excessive pore water pressure.	**Permeability:** High permeability of subbase limits the development of pore pressure and liquefaction.

A new approach to erosion testing in order to assess a rate of erosion under mechanical abrasion is introduced in this chapter. Prior to doing so, a model for share strength at the slab/subbase interface is described in Equations 6 and 7. Stabilized subbase layers have cohesive

strength (due to degree of bonding, *x*) and frictional strength while unstabilized layers have only frictional shear strength at slab/subbase interface.

Stabilized subbase:

$$f_e = \chi \cdot c + (1 - \chi) N \tan\emptyset = \chi \cdot N\mu_c + (1 - \chi) N\mu_f \quad (6)$$

Unstabilized subbase:

$$f_e = N\mu_e = N\mu_f \quad (7)$$

where:

f_e = shear strength of slab/subbase interface under erosion, (FL^{-2})

χ = degree of partial bonding where 0=unbonded and 1=fully bonded

c = cohesion, (FL^{-2})

N = normal stress, (FL^{-2})

$\emptyset$ = angle of friction of the slab/subbase interface, (deg)

μ_c = coefficient of cohesion

μ_f = coefficient of friction

μ_e = coefficient of erosion

NEW METHOD OF EROSION TESTING

Researchers configured a new laboratory test procedure to determine the erodibility of subbase materials under both dry and saturated (or wet) conditions. A dry condition test configuration was formulated using the rapid tri-axial test (RaTT) and the wet condition test configuration was formulated using the Hamburg Wheel-Tracking Device (HWTD). Both tests consist of a two component layer system: one being concrete and the other the subbase material of interest such as a cement-treated or flexible (define abbreviation as Flex) subbase. Test devices and results are further summarized below; the HWTD test procedure is detailed in Appendix B.

Erosion Testing

The dry condition testing method is a mechanical abrasive erosion test using the RaTT where the load levels of σ_1 and σ_3 are controlled through a rubber bladder that provides a cyclic deviatory stress at specified levels, as shown in Figure 4. This configuration provides mechanical abrasion and compression under an 80 psi normal stress where weight loss occurs due to frictional erosion and shear fracture of the subbase material at the interface of the two layers. Various shear stresses and load repetitions are applied to evaluate the rate of erosion under dry conditions. Normal stress and shear stress is calculated using Equations 8 and 9.

$$\sigma_n = \frac{\sigma_1+\sigma_3}{2} + \frac{\sigma_1-\sigma_3}{2} cos2\phi \quad (8)$$

$$\tau = \frac{\sigma_1-\sigma_3}{2} sin2\phi \quad (9)$$

where:

σ_n = normal stress, (FL^{-2})

τ = shear stress, (FL^{-2})

σ_1 = Vertical principal stress, (FL^{-2})

σ_3 = Horizontal principal stress, (FL^{-2})

$\emptyset$ = angle of friction of the slab/subbase interface, (deg)

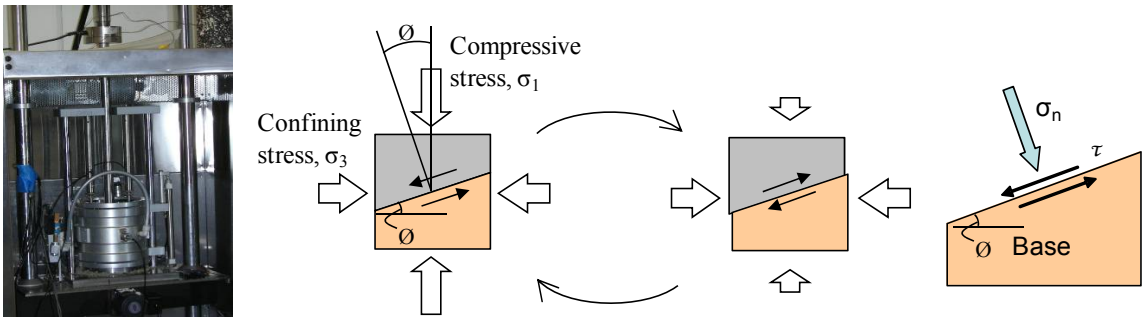

Figure 4 Schematic of Erosion Test Using RaTT Device.

The wet condition erosion test uses the HWTD since water is easily incorporated to transport abraded material due to mechanical and hydraulic shear generated by slab movement under an applied load at the erosion site on the surface of the base layer. The configuration of

the test device is the same as normally used with the HWTD except for the multi-layered sample shown in Figure 5. The test configuration consists of a 1 inch thick subbase material placed on a neoprene material below a 1 inch thick jointed concrete block (modification of the HWTD may allow for thicker slab layers). The test device allows for testing a laboratory compacted specimen or a core obtained from the field. A 158-lb wheel load is applied to the test samples at a 60 rpm load frequency up to 10,000 load repetitions under submerged condition at a temperature of 77°F. Measurements consist of the depth of erosion at 11 locations versus number of wheel load passes. In most cases, maximum deflection occurs at the measuring point number 5, 6, or 7. Shear stress can be calculated using Equation 10.

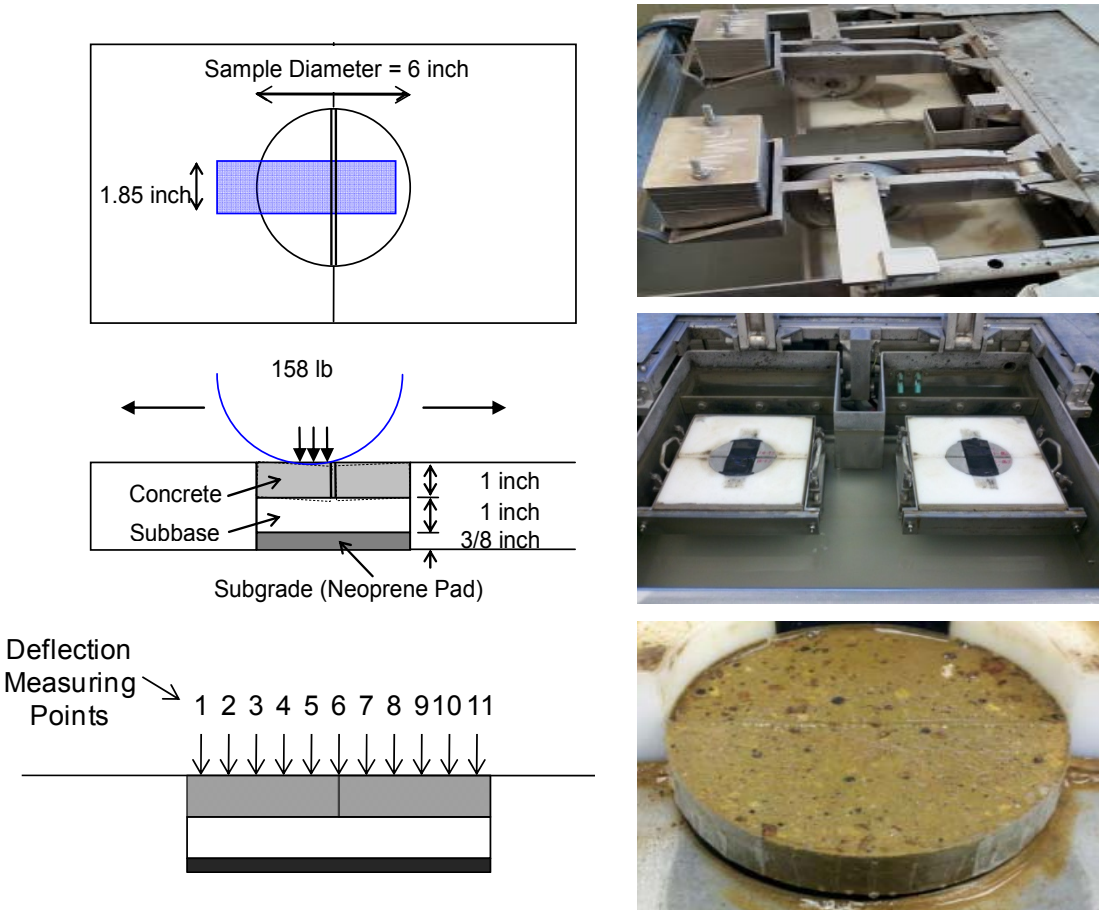

Figure 5 Erosion Test Using Hamburg Wheel-Tracking Device.

$$\tau = \mu N = (1 - \chi)\frac{\partial w}{\partial x}\left(\frac{E}{2(1+\nu)}\right) \quad (10)$$

where:

τ = shear stress, (FL^{-2})

μ = coefficient of friction of the slab/subbase interface

N = normal stress, (FL^{-2})

χ = degree of partial bonding where 0=unbonded and 1=fully bonded

$\frac{\partial w}{\partial x}$ = deflection rate under load between adjacent measuring points

E = elastic modulus of subbase material, (FL^{-2})

ν = Poisson's ratio of subbase material

Sample Preparation

The following three different sample types were selected for erosion testing. All samples were sieved according to the TxDOT standard and American Society of Testing Materials (ASTM), as shown in Table 18. Sieved materials are stabilized with different binder contents (0, 2, 4, and 6 percent cement) at optimum moisture content by weight:

- Flex sample–limestone base material (from the Bryan District);
- Recycled concrete (RC) sample–recycled crushed concrete; and
- RAP sample–30 percent RAP + base material (shell/dark soil) (from the Beaumont District).

All samples were prepared according to the test method "Tex-120-E, Soil-Cement Testing" and compacted according to the test method "Tex-113-E, Laboratory Compaction Characteristics and Moisture-density Relationship of Base Materials," using a 10-lb hammer, with an 18 inch drop, at 50 blows/layer in a 6 × 6 inch mold (with 5 inch disk insertion). All samples were cured more than 90 days (28 days will be the recommended time limit for curing cement stabilized samples) under 100 percent relative humidity conditions except for the untreated (0 percent cement treated) samples.

Table 18 Sieves for Aggregate Size Analysis.

Sieve Number	Sieve Size (in.)	Sieve Size (mm)
1 1/2	1.5	38
3/4	0.75	19
3/8	0.375	9.5
# 4	0.187	4.76
# 10	0.0787	2.0
# 40	0.0165	0.42
# 100	0.0059	0.149
# 200	0.0029	0.074

Erosion Test Results Using RATT Device

The 3 percent cement-treated base materials were tested with the RaTT device as pilot samples to examine the effects of shear stress and load repetition under dry conditions in which weight loss occurs due to frictional abrasion and compressive fracture of exposed material on the surface. The aggregate size distributions of the samples varied to some extent, as shown in Figure 6; the Flex and RC grading met the requirements of ASTM D 2940-03 but the RAP material grading consisted of an oversized distribution containing more fines than other materials. Test samples are dried 24 hours under dry conditions (humidity 30 percent and temperature 104°F) and cooled for 12 hours in room temperature before RaTT testing was carried out.

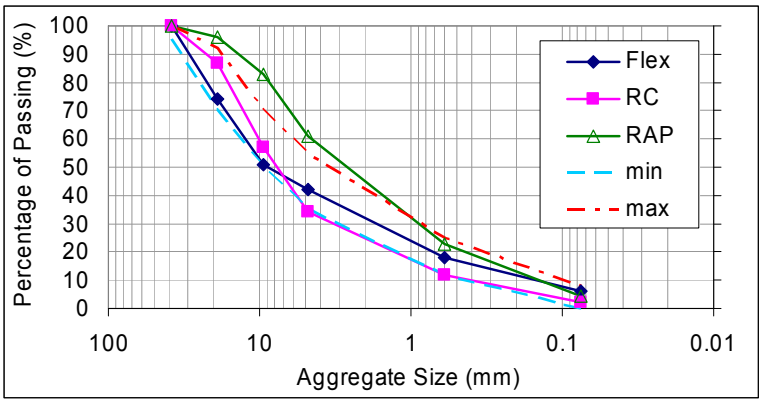

Figure 6 Aggregate Size Distributions of RaTT Erosion Test Samples.

Figure 7 shows the measured weight loss of abraded fines on the surface of the testing sample after 1,000 RaTT test load repetitions under various shear stress levels: 17, 25, 34, 42, and 50 psi. As expected, the greater the shear stress was the greater the weight loss. However, the rate of weight loss dropped off to some extent at higher stress levels—presumably due to a buildup of loose material on the interface, effectively reducing the interlayer coefficient of friction. RAP base samples experienced a greater weight loss than the RC base because of a higher fine content. It is clear the aggregate size distribution on surface affects the rate of abrasive erosion significantly under dry test conditions.

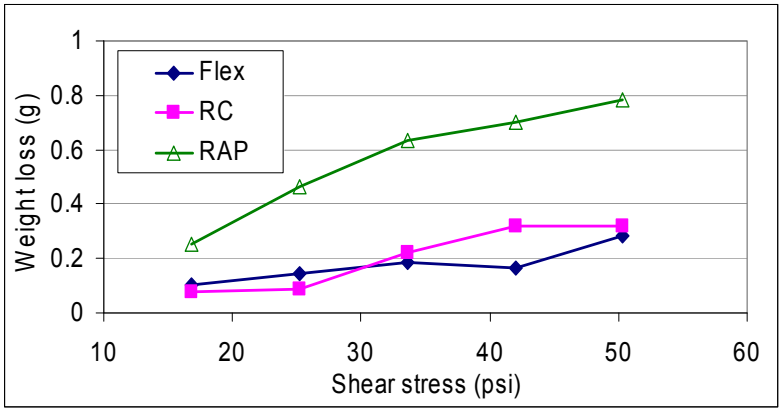

Figure 7 Weight Loss versus Various Levels of Shear Stress during RaTT Testing.

Figure 8 shows the effect of the number of loadings with a shear stress of 34 psi. Weight loss increased with loading repetition but the rate again diminished after 3,000 load repetitions. The one possible reason is the amount of generated fines causes a reduction in shear stress at the interface of the two layers. To minimize the effect of the accumulated fines on the induced shear stress, periodic cleaning of the interface was conducted as would take place under pumping action. The spikes in the results (Flex and RAP 3,000 repetition and RC 5,000 repetition) were caused by removal of large-sized aggregate in the mixture relative to other generated fines.

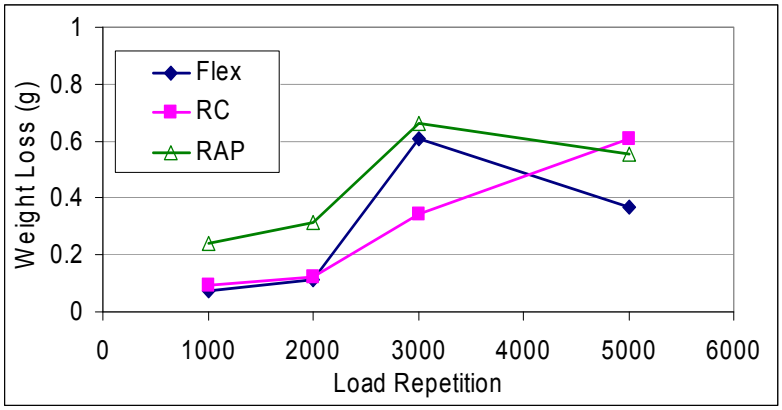

Figure 8 Weight Loss versus Various Number of Loading by RaTT.

Test for Maximum Aggregate Size Selection

Weight losses were deemed too small to allow use of the RaTT device in a practical test; for this reason, RaTT test was not given further consideration. Consequently, the HWTD test method appears to be a better choice for an erosion test method. In the discussion of the previous test results, it was noted that erosion testing was affected by the fineness of the gradation. Test results indicated a bias when layer particles were displaced during testing. Erosion samples should be prepared with fine gradations (i.e., aggregate size less than sieve number 40 [0.0165 in.]) as to be a better representation of a materials sensitivity to erosion.

Therefore, grading should be a factor for all subbase material types relative to the weight loss determinations. Figure 9 shows various grading distributions relative to the maximum aggregate size to maintain an allowable level of testing error due to the exposure of the larger aggregate sizes at the wearing surface.

Test materials were carefully graded in light of the sample thickness (1 inch) used for testing to limit the maximum aggregate size; with this respect, 4 different cases were considered: 0.8 inch, 0.4 inch, 0.2 inch, and 0.08 inch (20 mm, 10 mm, 5 mm, and 2 mm, respectively). Also, other aggregate size distributions were adjusted to achieve a similar sample density while keeping the percentage of fines (less than 0.006 inch [No. 100] sieve size) the same.

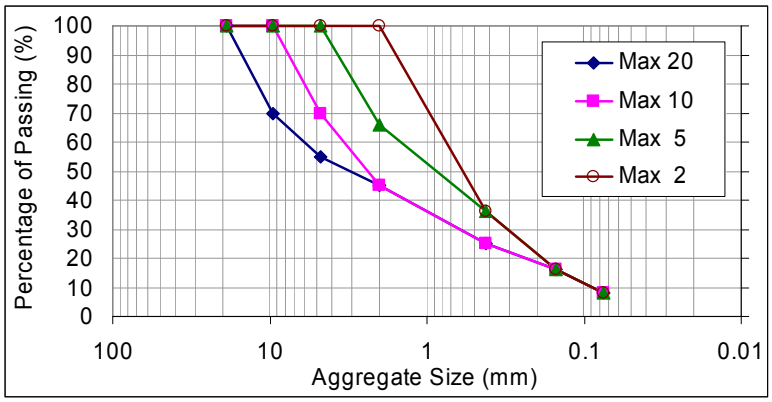

Figure 9 Aggregate Size Distributions of Erosion Test Samples.

Figure 10 shows the effect of different maximum aggregate size on aggregate gradation. There is no significant difference in the rate of erosion between Max 20, Max 5, and Max 10 gradation; while the erodibility of the Max 2 gradation is, comparatively speaking, excessive. Accordingly, the Max 5 gradation could be considered an optimum grading for erosion resistance due to improved grading and uniformity at the surface that contributes to reduced irregularity and due to the aggregate size distribution.

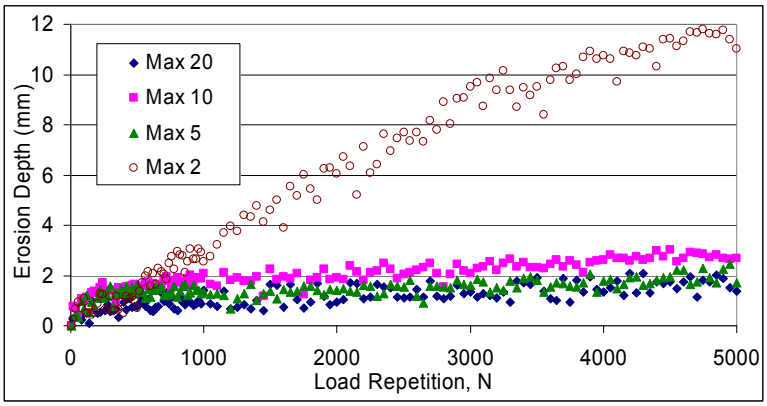

Figure 10 Erosion versus Number of Loading by HWTD Test.

Erosion Test Using HWTD

Based on the effect of aggregate grading, the samples for cement-treated base materials followed the Max 5 aggregate size distribution. Figure 11 shows the RaTT results of cement-treated samples where the erosion rate decreased with greater cement content. By the change in the aggregate size distribution from the grading shown in Figure 6, test results show a different erosion rate for each sample type. RC base shows the highest erosion rate, and the RAP base

shows the least erosion rate under dry conditions while maintaining the fine-size aggregate fraction is constant (i.e., 16 percent or less passing the 0.006 inch [0.15 mm], No.100 sieve size) since the amount of asphalt mastic increases shear strength.

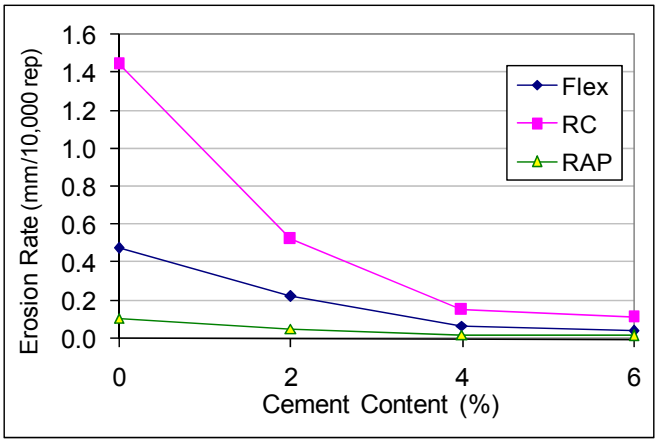

Figure 11 Erosion versus Change of Cement Percentage by RaTT.

HWTD test results after 10,000 load repetitions shown in Figure 12 indicate as the percentage of cement increases the erosion depth decreases. Two percent cement for Flex and RAP subbases, however, does not reduce the erosion depth significantly, but 4 percent cement reduces erosion remarkably when compared with unstabilized materials.

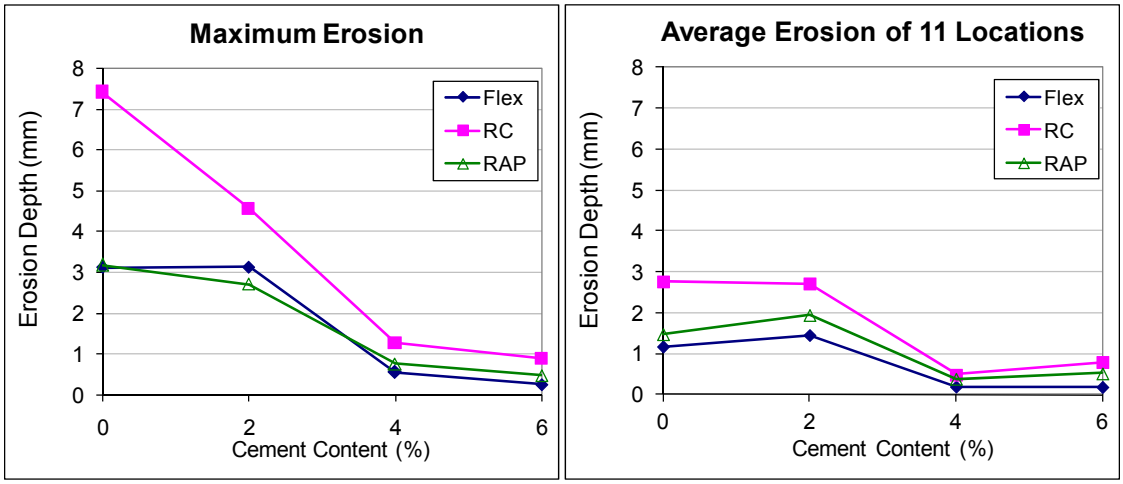

Figure 12 Erosion Depth Changes of HWTD Erosion Test due to Cement Percentage Modification.

Figure 13 shows the maximum erosion depth and Figure 14 shows the average of 11 erosion depths across the sample erosion profile relative to HWTD load repetition. Erosion occurred rapidly from the start of the test but its rate decreased as the void deepened since the sample was saturated, and the hydraulic shear was higher when the void between concrete and sample was smaller. (Phu and Ray [*20*] indicated [at a constant slab deflection speed] that if the void is larger than 0.04 inch [1 mm] the rate of erosion will diminish with an increase in void depth.) Test results show a fluctuation of erosion depth with the number of loading most likely due to relatively large aggregates being dislocated by pumping action while small fines are more uniform hydraulically transported through the joint.

The dry and wet conditions under which the RaTT and HWTD erosion tests were conducted represent free edge conditions (i.e., no load transfer). However, separation between the slab and the base must occur for sufficient pumping action to initiate erosion (over dry and wet periods). In design, the calculated erosion depth should therefore be weighted over dry and wet performance periods as well as load magnitude and applied interfacial shear. Moreover, local conditions in design such as frequency of joint sealing maintenance, changes in drainage conditions, and annual precipitation also are important to assure erosion depth.

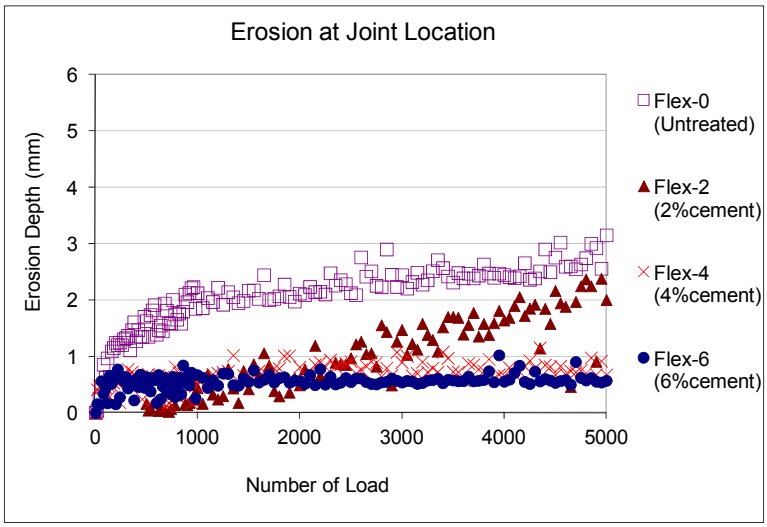

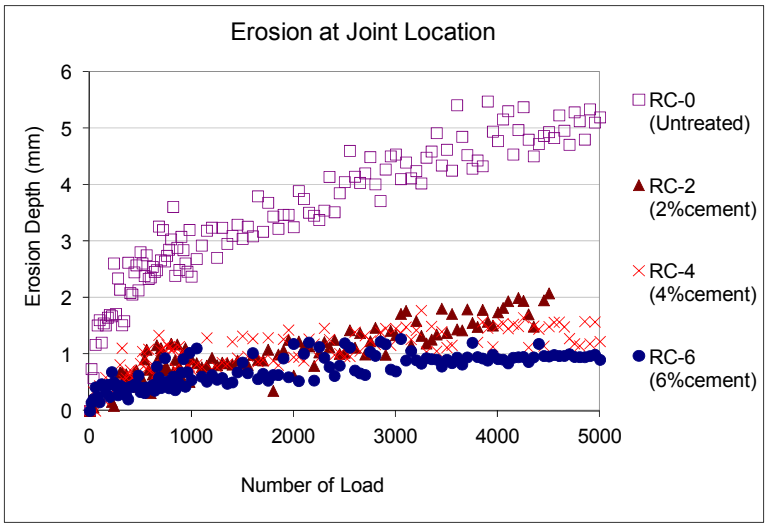

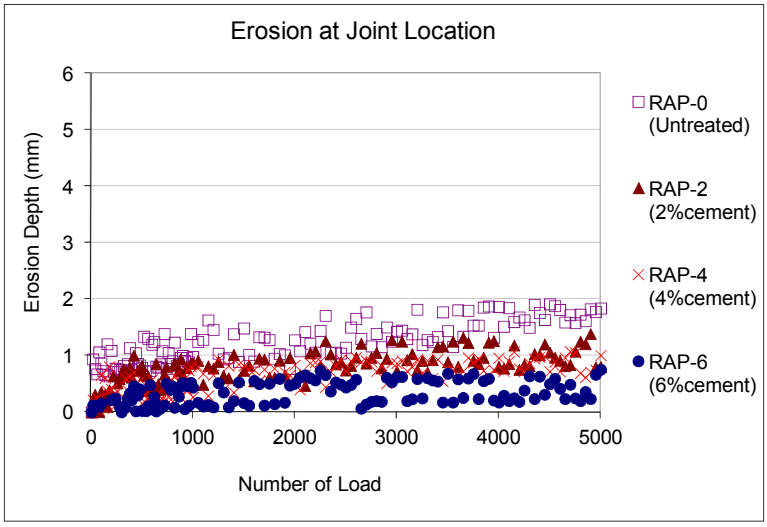

Figure 13 Maximum Erosion Depth at Joint Location versus Number of Load by HWTD Test.

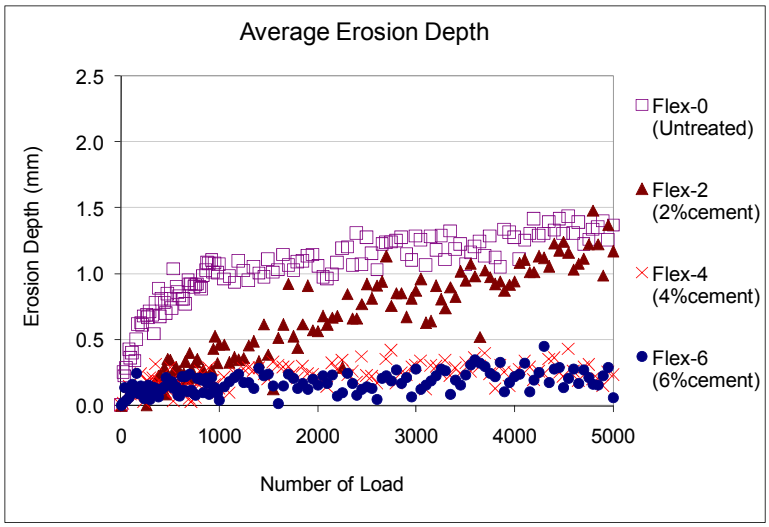

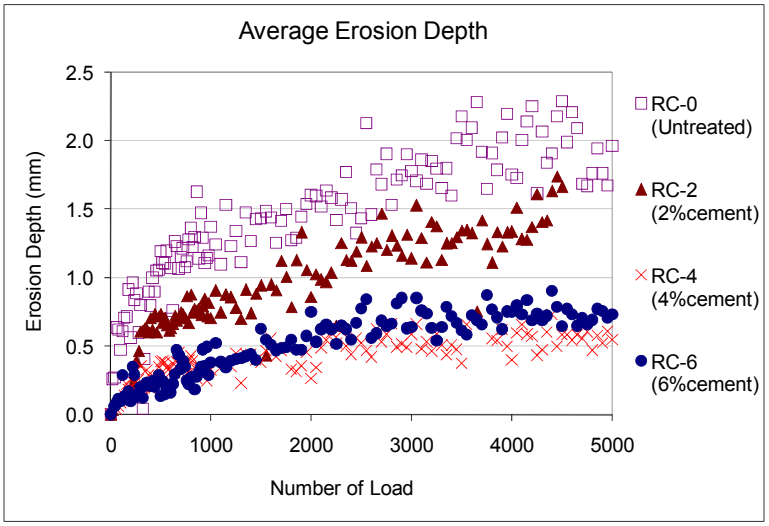

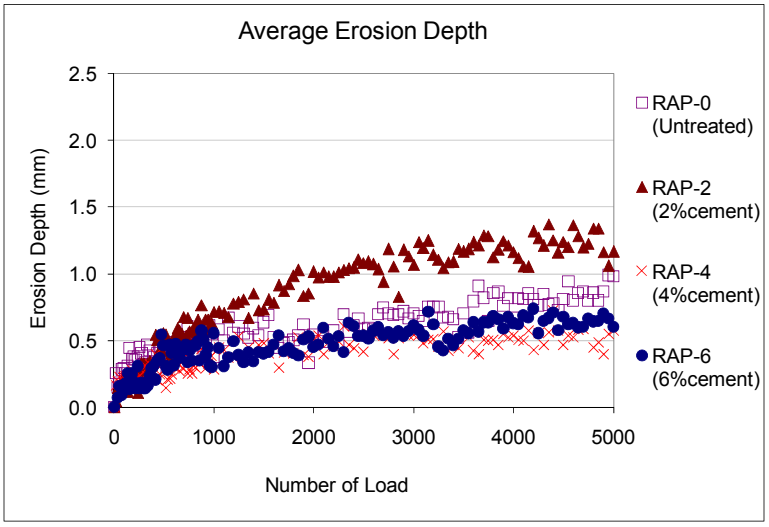

Figure 14 Mean Erosion Depth of 11 Measuring Spots versus Number of Load by HWTD Test.

EROSION MODEL DEVELOPMENT

A mechanistic empirical model for subbase erosion (Equation 11) was proposed by Jeong and Zollinger based on the work of Van Wijk and Phu and Ray (*7, 12, 20*). Figure 15 conceptually illustrates slab movement under load at a transverse (jointed concrete) or along a longitudinal (CRC) joint and the induced shearing action along the slab/subbase interface that mechanically creates a loose layer of subbase material. This layer of material is readily saturated and liquefied in the presence of water. Hydraulically induced shear stresses in this liquefied layer are developed as a function of the slab movement, vehicle speed, and ambient temperature as well as the stiffness of the crack or joint, which are represented in the subsequently discussed performance model.

Transport potential increases with higher initial edge gaps and liftoff distances due to the effect of upward curling along slab corners and edges inducing hydraulic shear stress at the surface of the base layer by pumping of trapped water. The magnitude of hydraulic shear stress depends on the dynamic viscosity of water governed by water temperature and the speed of slab deflection. Greater slab deflection velocity and lower viscosity of water result in greater transportation of fines, while better load transfer reduces the deflection velocity as represented in the performance equation.

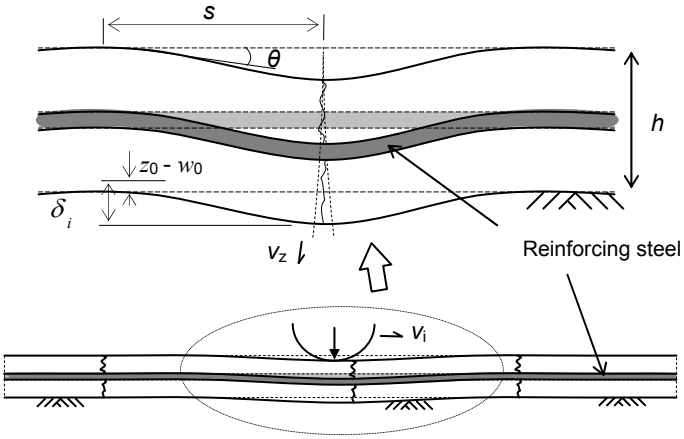

Figure 15 Slab Configuration of Erosion Modeling.

$$f_i = f_0 e^{-\left(\frac{\rho}{N_i - N_e}\right)^a} \quad (11)$$

where:

f_i = erosion depth, (L)

f_0 = ultimate erosion depth, (L)

ρ = calibration erosion coefficient based on local performance

N_i = number of axle loads contributing to erosion

N_e = calibration coefficient represents the number of wheel loads (or time) to occur layer debonding of the slab and subbase and to initiate erosion, 0 for lab test

a = composite calibration rate coefficient based on field and laboratory performance

$= \alpha' \alpha_f$

α' = calibration rate coefficient based on local performance

α_f = laboratory determined rate of void development

$$= \left[\frac{\partial f_i}{\partial t}\right] = \left[\frac{\partial f_i}{\partial N}\frac{\partial N}{\partial t}\right] = \left[\frac{Log^{-1}(a_m \tau_i + b_m)}{\gamma_b}\right]$$

$\frac{\partial f_i}{\partial t}$ = rate of erosion from laboratory testing = $(1-x)\frac{\partial f_{i-dry}}{\partial N} + x\frac{\partial f_{i-wet}}{\partial N}$

x = percent of saturated time on the interface between subbase and slab–determine by calibration

$\frac{\partial N}{\partial t}$ = equivalent traffic rate = $\frac{\partial}{\partial t}[EWF \cdot \sum\{EAF \cdot \sum(ELF \cdot n)\}]$

N = number of design traffic

EWF = equivalent wandering factor = $e^{(a+b\sqrt{t}+c\cdot LTE^{1.5})}$

$a = -0.0017D^2 - 0.0948D + 5.2251$,

$b = 0.0002D^2 - 0.0113D - 1.221$,

$c = -2\times10^{-7}D^2 - 2\times10^{-5}D - 0.003$,

D = distance to outside wheel path from the edge of pavement

EAF = equivalent axle factor = $\frac{DE_{i-axle}}{DE_{18\ kip-single\ axle}}$

ELF = equivalent load factor = $\frac{DE_{i-load}}{DE_{18\ kip-load}}$

n = number of load

ℓ = radius of relative stiffness, (L) = $\sqrt[4]{\frac{Eh^3}{12(1-\nu^2)k}}$

h = PCC slab thickness, (L)

k = modulus of sub-layer reaction, (FL^{-3})

LTE_i = joint or crack load transfer efficiency (%) and is subject to wear out or dowel degradation

$$= \frac{1}{1+\log^{-1}\left[0.214-0.183\left(\frac{r}{\ell}\right)-\log(J_i)\Big/1.180\right]}$$

J_i = total joint stiffness = $J_S + J_{AI}$

J_S = joint stiffness of reinforcing steel

J_{AI} = joint stiffness of aggregate interlock

r = loaded radius, (L)

τ_i = interfacial shear stress, (FL^{-2}) = $\tau_{i\text{-}fri} + \tau_{i\text{-}hyd}$

$\tau_{i\text{-}fri}$ = interfacial frictional shear stress, (FL^{-2}) = $\mu\left(\frac{h}{12}+\frac{DE_i}{\delta_i}\right)$

μ = coefficient of friction of sub-layer

DE_i = deformation energy, (FL^{-2}) = $\frac{k}{2}\delta_i^2\left\{1-\left(\frac{LTE_i}{100}\right)^2\right\}$

δ_i = loaded slab deflection, (L) = $\delta_{void} + w_{LTE} + z_0 - w_0$

w_{LTE} = slab deflection with load transfer, (L)

$$= \frac{P_i}{k\ell(1+\frac{LTE_i}{100})}\left\{1.1-0.88\left(\frac{r\sqrt{2}}{\ell}\right)\right\}$$

P_i = axle load, (F)

s = slab liftoff distance, (L) = $\sqrt{2}\ell\left[\sqrt{\frac{z_0}{w_0}}-1\right]$

z_0 = edge gap, (L) = $\frac{(1+\nu)}{h}\Delta\varepsilon_{tot}\ell^2$

$\Delta\varepsilon_{tot}$ = total strain due to moisture and temperature gradient

w_0 = deflection of slab by self weight, (L)= $\frac{\rho h}{k}$

ρ = density of concrete, (FL^{-3})

$\tau_{i\text{-}hyd}$ = interfacial hydraulic shear stress, (FL^{-2}) = $\frac{\eta B_i}{\delta_{void}}\left(1-\left(\frac{LTE_i}{100}\right)^2\right)$

η = dynamic viscosity of water, ($FL^{-2}t$)

$= \left\{2056.82 + 10.56T - 284.93\sqrt{T} - 265.02e^{-T}\right\}10^{-6}$

T = water temperature, (°C)

$B_i = V_{z_i}\sin\theta + 6V_{z_i}\left[\frac{\sin\theta}{2} + \frac{\cos^2\theta}{\sin\theta}\right]$, ($Lt^{-1}$)

V_{z_i} = slab deflection velocity, (LT^{-1}) = $\frac{\delta_{total}}{s/V_i}$

V_i = vehicle speed, (LT^{-1})

θ = slab angle, (rad) = $\tan^{-1}\left[\frac{z_0}{s}\right]$

δ_{void} = void space below slab for water movement, (L)

The advantage of this model is its capability of translating the laboratory test results to any layer combination or thickness in the field based on the resulting deflection. In order to validate the proposed erosion model, HWTD test results have been used to obtain a and ρ that are governed by material type and the percentage of cement treatment facilitated by the following development (Equations 12 and 13):

$$\frac{f_i}{f_0} = e^{-\left(\frac{\rho}{N_i}\right)^a} \tag{12}$$

$$\ln f_i = \ln f_0 - \left(\frac{\rho}{N_i}\right)^a \tag{13}$$

Taking the derivative of Equation 13 with respect to N_i:

$$\frac{\partial \ln f_i}{\partial N_i} = \frac{\partial \ln f_i}{\partial f_i} \cdot \frac{\partial f_i}{\partial N_i} = \frac{1}{f_i} \frac{\partial f_i}{\partial N_i} \tag{14}$$

Combining Equation 13 and Equation 14:

$$\frac{\partial f_i}{\partial N_i} \cdot \frac{1}{f_i} = \frac{\partial \left(\ln f_0 - \left(\frac{\rho}{N_i} \right)^a \right)}{\partial N_i} \tag{15}$$

Since f_0 is assumed to also be a material parameter, its derivative with respect to N_i is assumed to be zero. Hence, Equation 15 is converted as:

$$\frac{\partial f_i}{\partial N_i} \cdot \frac{1}{f_i} = \frac{\partial \left(-\left(\frac{\rho}{N_i} \right)^a \right)}{\partial N_i} = a \cdot \left(\frac{\rho}{N_i} \right)^{a-1} \frac{\rho}{N_i^2} = a \cdot \left(\frac{\rho}{N_i} \right)^a \frac{1}{N_i} \tag{16}$$

$$\left(\frac{N_i}{f_i} \left(\frac{\partial f}{\partial N} \right)_i \right) = \left(\frac{\partial f / f_i}{\partial N / N_i} \right) = \frac{a \rho^a}{N_i^a} \tag{17}$$

Taking logarithm for both sides of Equation 17, we get:

$$\ln \left(\frac{\partial f / f_i}{\partial N / N_i} \right) = \ln \left(\frac{\partial \ln f_i}{\partial \ln N_i} \right) = \ln a \rho^a - a \ln N_i \tag{18}$$

Considering Equation 18 to be in the form of $y = mx + b$, $-a$ is the slope m of values of $x = \ln N_i$ plotted against values of $y = \ln \left(\frac{\partial \ln f_i}{\partial \ln N_i} \right)$, and $\ln a \rho^a$ is the intercept b. The slope and intercept from linear regression analysis of the test data are used as Equation 19 and Equation 20 to determine a and ρ.

$$a = -m \tag{19}$$

$$\rho = e^{\frac{b - \ln a}{a}} \tag{20}$$

Once ρ is defined, it is advantageous to determine the coefficients a_m and b_m of ρ_o since:

$$a_f = \frac{10^{a_m \tau_i + b_m}}{\gamma_b} \tag{21}$$

$$\log a_f = a_m \tau_i + b_m - \log \gamma_b \tag{22}$$

If the above expression is in the form of $y = mx + b$, a_m is the slope m of values of $x = \tau_i$ plotted against values of $y = \log a_f$, and $b_m - \log \gamma_b$ is the intercept b. Therefore, a_m and b_m are similar to Equation 23 and Equation 24.

$$a_m = m \tag{23}$$

$$b_m = b + \log \gamma_b \tag{24}$$

f_0 can be found by averaging multiple values from Equation 12 above.

Figure 16 shows an example plot to estimate *a* and *ρ* from slope and intercept of the linearly regressed lines for HWTD test results.

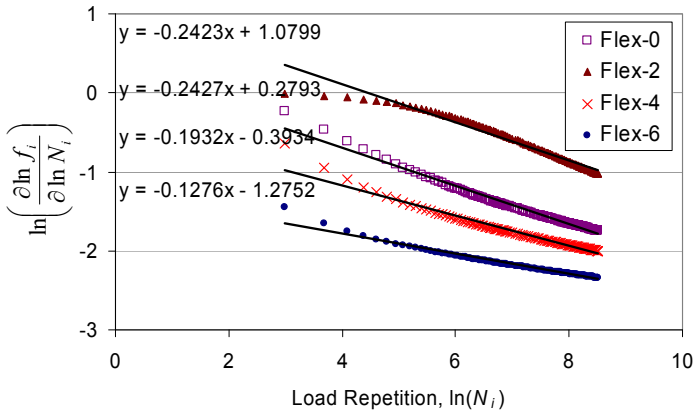

Figure 16 Log Plot to Acquire *a* and *ρ* from HWTD Test.

Figure 17 shows the comparison of the model predictions (lines) versus the HWTD test results (dots). The erosion model shows a similar trend with test data.

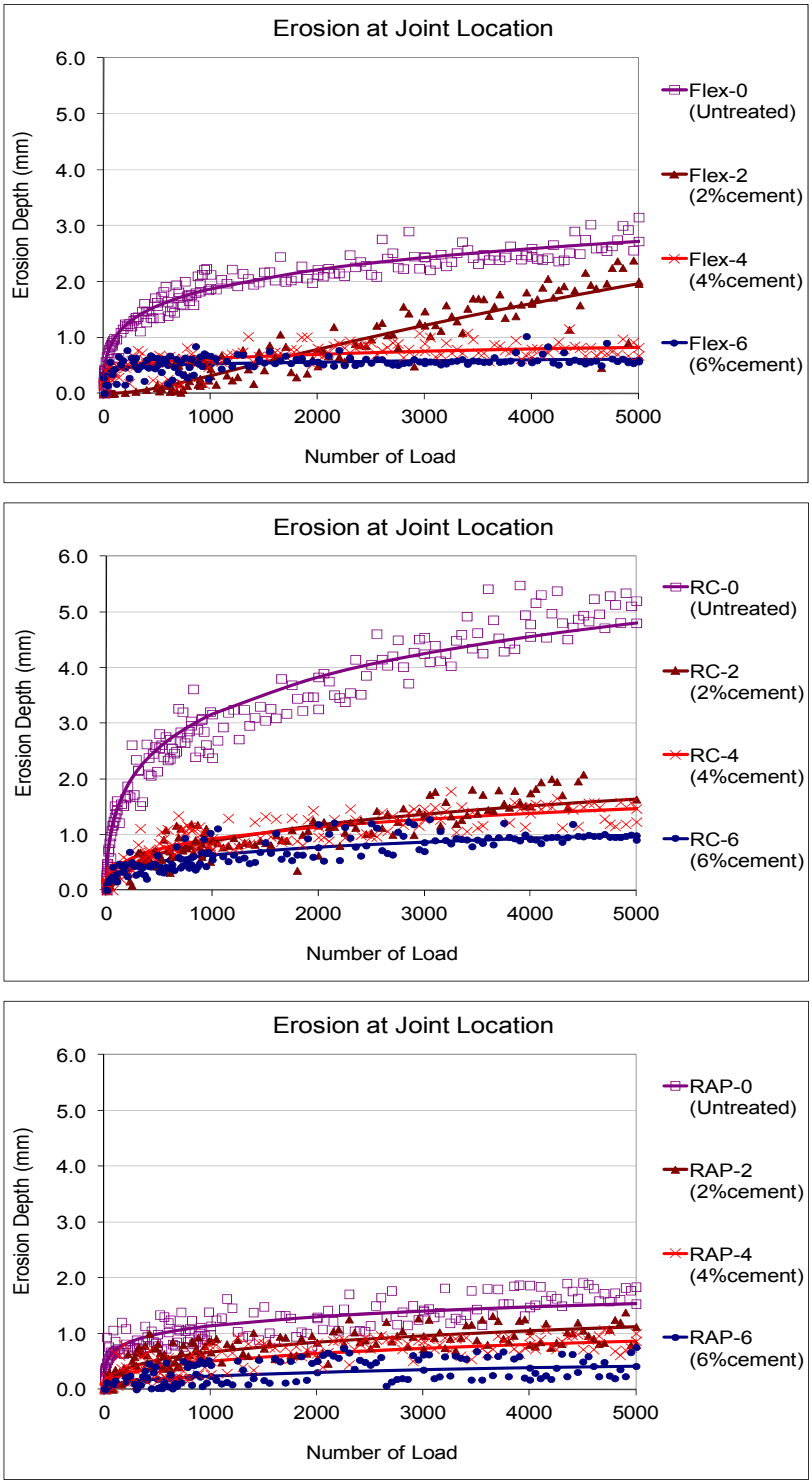

Figure 17 Erosion Model Fitting to HWTD Test Results.

The data in Figure 18 show the correlation between observed and model fitted erosion depth of all test materials. The closer the data plots are to a diagonal line, the better the fit of the model to the test data. An R-squared value of 93 percent indicates a good fit of the test data. The underestimated erosion near the maximum erosion is perhaps due to increasing shear conditions in the laboratory test apparatus. Fluctuation in the measured data due to irregular movements due to erosion below the concrete cap may also induce divergence in the test data.

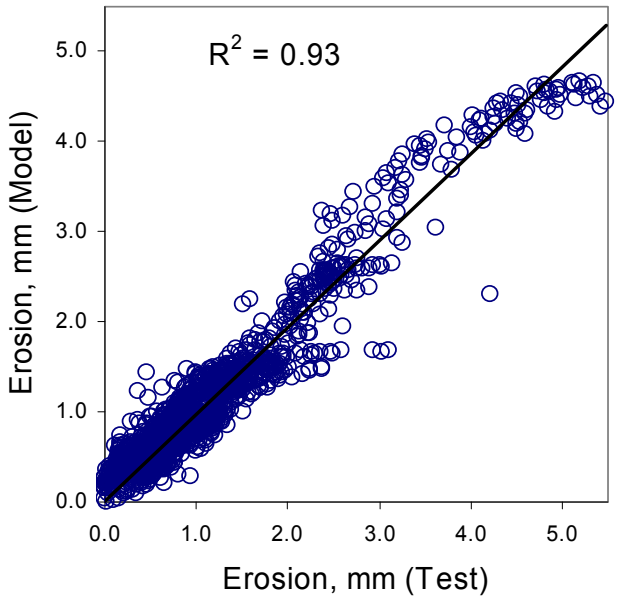

Figure 18 Model Fitted Erosion versus Measured Erosion from HWTD Test.

A paired t-test analysis was conducted to validate proposed erosion model at a confidence level of 95 percent based on the null hypothesis of no difference between the means of observed erosion and model fitted erosion depth. Table 19 shows the results of the p-value are greater than 0.05, which indicates there is statistically no difference between measured and fitted values.

Table 19 Results of Paired T-test Statistic on Measured and Modeled Erosion.

Statistical Quantity	Test Results	Model
Mean	1.13	1.13
Variance	0.95	0.85
Observations	1527	1527
Pearson Correlation	0.97	
Hypothesized Mean Difference	0.00	
df	1526	
t Stat	0.78	
P(T<=t) one-tail	0.22	
t Critical one-tail	1.65	
P(T<=t) two-tail	0.44	
t Critical two-tail	1.96	

CHAPTER 4
SUBBASE PERFORMANCE FACTORS

A variety of materials have been used in subbase layers over the years. Specifically, hot mixed asphalt material has been widely used as a subbase layer material for PCC pavements. However, it has been recently realized that the use of the asphalt material in subbase layers has unduly increased construction cost. For these reasons, this study has focused on the assessment of design and performance implications related to the use of alternative subbase materials instead of hot mixed asphalt concrete.

To evaluate the structural aspects of subbase performance, three variables including subbase friction, stiffness, and erosion are considered. The first two variables are key to the overall composite stiffness of the pavement section to resist load stress and deflection. Moreover, finite element analysis in the form of selected pavement analysis programs is used to validate structural responses of a PCC slab in terms of these parameters.

Friction at the interface between a concrete slab and subbase plays a role in resisting slab deflection. This resistance also induces a certain level of horizontally oriented tensile stress in concrete slab and contributes, for instance, to development of the cracking pattern in CRC pavement. Also, the width of these cracks may affect LTE in these types of pavement as well as punchout potential. Therefore, frictional characteristics are one of the key subbase factors for assessing the performance of a concrete pavement system.

Subbase support stiffness is another important factor to evaluate performance. The thicker and stiffer subbase layer will have greater load-carrying capacity of the slab. However, disadvantages arise with respect to temperature and moisture-induced slab deformation and stress. Curling and warping of a CRC pavement slab segment tends to increase transverse design stresses, which are enhanced due to the stiffness of the subbase support. Although higher k-values reduce load-induced deflection and stress, a high k-value support system promotes greater environmentally induced stress possibly leading to a greater incidence of longitudinal cracking potential as a contributor to punchout potential.

Erosion could be the most important of all factors related to subbase performance effects relative to the continuity of the slab support. Erosion-related loss of support along pavement shoulder and longitudinal joint areas has been identified as a key factor in the development of punchout distress in CRC pavement systems. Erosion plays a prominent role in the punchout

process since it directly impacts shear stress on the face of transverse cracks where interlocking of the exposed aggregate transfers load between adjacent slab segments. Increase in shear stress due to the loss of support will increase the rate of aggregate wear out that ultimately leads to lower load transfer and increased lateral bending stress. However, as long as support conditions can be maintained and wear out of aggregate interlock minimized, bending stresses in CRC pavement systems will be relatively small, which results, for all practical purposes, in an infinitely long fatigue life. Otherwise, it is critical in the design stage to account for less than full support conditions in slab areas where erosion has a potential of occurring.

EVALUATION OF SUBBASE FRICTION, STIFFNESS, AND EROSION

The determination of the proper computer programs to assess selected subbase parameters included CRCP-10, ISLAB 2000, and the MEPDG software. These programs are based on the finite element analysis (FEA) method and can be used to varying degrees to assess the effects of the above parameters on performance.

Subbase Friction

To evaluate effects of subbase friction, the CRCP-10 computer program was used. This program is useful for modeling a crack development in a CRC pavement, but also for analyzing long-term performance including mean crack spacing, mean crack width, steel stress, and punchout performances.

Table 20 shows geometry input values, which were used in this analysis. Also, the range of subgrade reaction modulus value changed from 100 psi/inch to 800 psi/inch.

Table 20 Input Values.

Thickness	10 inches
Elastic Modulus	4.56×10^6 psi
Poisson's Ratio	0.15
Aggregate	SRG
Unit Weight	150 pcf
Steel Ratio	0.6

To consider frictional effects between the concrete slab and the subbase, the concept of friction stiffness was introduced. Figure 19 shows the concept of friction stiffness. When pushing the concrete slab horizontally, the measured slope of frictional resistance (psi) and horizontal movement of the slab (inch) is presented as frictional stiffness, which has units of psi/inch. CRCP-10 computer program provides typical frictional stiffness values corresponding to various subbase types. Table 21 presents the typical frictional stiffness values provided by CRCP-10.

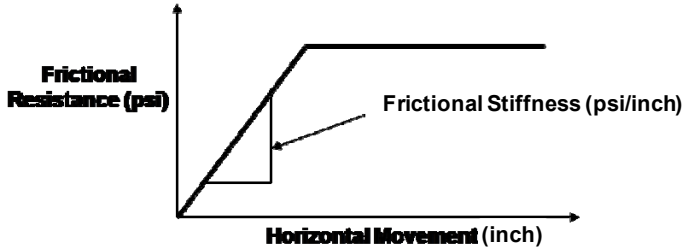

Figure 19 Concept of Friction Stiffness.

Table 21 Frictional Stiffness Values.

Subbase Type	Frictional Stiffness (psi/inch)
Flexible	145.5
Asphalt-Stabilized	55.9
Cement-Stabilized	15,400
Lime-Treated Clay	154.5
Untreated Clay	22

In this analysis the modulus of subgrade reaction value was fixed at 500 psi/inch and various friction stiffness values were employed (ranging from 50 psi/inch to 10,000 psi/inch) to study the effect of subbase friction level. Figure 20 and Figure 21 show the results of the frictional analysis with respect to the mean crack spacing, mean crack width, steel stress, and punchout performance. As shown in Figure 20, mean crack spacing and mean crack width decrease as frictional stiffness increases. More cracks would be generated under high friction conditions because of friction-induced restraint at the interface between a concrete slab and the underlying subbase resisting movement of the concrete slab, and thus leading to high tensile

stress in the concrete slab. Also, with more cracks, the steel stress at crack is redistributed and reduced because strains at cracks are smaller. Finally, the predicted amount of punchout distress generally increases as the frictional resistance increases because the mean crack spacing is relatively shorter increasing the probability of punchout (which again ignores the effect of crack width on load transfer).

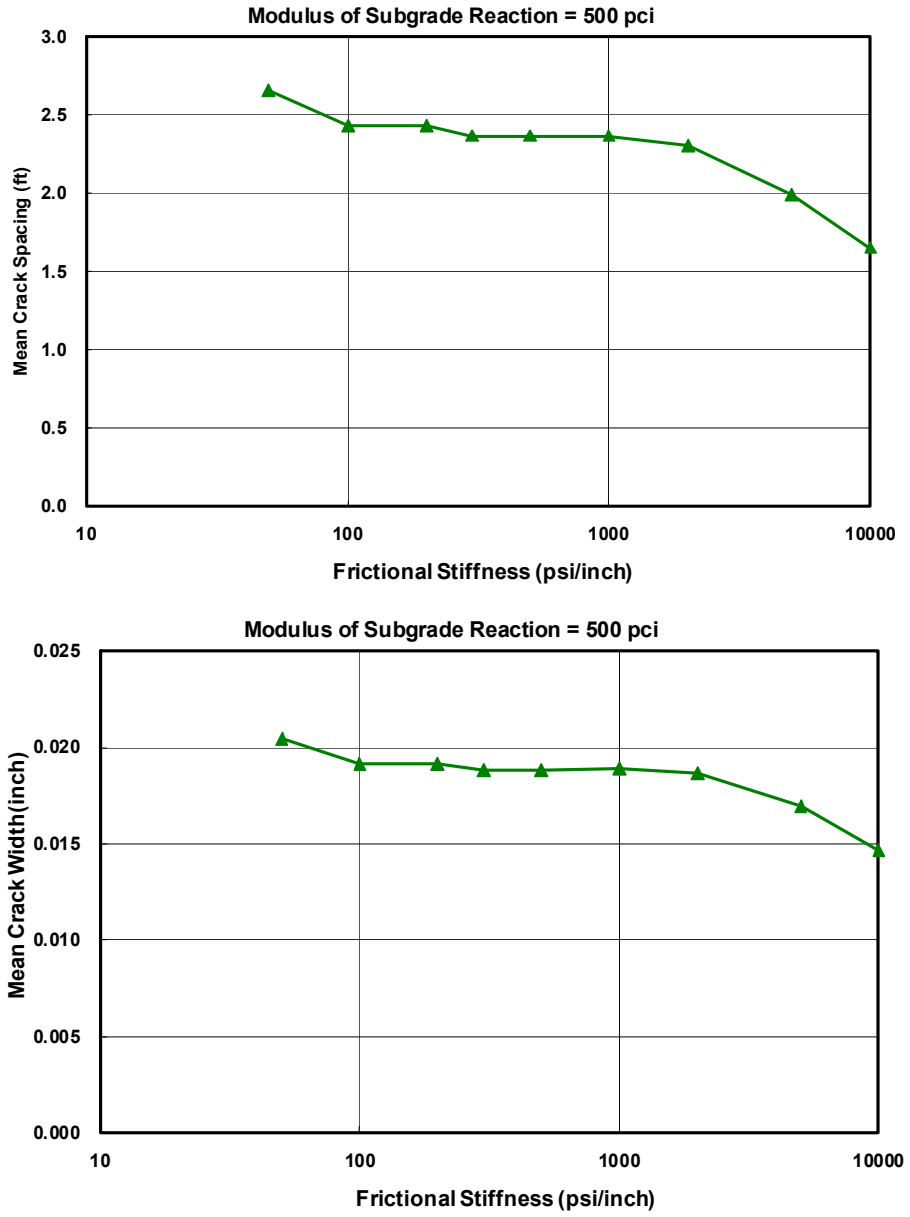

Figure 20 Analysis of Frictional Effects: Crack Width and Spacing.

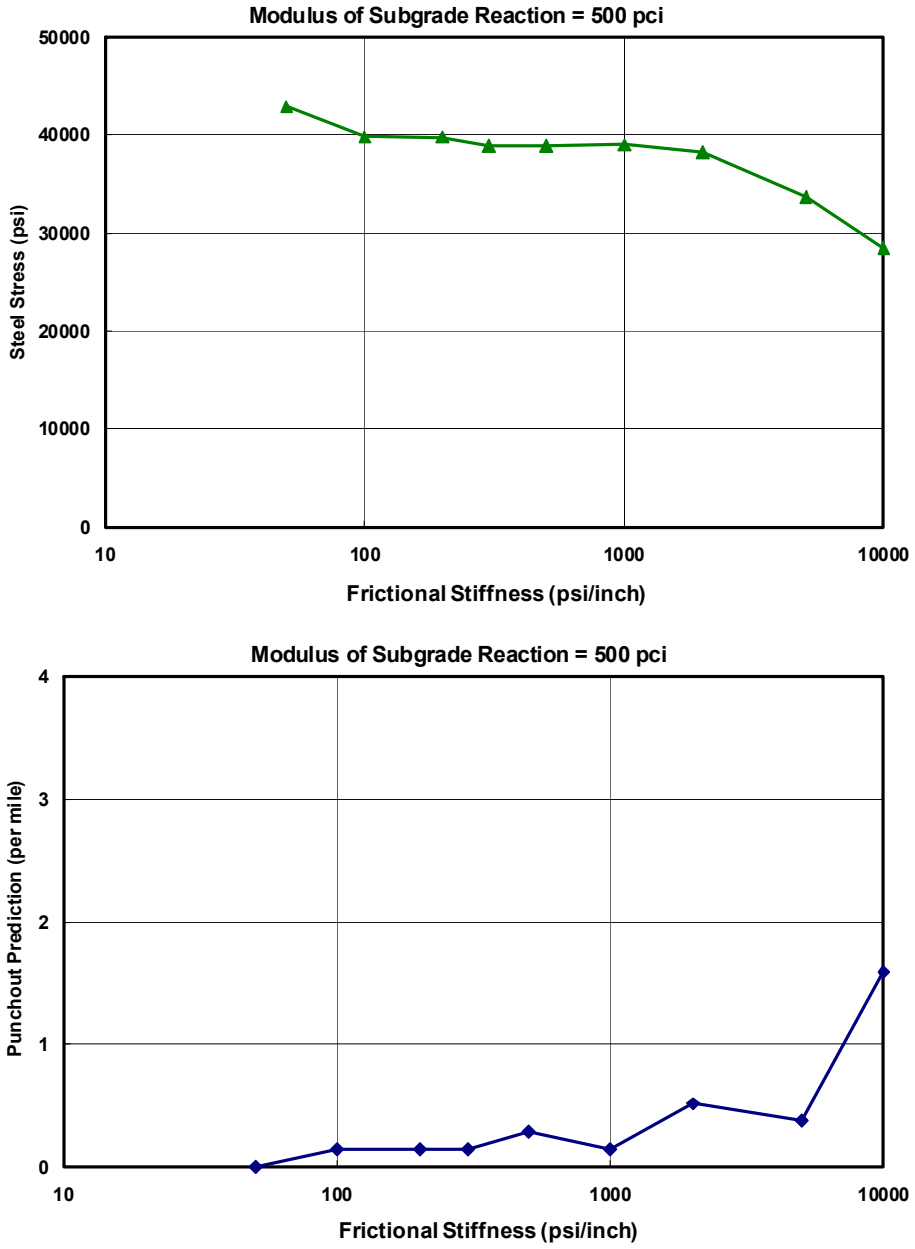

Figure 21 Analysis of Frictional Effects: Steel Stress and Punchout.

To further evaluate effects of frictional stiffness, the MEPDG computer program was also used. Indications are that a good correlation exists between predicted cracking patterns from the MEPDG to those manifests in CRC pavements placed under field conditions. In this program, many aspects of design and performance can be considered and evaluated in terms of mean crack spacing, crack width, LTE, punchout, and international roughness index (IRI). In this analysis, a 10 inch CRC pavement with 0.6 percent steel and #6 rebar was used. A range of input value of frictional coefficients used covered from 5 to 25 where typical values of frictional coefficients corresponding to different subbase types are listed in Table 22.

Table 22 Value Range of Frictional Coefficient.

Subbase Type	Frictional Coefficient (Low – Mean – High)
Fine-grained soil	0.5 – 1.1 – 2.0
Aggregate	0.5 – 2.5 – 4.0
Lime-stabilized clay	3.0 – 4.1 – 5.3
ATB	2.5 – 7.5 – 15.0
CTB	3.5 – 8.9 – 13.0
Soil cement	6.0 – 7.9 – 23.0
LCB	1.0 – 6.6 – 20.0

Figure 22 and Figure 23 present the variation of mean crack spacing and crack width, respectively, against the subbase friction coefficient. Figure 22 clearly shows that mean crack spacing decreases as the friction coefficient increases. This decrease occurs because high friction conditions tend to minimize concrete slab movement through higher tensile stresses, which lead to greater crack generation in a concrete slab. Also, shorter mean crack spacing corresponds to narrower crack widths. Therefore, the concrete pavement system with higher frictional conditions contains cracks, which have narrower crack widths than one with low frictional conditions.

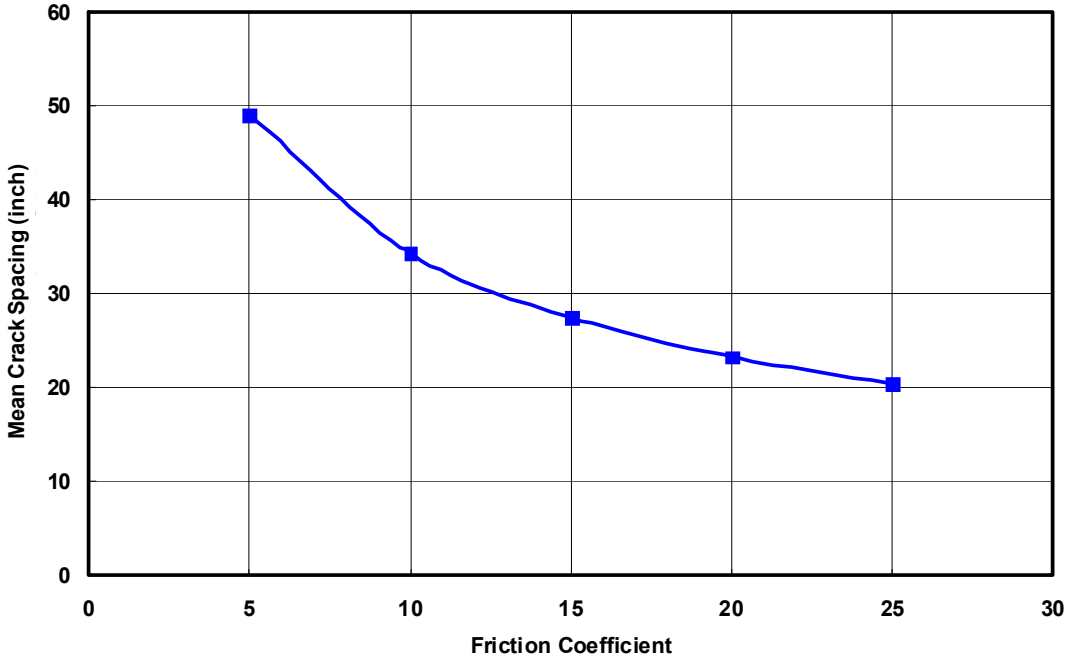

Figure 22 Mean Crack Spacing Analysis of Frictional Effects.

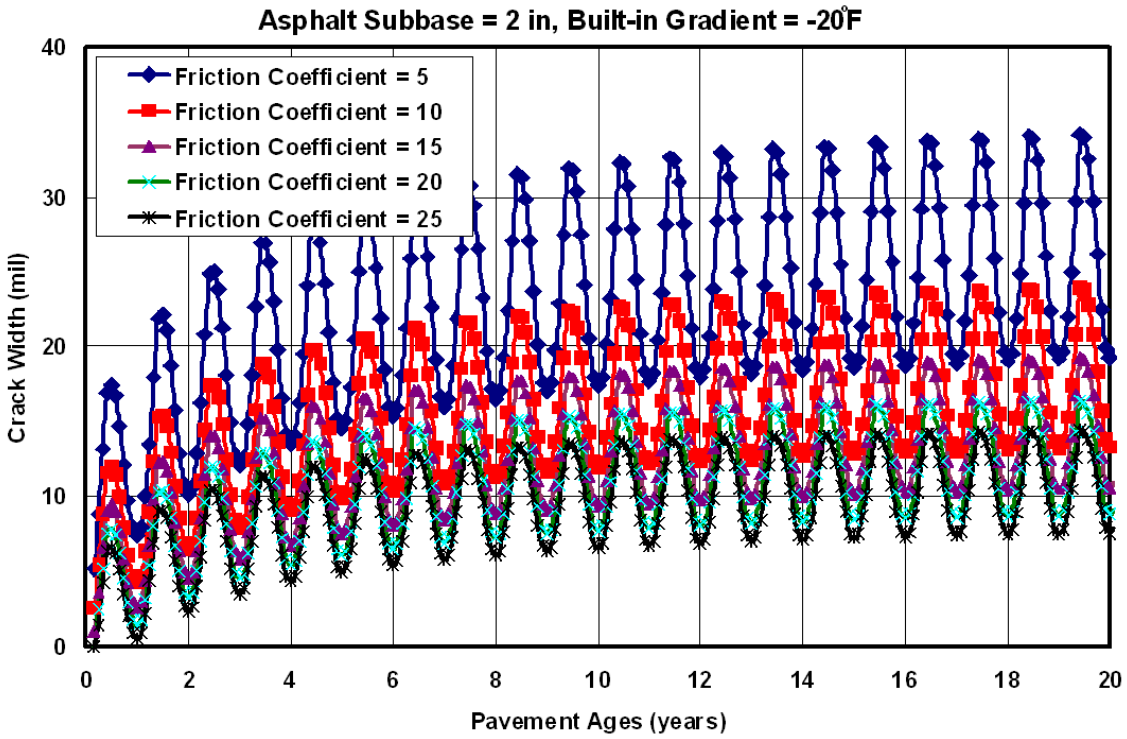

Figure 23 Crack Width Analysis of Frictional Effects.

Also as an additional dimension in which to evaluate frictional effects, long-term performance including LTE, punchout, and IRI were considered by MEPDG. Figure 24, Figure 25, and Figure 26 show the results in terms of LTE, punchout, and IRI projections, respectively. LTE decreases under low frictional conditions because low friction yields longer mean crack spacing and wider crack widths. Therefore, the efficiency of load transfer is lower under low frictional conditions. Also, MEPDG analysis results show that if the friction coefficient is small, more punchouts will be generated than would be the case under high frictional conditions, which is opposite that predicted by CRCP-10. The reason is due to the fact that low LTE conditions limit effective distribution of the vehicle wheel load stress, thus causing a higher bending stress and a greater punchout rate than under high LTE conditions. Furthermore, the roughness of the pavement becomes worse. In other words, pavement IRI will be greater under low friction conditions. In this analysis, thickness of asphalt subbase and the built-in temperature gradient are fixed at 2 inches and 20°F, respectively.

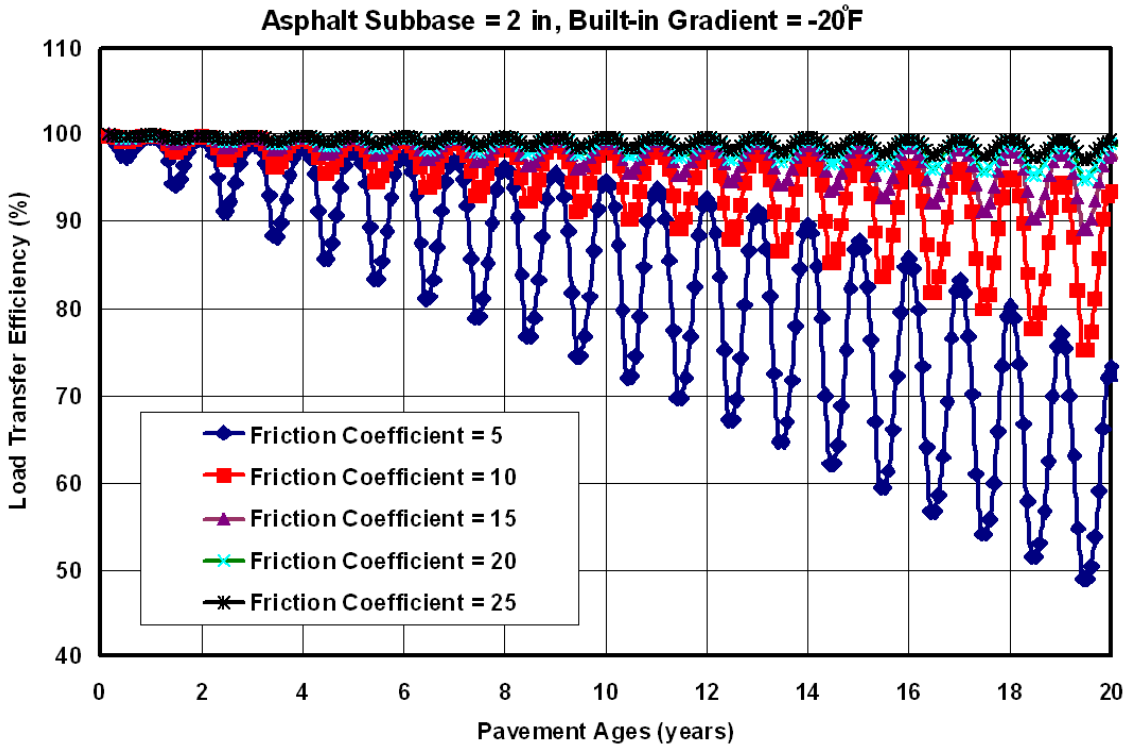

Figure 24 LTE Analysis of Frictional Effects.

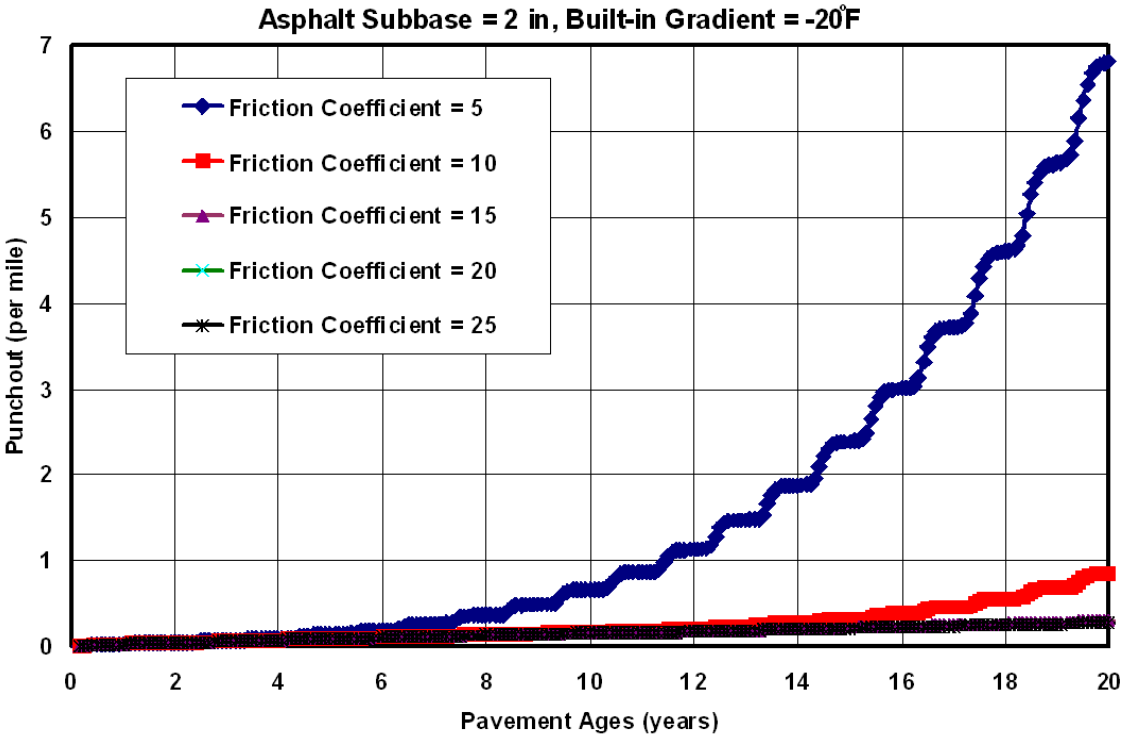

Figure 25 Punchout Analysis of Frictional Effects.

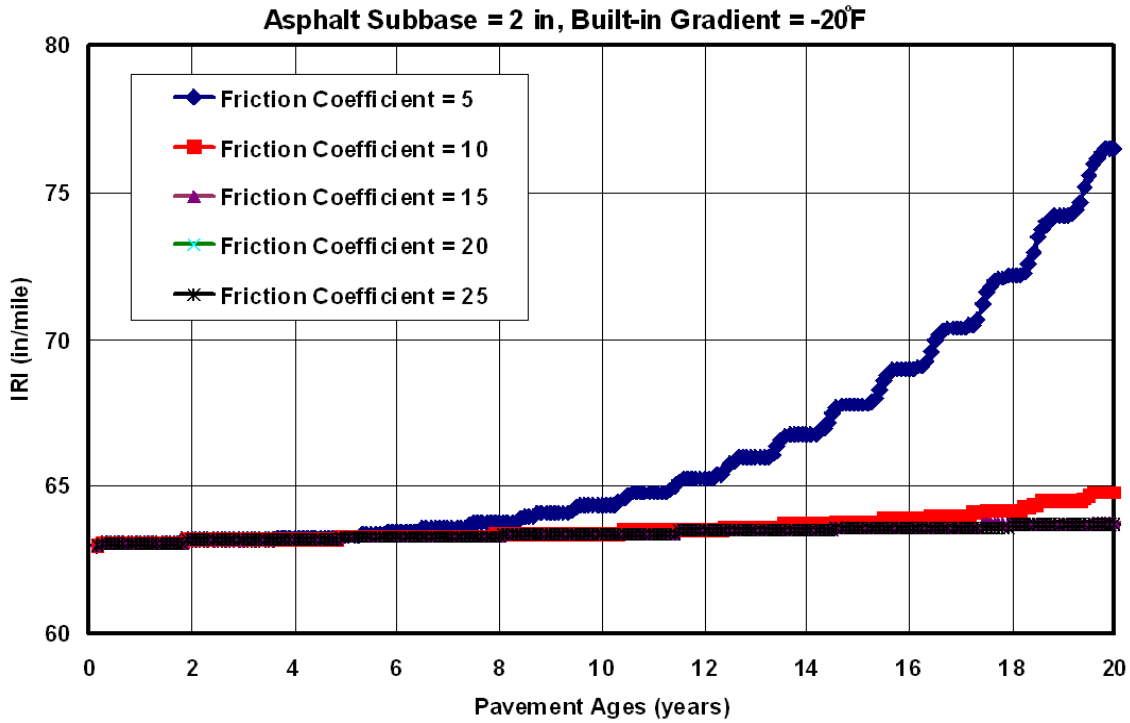

Figure 26 IRI Analysis of Frictional Effects.

Subbase Support Stiffness

A key aspect of long-term concrete pavement performance (particularly those of the unbonded jointed concrete options) is the quality and the nature of the curing effort relative to keeping the set temperature gradient to a minimum during and shortly after construction. The set gradient plays a major part of the magnitude and effect of the resulting curling and warping stresses that often are the cause of early, random cracking that are mainly dictated by the prevailing weather and curing conditions at the time the construction takes place. Tensile stresses and cracking in a concrete pavement often result from temperature and shrinkage effects during the early stages of hydration while the concrete is maturing and developing stiffness. Due to exposure to ambient conditions, a concrete pavement may cool to a minimum temperature as well as shrink due to moisture loss after cycling through a maximum temperature such that tensile stresses can be induced in the concrete slab. Stress development may become significant very soon after placement, perhaps even before the concrete has attained full hydration. Crack development in concrete pavement has been noted to be sensitive to diurnal temperature and wind effects. The tendency to curl and warp is restrained by the concrete slab weight in which the resulting level of stress development is a function of the stiffness of the underlying subbase layer as reflected in the radius of relative stiffness (ℓ- value subsequently defined). When the slab curls and warps in an upward configuration at the corners, tensile stresses are induced in the surface of the mid-slab area. Analysis of stress induced by a linear temperature gradient in a rigid pavement was originally developed by Westergaard (*21*).

As previously noted, early aged curling and warping stress can be a major concern during paving, particularly on the stiff support conditions justifying calls for special measures to be taken to assure the quality of construction and the long-term performance of the pavement. One option to limit these types of stresses is through proper selection of the spacing between the sawcut joints. Section 337 under Item (b) of the federal aviation association (FAA) Advisory Circular 150-5320 notes the design spacing for jointed concrete construction is elaborated. The text of this discussion is in the form of guidelines for concrete pavement sections containing both stabilized and unstabilized bases. Quoting directly from the circular:

> **"With Stabilized Subbase.** Rigid pavements supported on stabilized subbase are subject to higher warping and curling stresses than those supported on unstabilized foundations.

When designing a rigid pavement supported on a stabilized subbase a different procedure is recommended to determine joint spacing. Joint spacing should be a function of the radius of relative stiffness of the slab. The joint spacing should be selected such that the ratio of the joint spacing to the radius of relative stiffness is between 4 and 6. The radius of relative stiffness is defined by Westergaard as the stiffness of the slab relative to the stiffness of the foundation. It is determined by the following formula:

$$\ell = \left(\frac{Eh^3}{12\left(1-\upsilon^2\right)k} \right)^{\frac{1}{4}} \tag{25}$$

where: E = modulus of elasticity of the concrete, usually 4 million psi
h = slab thickness, in
ν = Poisson's ratio for concrete, usually 0.15
k = modulus of subgrade reaction, pci

The radius of relative stiffness has the dimension of length and when calculated in accordance with the above, the units of ℓ are inches."

The basis for the FAA advisory circular guidance is imbedded in the fundamental considerations originally elaborated by Westergaard (*21*), which are only briefly elaborated here. Westergaard presented solutions that considered curling stresses in a slab of infinite and semi-infinite dimensions based on the following governing equation:

$$\ell^4 \frac{d^4w}{dy^4} + kw = 0 \tag{26}$$

where: w = vertical displacement in the y direction.

Although the slab weight restrains the curling, the weight is not included in the equation. However, the displacement (w) caused by curling can be considered only part of the slab displacement. There are two boundary conditions that Westergaard addressed to solve the above expression, which are defined relative to an infinitely long slab of a finite width and for a semi-infinite slab. A pavement slab is considered to be of infinite extent with respect to the length of the slab when the tendency to curl in longitudinal direction is fully restrained or $w = 0$ at the

longitudinal center. With a positive Δt (temperature at the top higher than the temperature at the bottom), the maximum tensile stress is at the bottom surface of the slab in longitudinal direction, whose value is:

$$\sigma_x = \frac{E\alpha\Delta t}{2(1-\nu)} \tag{27}$$

where: α = thermal coefficient of expansion in the concrete.

The tensile stress pattern in concrete slab is shown in Figure 27. For a slab of finite dimensions, Bradbury (*22*) suggested an approximate formula to estimate the maximum stress, where two coefficients were given based on the Westergaard analysis. Bradbury developed a chart to determine the correction factors that were based upon the Westergaard equation to determine the curling stress in the slab. The Bradbury coefficient depends on radius relative stiffness of the slab, length of the slab, modulus of elasticity of concrete, thickness of the slab, Poisson ratio of concrete, and modulus of subgrade reaction, as indicated in Figure 28.

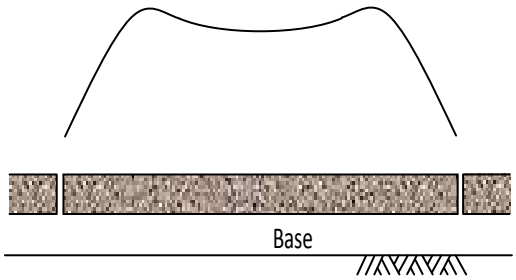

Figure 27 Tensile Stress Pattern in Slabs (*23*).

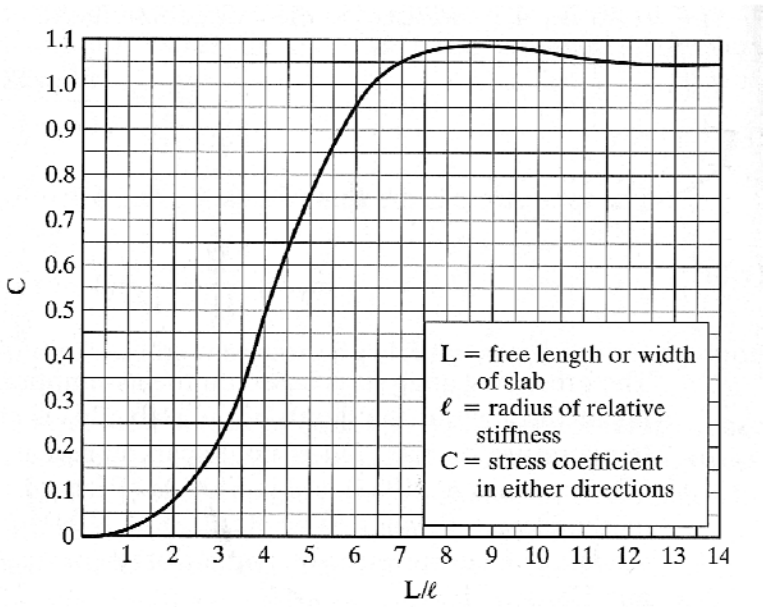

Figure 28 Coefficients for Maximum Stress in Curled Slab (*22*).

When a slab with a finite length (L_x) and a finite width (L_y) is curled (or warped) as subjected to a temperature gradient, stress distributions can be found analytically. For estimating the maximum σ in a finite slab, Bradbury proposed an approximate formula as follows (*21, 22, 24*):

$$\sigma_x = \frac{E\alpha\Delta t}{2}\left(\frac{C_1 + \nu C_2}{1-\nu^2}\right) \tag{28}$$

where:

C = the Bradbury coefficient

$$= 1 - \left(\frac{2\cos\lambda\cosh\lambda}{\sin 2\lambda + \sinh 2\lambda}\right)\left[\begin{array}{l}(\tan\lambda + \tanh\lambda)\cos\dfrac{y}{\sqrt{2}\ell}\cosh\dfrac{y}{\sqrt{2}\ell} \\ +(\tan\lambda - \tanh\lambda)\sin\dfrac{y}{\sqrt{2}\ell}\sinh\dfrac{y}{\sqrt{2}\ell}\end{array}\right] \tag{29}$$

$$\lambda = \frac{x}{\sqrt{8}\ell}$$

The coefficient C_1 is typically in the longitudinal direction, whereas C_2 is for the perpendicular direction. Coefficient C_1 increases as the ratio L/ℓ increases, having a value of C = 1.0 for L = 6.7ℓ, reaching a maximum value of 1.084 for L=8.88ℓ. In summary, the magnitude of the restraint stress is affected by slab dimensions and support stiffness. When the coefficient C has a maximum value of 1.084, the maximum tensile stress due to curling is 0.638 $E\varepsilon^t$ (where $E\varepsilon^t = E\alpha\Delta t$ and $\nu = 0.15$), which implies that the maximum curling stress cannot exceed 63.8 percent of total possible restrained tensile stress. Any additional contributors to the tensile stress in the slab such as those induced by reinforced steel bar and friction between subgrade and slab may add to the balance of stresses, but the total tensile stress should not exceed $E\varepsilon^t$.

To evaluate the effects of subbase support stiffness (i.e., k-value) under temperature effects, the ISLAB2000 (*6*) FEA computer program was used. Table 23 shows geometry input values used in this analysis. In this analysis, the range of k-value was from 50 psi/inch to 1000 psi/inch

Table 23 Geometry Input Values.

Slab Dimension	12 ft × 12 ft
Thickness	12 inches
Elastic Modulus	5.0×10^6 psi
Poisson's Ratio	0.15
Coefficient of Thermal Expansion (CTE)	6.0×10^{-6} /°F
Unit Weight	145 pcf
k-value	50 ~ 1,000 psi/in

Loading inputs pertained to temperature only; nighttime temperature conditions and daytime temperature conditions were represented by the temperature input values. Figure 29

shows the input temperature distributions along the concrete slab depth. The temperature gradients, which have the same absolute value between top and bottom, were used to compare the nighttime and daytime conditions.

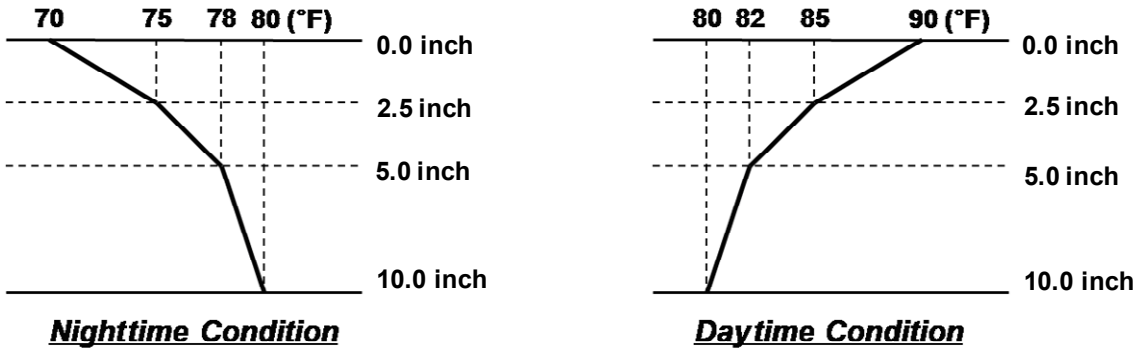

Figure 29 Temperature Loading Conditions.

Figure 30 presents the analysis output values. Three output values were considered in this analysis as: (1) the deflection of top surface at slab center from datum line, (2) deflection of top surface at slab corner from datum line, and (3) the relative deflection between center and corner of the concrete slab.

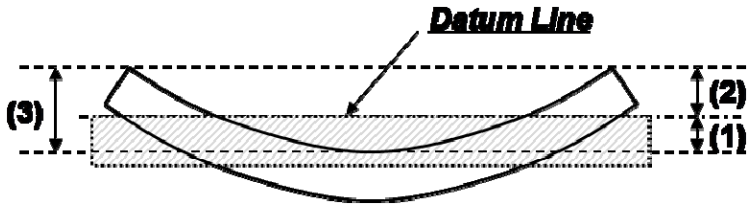

Figure 30 Output Values.

Figure 31 and Figure 32 show the results of the modulus of subgrade reaction effects under nighttime and daytime temperature conditions. As shown in the figures, the deflections decrease as the k-value increases. If the k-value is larger than 300 psi/inch, however, the change of deflection is very small.

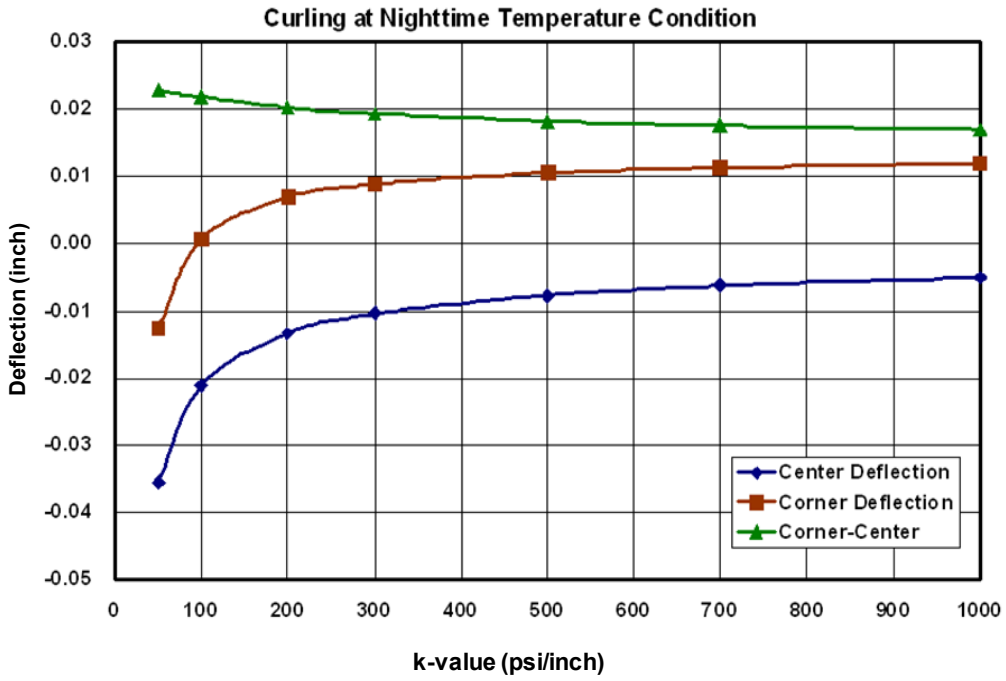

Figure 31 Modulus of Subgrade Reaction Effects under Nighttime Temperature Condition.

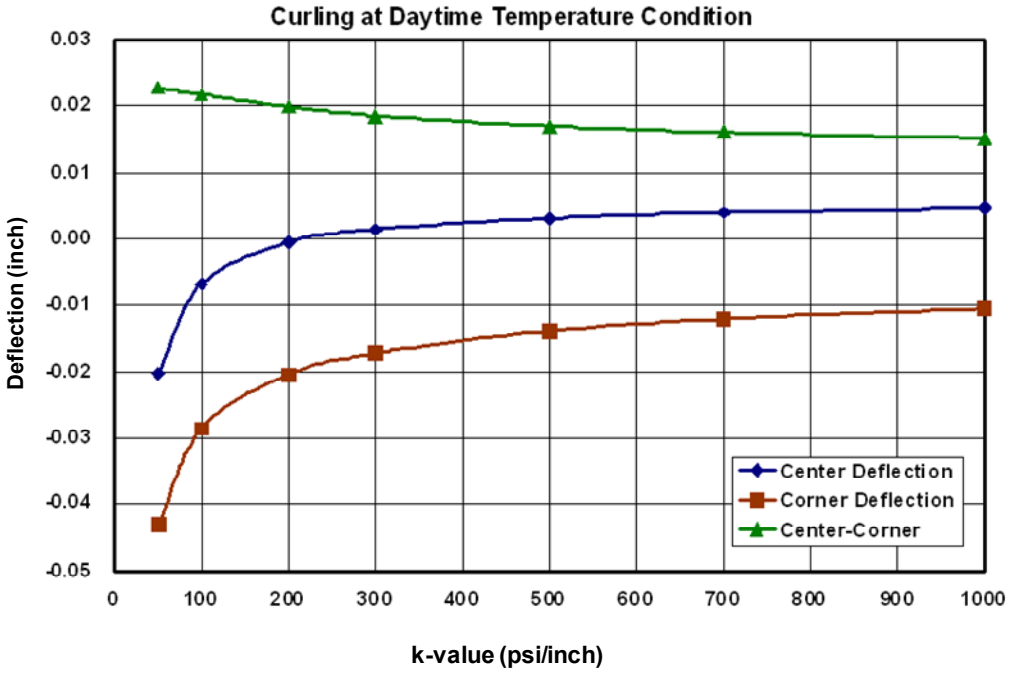

Figure 32 Modulus of Subgrade Reaction Effects under Daytime Temperature Condition.

Figure 33 shows the comparison of modulus of composite k-value effects between the nighttime temperature loading and the static 9000 lb, mid-slab vehicle loading condition. The vertical axis presents the maximum tensile stress on the top surface of the concrete slab. As shown in the figure, load stress decreases as k-value increases, as expected. On the other hand, the temperature-induced stress increases with k-value suggesting that subbase stiffness should be minimized since climatic-induced stresses have greater sensitivity to k-value than load-induced stresses.

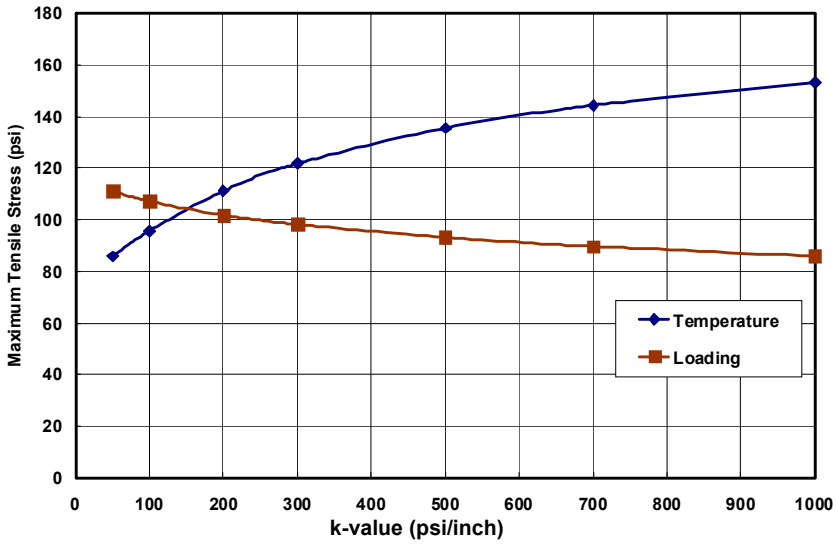

Figure 33 Modulus of Subgrade Reaction Effects under Temperature and Vehicle Loads.

From ISLAB2000 (*25*) analysis, it is evident (as shown in Figure 34a and b) that relative to pavement type, a CRC design has a definite advantage over a jointed or a contraction design although the curing behavior is a concern for both pavement types. Curing stresses are shown as a function of slab thickness, temperature gradient, base thickness, and stiffness. Curing stresses for a contraction design are shown in the longitudinal direction while the curling stresses for the CRC are in the transverse direction.

Elaborating further on the Figure 34 illustrated behavior, the Bradbury and Westergaard characterization is limited to a single slab on grade configuration, and converting a multi-layer configuration to a single slab configuration allows a way to illustrate the exceptional dominance of the stiffness of a stiff layer on curling stress. As indicated in Figure 35, the single layer k-value used for curl stress analysis where a stiff subbase is involved may be much greater than

that indicated from Section 330 in the FAA design charts. The k-value on top of a stiff layer that effectively creates the curling stress as back calculated using the Westergaard formulation for the Bradbury C and equating the curling stress from the ISLAB2000 analysis (taking the multiple layer into account) to $\sigma = C^*\sigma_0$ (where $\sigma_0 = E_c\alpha\Delta t$) a single layer composite k-value can be back calculated. This effect of course becomes less dominant in pavement sections of lower base thicknesses. Nonetheless, high composite k-values can be the source of damage that could ultimately shorten the fatigue life, particularly of a contraction design.

Clearly, climatically induced stresses should be a key consideration in the pavement design and type selection, particularly in the cases where an exceptionally stiff support platform exists. Under circumstances such as these, load stresses are rarely the issue but environmental stresses are raising the potential for shortened fatigue life and several instances of randomly cracked slabs prior to a single load being applied to the pavement. Ideally, bonded overlays are the best option for thick, stiff support layers because many of the construction-related issues described above are eliminated.

Using an AC interlayer under a concrete slab will moderate the frictional interface yet it reduces the structural capacity of the slab to carry load through a partial bond between the surface and the subbase. It also allows for the inducement of slab pumping action under which erosion can take place, possibly causing joint-related performance issues. Analysis of concrete pavement performance including mean crack spacing, mean crack width, steel stress, and punchout performance due to change of the modulus of subgrade reaction was performed. In this analysis, the friction stiffness value was fixed by 100 psi/inch. Figure 36 and Figure 37 present the analysis results. As the modulus of subgrade reaction value increases, the mean crack spacing and mean crack width increase. Clearly, since the CRCP-10 program only accounts for load and horizontal stresses on the cracking stress, crack spacing will increase as k-value increases. Since the CRCP-10 punchout model is basically fatigue-based as well as independent of crack width effects on load transfer, the punchout rate also decreases with increasing k-value.

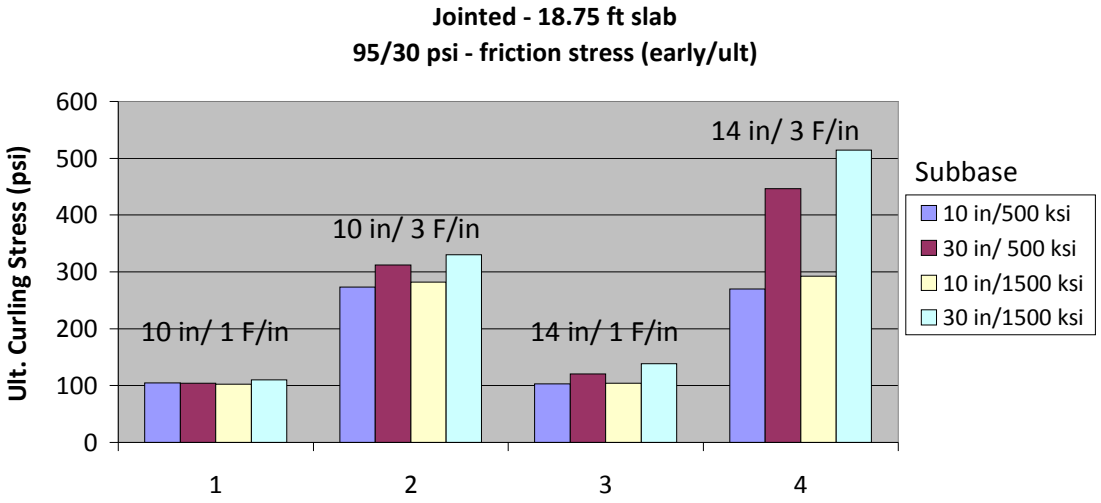

(a) Curling Stresses for a Jointed 18.75 ft Slab - Longitudinal.

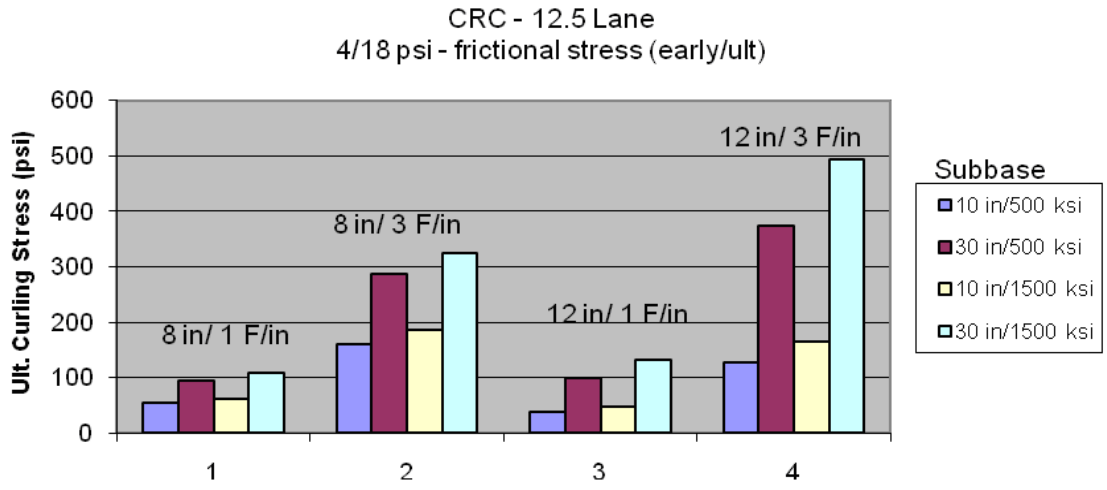

(b) Curling Stresses for a CRC Pavement - Transverse.

Figure 34 Curling Stresses.

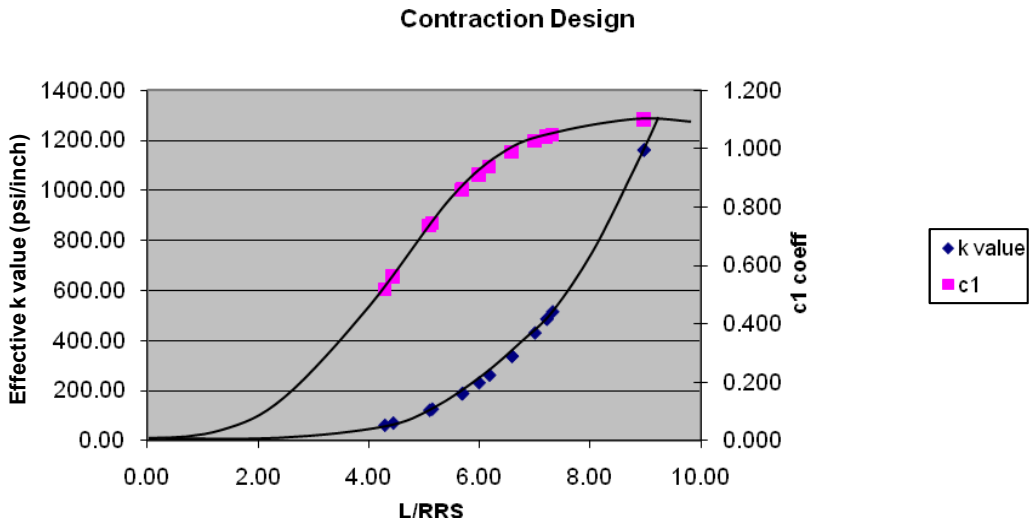

Figure 35 Relationship between the Effective k-value and the Bradbury C Factor.

To further verify the effect of k-value, another analysis was conducted. In this analysis, the friction coefficient and the built-in temperature gradient were fixed at 10 and 20°F, respectively. Figure 38 and Figure 39 present the results of punchout and IRI under different dynamic k-value conditions, respectively, using the MEPDG program. Punchout and roughness increased as dynamic k-value increased. Due to the MEPDG punchout definition and the effect of bending stress, climatic stress and the rate of punchout will be larger, particularly under a negative temperature gradient as k-value increases. Although this trend is consistent with bending stress factors, it is not necessarily consistent with field experience in the case of stiff support. Likewise, the roughness of the pavement system increases as k-value increases. Additional analysis of the behavior of PCC slabs placed on stiff subbases is provided in Appendix A.

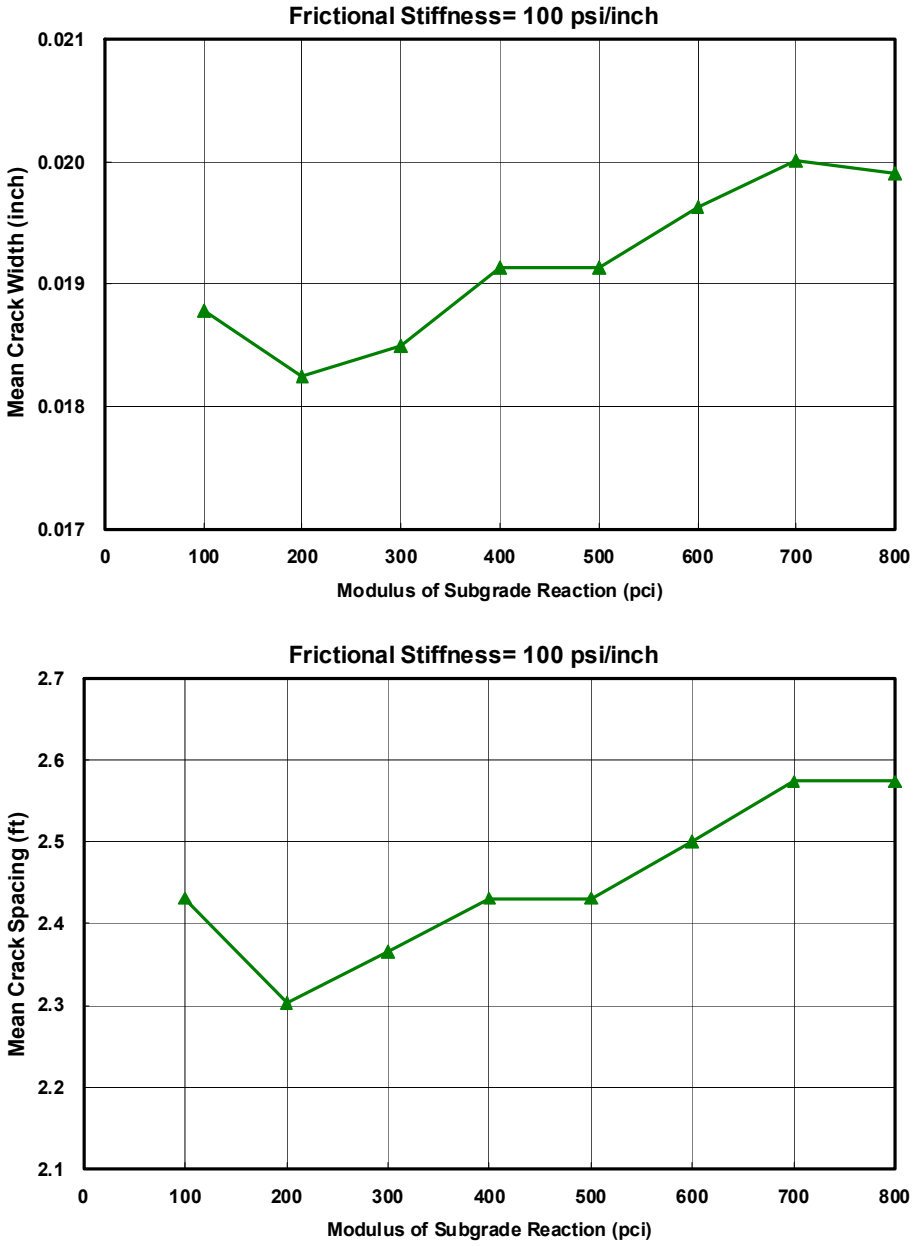

Figure 36 Analysis of Modulus of Subgrade Reaction Effects: Crack Width and Spacing.

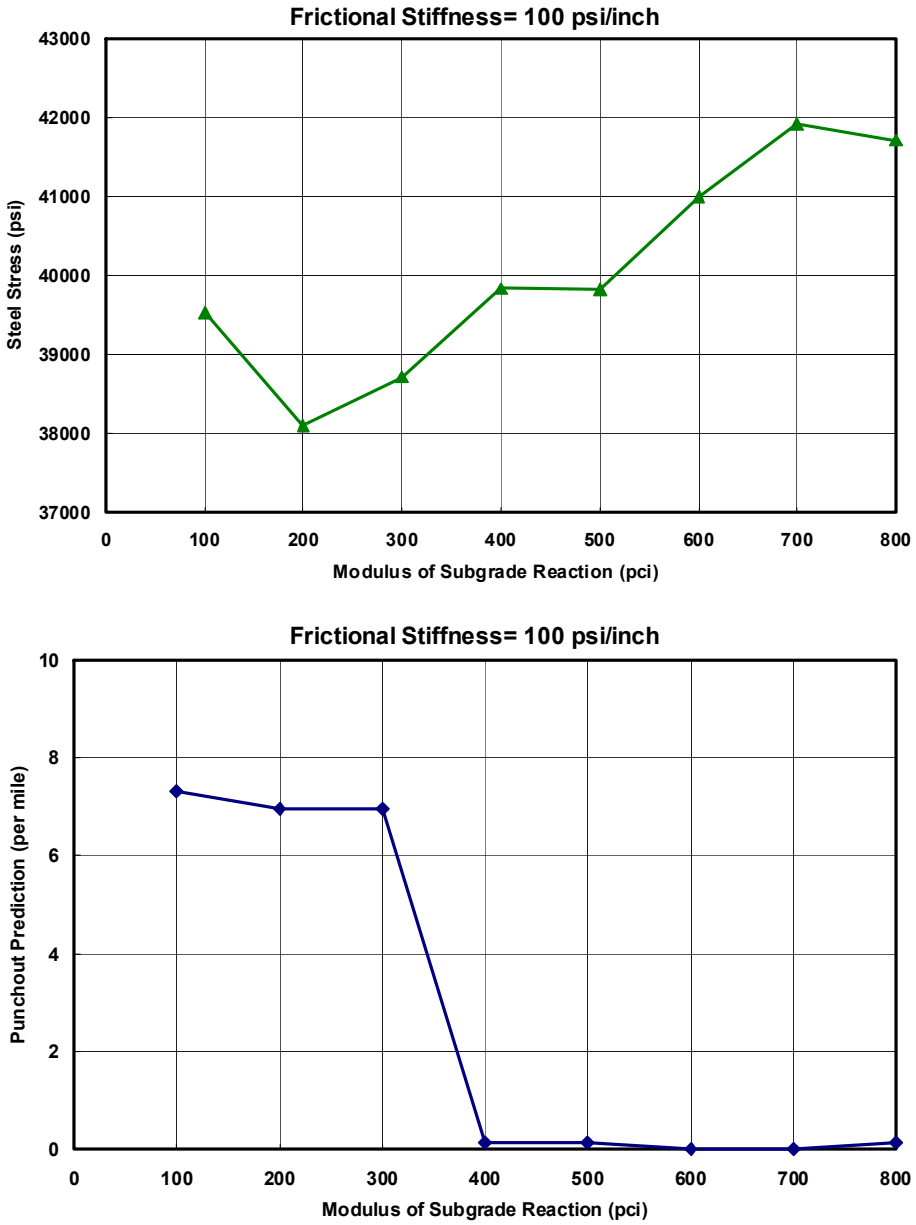

Figure 37 Analysis of Modulus of Subgrade Reaction Effects: Steel Stress and Punchout.

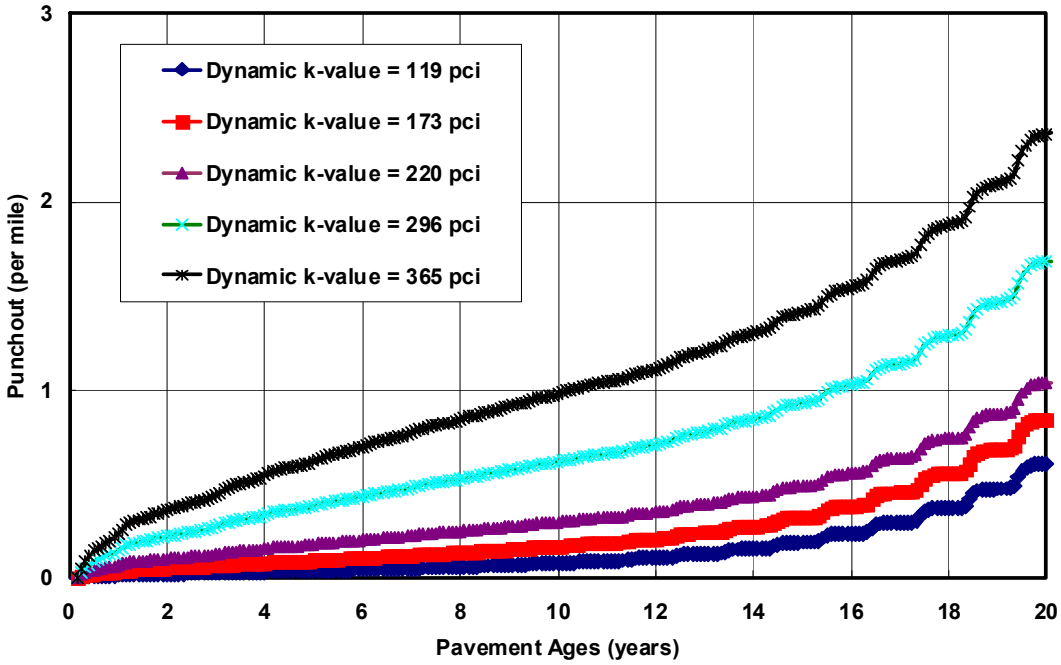

Figure 38 Punchout Analysis of Modulus of Subgrade Reaction Effects.

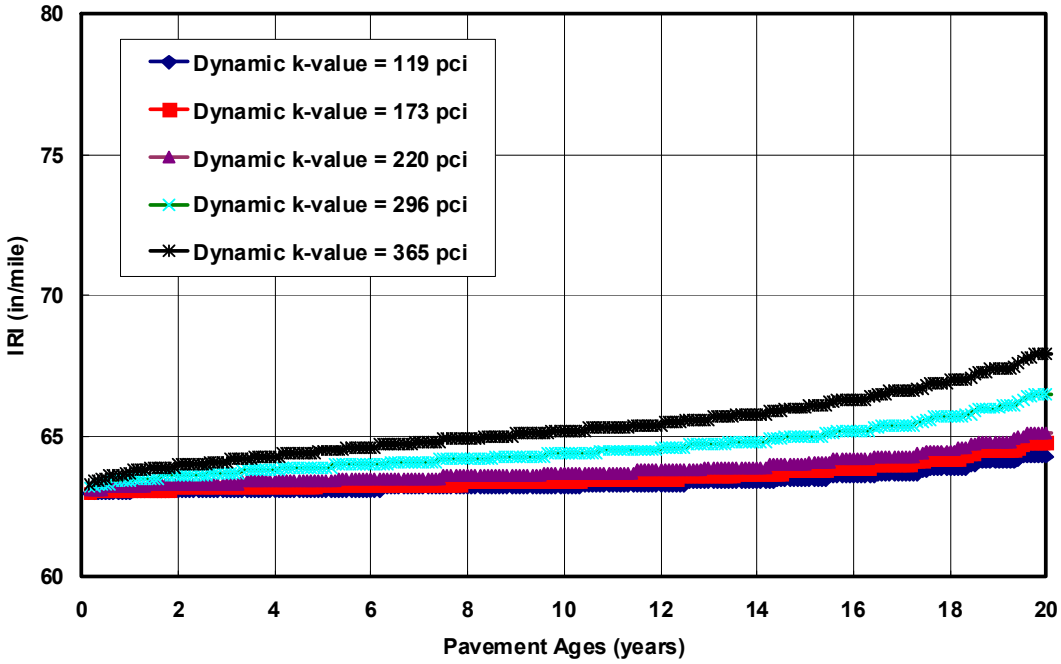

Figure 39 IRI Analysis of Modulus of Subgrade Reaction Effects.

Erodibility Effects

The MEPDG computer program includes five classes of erodibility, as input values shown in Table 24. In this classification, Class 1 contains extremely erosion-resistant materials such as lean concrete base, stabilized soil layer, or a hot mixed asphalt concrete. Class 2 includes very erosion-resistant materials including cement or asphalt treated granular material. Class 3 includes erosion-resistant materials such as cement or asphalt treated granular material. Class 4 contains fairly erodible materials such as unbounded crushed granular material having dense gradation and high quality aggregates. Finally, Class 5 includes very erodible materials including untreated subgrade compacted soils (*19*).

According to the MEPDG analysis, erodibility could affect long-term performance of the concrete pavement system. As a means to illustrate some of the factors involved with erosion-related distress, Figure 40 presents the effects of base erodibility on predicted faulting in jointed plain concrete pavements (JPCP). Punchout distress in CRC pavement is affected by many of the same factors involved with faulting in JPC pavements since the root cause is erosion where a subbase layer classified in the low erodibility category could provide good performance.

Table 24 Erodibility Classification.

Erodibility Class	Description
Class 1	Extremely erosion-resistant materials
Class 2	Very erosion-resistant materials
Class 3	Erosion-resistant materials
Class 4	Fairly erodible materials
Class 5	Very erodible materials

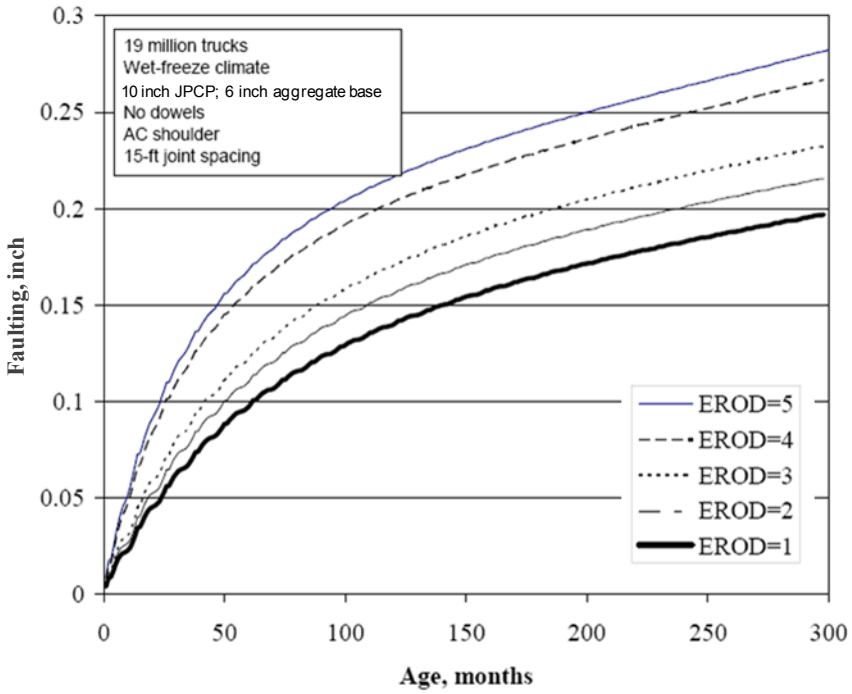

(a) Undoweled

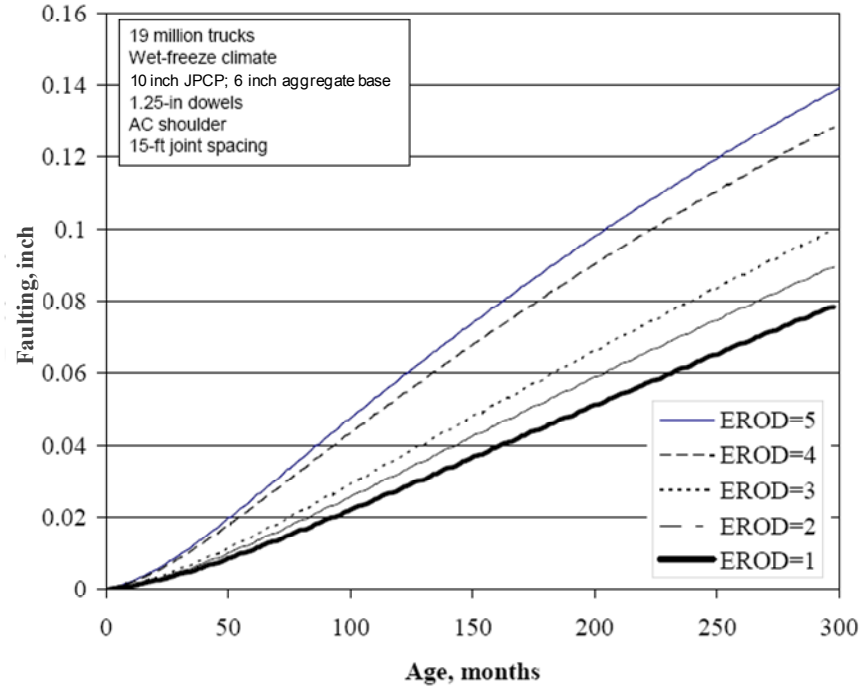

(b) Doweled

Figure 40 Effect of Base Erodibility on Predicted Faulting at JPCP (*19*).

CONCLUSIONS

To assess the effect of subbase behavior on performance, this study was conducted. Effects of friction characteristic between concrete slab and the subbase and effects of the subbase support stiffness, which is expressed in terms of composite k-value, were analyzed using several computer programs such as ISLAB2000, CRCP-10, and MEPDG. CRCP-10 and MEPDG were used to verify friction effects and ISLAB2000, CRCP-10, and MEPDG were used for evaluation of subbase support stiffness effects. Crack spacing, crack width, steel stress, punchout, and roughness were considered as indicators to assess the long-term performance of the concrete pavement system.

Also, on the basis of the finite element (FE) analysis elaborated in Appendix A, the nighttime nonlinear temperature gradient condition leads to the critical stress condition in PCC slab. Therefore, the critical temperature input should be the nighttime nonlinear case. Moreover, the modified FE analysis as presented indicated as the subbase thickness increases, the subbase support stiffness increases.

CHAPTER 5
GUIDELINES FOR THE DESIGN OF CONCRETE PAVEMENT SUBBASE

The objective of this guideline are to provide assistance for the economical and sustainable design of concrete pavement subbase layers. The target audiences are district pavement design and construction engineers. A decision flowchart provides the guidance for an effective design process of a concrete pavement subbase. Many design factors that affect the performance of the subbase are considered; however, the service history of existing subbases with similar layer properties and environmental conditions should be considered first if such information is available. These guidelines are provided in terms of design recommendations, material specification, and test methods.

SUBBASE PERFORMANCE CONSIDERATIONS

A primary focus of subbase layer design is to achieve long-term performance in a cost effective and reliable manner. During construction, a subbase needs to provide a stable construction platform and over the service-life uniform slab support. The role of uniform support cannot be overstated in the performance of long-lasting concrete pavement systems; good performing concrete pavements can coexist with a wide range of support strength, but variation from the slab center to the edge or corner area or differences in support between segments cannot be tolerated to any great extent, which is why erosion is a key factor in performance.

Erosion creates a nonuniform support condition that often leads to faulting in jointed pavements and punchout-related distress in CRC pavements. Erosion potential is greatest where upward curling and warping along edge and corner areas separate the slab from the subbase enabling the slab to "pump" any water that may be trapped under applied wheel loads back and forth across the slab/subbase interface. Unfortunately, most CTBs are not sufficiently erosion-resistant or permeable to allow for an acceptable means of removal of water to avoid erosion damage. The use of an asphalt interlayer has certainly improved the erosion resistance of CTB but the main reason for using such materials has been to reduce the frictional resistance between the slab and the subbase to ensure proper development of the crack pattern, particularly in CRC

pavements. Clearly, use of an asphalt interlayer has successfully served these two purposes well as far as CRC pavement design and performance.

Subbase layers certainly can add structural capacity to a concrete pavement, but only to the degree the interlayer bond or friction can be employed to contribute to the inherent load spreading capability of the slab. Consequently, increasing slab support is not always accomplished depending upon the type of subbase material used. Another more important feature is provision of a gradual change in layer stiffness from the slab to the top of the subgrade layer. Abrupt changes in this regard can lead to undesirable load-induced shear stress concentrations along the corners and pavement edges, enhancing the potential of poor support conditions developing over time and loading cycles. Stiff subbases, unless fully bonded to the slab, also tend to magnify the environmentally induced load stresses in the slab and shorten the fatigue life of the pavement system. Nonetheless, even though the use of an AC interlayer will prohibit development of full bond, it can help reduce these types of stresses and promote to some extent slab/subbase bonding, which tends to prolong the fatigue life of the slab by reducing the curling and warping-related stresses.

SUBBASE DESIGN FLOWCHART

The decision process for the design and subbase material type selection shown in Figure 41 is categorized into three areas of consideration or criteria: materials, design, and sustainability. The process begins with the selection of material factors such as type, strength, and erodibility requirements. Design factors include friction/bond characteristics, layer thickness, and traffic considerations. Finally, the design engineer considers the sustainability the subbase layer affords the overall pavement design. Load transfer, constructability, and drainability, as well as precipitation and joint sealing maintenances should be considered in the design process in order to fully account for erosion damage. Accordingly, following this decision process, the design engineer should evaluate the key factors associated with a given subbase configuration. A step by step design process with a design guide spreadsheet and example is detailed at the end of this chapter.

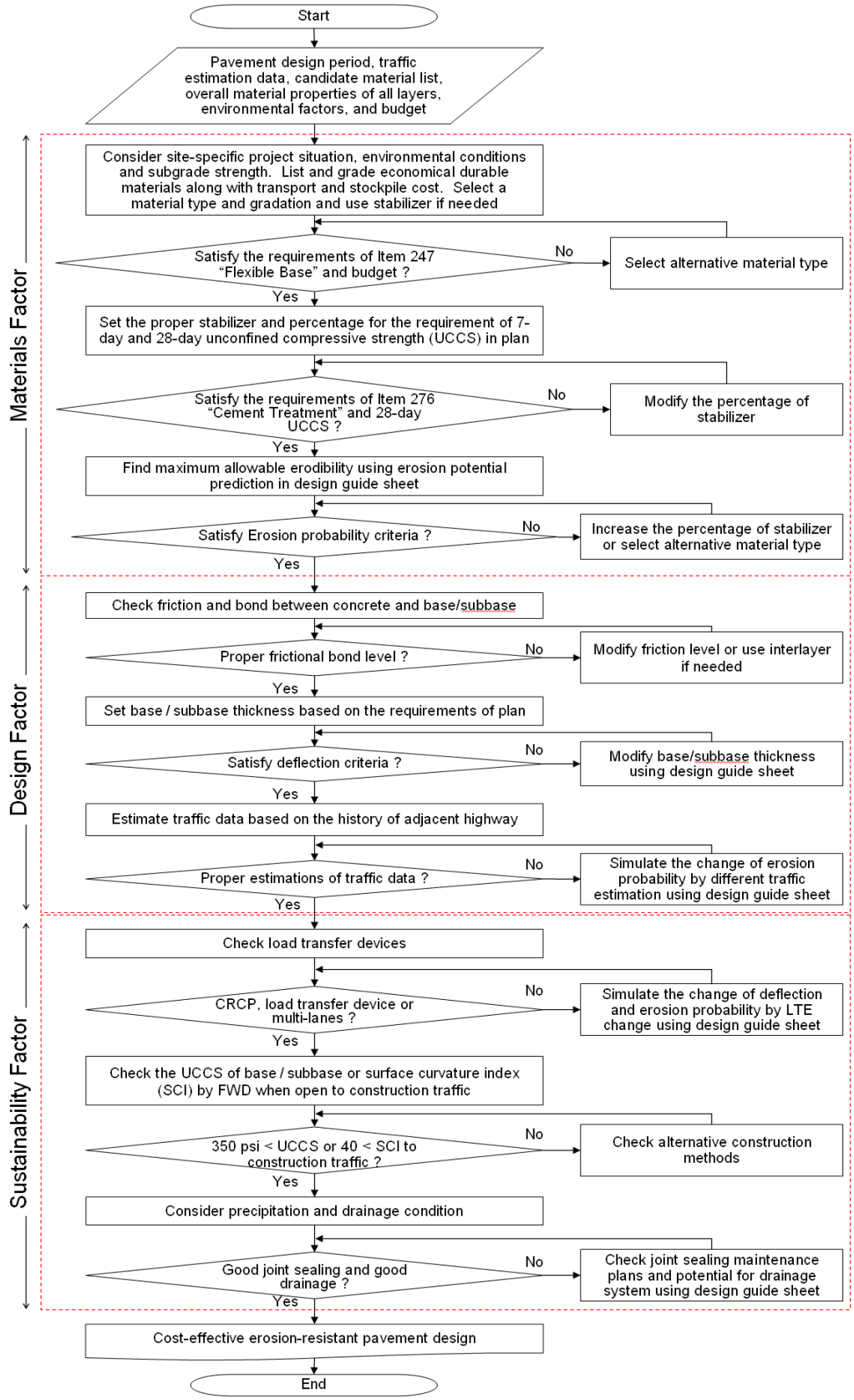

Figure 41 Decision Flowchart for Subbase Design of Concrete Pavement.

Material Factors

Subbase design-related decisions should account for many material characteristics and project-related environmental conditions. The longevity of material beneath the slab is an important sustainability-related factor that needs to be addressed in subbase material selection. In this regard, material factors such as material type, stiffness, strength, and erodibility resistance of the subbase and subgrade are important factors. Table 25 shows an ordered list of decision factors and their attributes.

Table 25 Subbase Design Considerations.

Factor	Item	Criteria Parameter	Test Method
Materials	Type	Minimum requirement, cost	Standard, budget
	Compressive Strength	7-day and 28-day compressive strength Elastic modulus	Compressive strength test, Suction test
	Erodibility	Rate of erosion	Hamburg wheel-tracking test
Design	Friction/Bond	Coefficient of friction	Friction test
	Thickness	Deflection	Composite deflection
	Traffic	Volume, load, and axle group	Distribution
Sustainability	Load Transfer	Radius of relative stiffness	Effective k-value FWD
	Constructability	Material functionality, cost	Cost Analysis, Impact Assessment
	Drainability	Moisture susceptibility	Suction test, Durability testing

Material Type

Typically, locally available, economical, and durable materials are used for subbase layer construction to keep transportation costs low. Moreover, recyclable materials are suggested to promote environmentally friendly designs; stabilization may be needed to properly assure the agency's requirements. With these suggested features, CTB using RAP, recycled concrete, or other locally available materials can be feasible candidate alternatives for subbase layers.

When a stabilized subbase is planned, sufficient stabilization is necessary to provide the needed erosion resistance. Typically, the cement percent for CTB should be higher than 4 percent to reduce erosion damage. Otherwise, projected traffic levels can be used to gauge necessary cement contents (as a function of strength). Moreover, the percentage passing the No. 200 (0.075 mm) sieve size in granular materials should not exceed 8 percent by weight for untreated subbase.

Modified material specifications are provided in Appendix C. In Item 247 "Flexible Base," the following sentence is included in Section 247.2.A.3.a, "Limits on Percentage":

> When RAP and other recycled materials are applied as the aggregates for Item 276 "Cement Treatment (Plant-Mixed)," more than 20% RAP by weight and other percentage limitations are allowed only if the strength and erosion requirements in Item 276 "Cement Treatment (Plant-Mixed)" are satisfied.

Section 276.2.E, "Mix Design" in Item 276 "Cement Treatment (Plant-Mixed)" is modified as following sentence using new table for erosion requirements.

> **E. Mix Design.** Using the materials proposed for the project, the Engineer will determine the target cement content and optimum moisture content necessary to produce a stabilized mixture meeting the strength and erosion requirements shown in Table 1 and 2 for the class specified on the plans. The mix will be designed in accordance with Tex-120-E. The Contractor may propose a mix design developed in accordance with Tex-120-E. The Engineer will use Tex-120-E to verify the Contractor's proposed mix design before acceptance. The Engineer may use project materials sampled from the plant or the quarry, and sampled by the Engineer or the Contractor, as determined by the Engineer. Limit the amount of asphalt concrete pavement to no more than 50% of the mix unless otherwise shown on the plans or directed.

Table 1 Strength Requirements.

Class	7-Day Unconfined Compressive Strength, Min. psi
K	500
L	300
M	175
N	As shown on the plans or 500

Table 2 Erosion Requirements.

Environment and Drainage	28-Day Erodibility Using Hamburg Wheel-Tracking Device Test, mm/10,000 load repetitions	
	With Subsurface Drainage	Without Subsurface Drainage
Rainfall less than or equal 10 inch/yr	0.75	0.25
Rainfall greater than 10 inch/yr	0.5	0.13

The advantage of a CTB is the higher material strength, stiffness, and resistance to erosion whether or not it is fully bonded to the concrete slab. A CTB layer is practically impervious and insensitive to the cyclic damage of freeze and thaw, which improves with time since it gains sufficient strength with age (*4*). However, CTB may have a tendency to reflect cracking through a bonded surface layer, which is one reason why asphaltic interlayer is commonly used with a CRC pavement construction; however, this could be mitigated to some extent through sawcutting the base layer if full bond is a desired design option. Use of a fully bonded CTB may cause irregularities in the cracking pattern, which again could be offset by adjustments in the steel percentages in a CRC pavement design. Otherwise, the main consideration in the design of a CTB layer is the need to balance erodibility against layer stiffness and interlayer friction. A consequence of not maintaining this balance is then the need to use an interlayer bond breaker.

RAP has economical and environmental benefits since its use potentially saves material, energy, and disposal costs, as well as conserves natural resources. RAP also typically has good availability for construction since it typically can be obtained, processed, and used onsite. RAP may also provide relatively low friction between the concrete slab and the subbase layer (*4*). The quality of RAP is highly governed by its constituent materials, potentially leading to substantial

variation in aggregate quality, size, and consistency depending on the source of the original material. Moreover, milling and crushing during processing can cause aggregate degradation and the amount of fines generated. This variation can cause reduction in subbase stiffness and strength possibly creating low erosion resistance (*5*).

Similar to RAP, the use of recycled concrete may have many economical and environmental advantages such as a lower haul distance, reduced usage of natural aggregates, and lower energy consumption and waste. Previous research has found that recycled concrete (RC) materials cause CTB mixtures to set quicker with slightly higher density (about 2 percent) than mixtures with conventional aggregates as well as higher long-term strength (*26*). Benefits using RC bases could only be realized where sufficient quantities of recycled concrete materials are available near the construction site. RCB may segregate when worked excessively during compaction (*27*).

Compressive Strength

Subbase strengths are typically of low strength since the concrete layer is expected to provide most of the load carrying capacity of the slab. Excessively high subbases are generally avoided to minimize shrinkage cracking in early stages of curing. A compressive strength of 350 psi is often sufficient to support construction traffic; a 7-day strength range from 500 to 800 psi is recommendable. Even if a high strength subbase is utilized, the subbase strength should not exceed a 7-day compressive strength of 1,000 psi to prevent early-age cracking (*28*).

Erodibility

Erosion is often the dominant subbase deterioration mechanism resulting in faulting or punchout distress. Certainly, erodibility is related to subbase material type, stiffness, and strength that can be to some extent evaluated on the basis of erosion testing results. Stabilization does decrease erodibility; however, the resulting increased stiffness by stabilization could generate other consequences as discussed previously. Proper stabilization level should be determined based on stiffness and erosion analysis for a given material type, design traffic, annual precipitation, and drainage condition. Table 26 shows the general guideline for three erosion resistance levels measured by the HWTD test.

The erosion depth criteria list in Table 26 is weighted against the rate found from the HWTD test (detailed in Appendix B). The erosion rate may also be confirmed against key design and sustainability factors listed in the decision process for subbase design.

Table 26 Subbase Erosion Resistance Criteria in Design Factors.

Erosion Resistance	Mean Erosion Depth (ER) Using HWTD (mm/10,000 load repetitions)	Design Recommendation
Good	ER < 0.5	Acceptable
Moderate	0.5 < ER < 1	Add more stabilizer if frequently saturated condition
Poor	1 < ER	Add more stabilizer or change material type or gradation

Design Factors

These factors are related to those most likely to be governed by the design engineer, although traffic considerations may override project-related engineering limitations. Nonetheless, the engineer should have some influence over their selection.

Friction or Bond

Obtaining friction resistance or chemical bond between a concrete slab and the subbase is also an important factor for subbase design. Subbases with high friction or chemical bonded properties have been found to be problematic relative to the formation of bottom up reflection cracking in JC pavement (or from embedded items) and poor cracking pattern distribution in CRC pavement due to effectively reduced steel contents (which may result in crack spacing too long inducing wide crack widths). However, this problem tends to be mitigated if the potential for chemical bond is eliminated or if interfacial friction is lowered by the use of an unmilled asphalt concrete layer. High friction or full bond effects could be offset by increased steel percentages in a CRC pavement design. On the other hand, maintaining a medium level of frictional restraint (i.e., using an asphaltic interlayer) is desired to minimize the shear stress between the concrete and the base layer. The use of an asphalt interlayer does reduce excessive subbase friction where a CTB layer is included in the design while protecting against the low

erosion potential most CTB materials seem to have. Other bond breaker types (i.e., fabrics) are possible but they may need extensive field evaluation to validate their successful use.

Subbase Thickness

Subbase thickness and stiffness properties affect the overall composite design thickness of the pavement; its design includes considerations for the projected traffic level as well as the structural capacity needs of pavement system such as deflection criteria, subgrade strength and type, and load transfer of the joints and cracks. The deflection of composite layer could be a criterion for subbase thickness design. If expansive subgrade soils are a concern, measures to mitigate swell potential should be taken.

Subbase stiffness (or modulus) is conveniently expressed in terms of the radius of relative stiffness (ℓ) for design purposes. Higher subbase stiffness can reduce deflection and erosion potential of the subgrade but may increase interfacial friction and curling stress in the concrete slab. If the governing design criteria is acceptable to deflection, lower stiffness would perhaps be preferable in light of reduced interfacial friction and curling stress.

Figure 42 is an example of a deflection design chart presented in terms of the composite or effective ℓ -value and overall pavement thickness for a 300 psi/inch composite k-value (relative to a variable slab thickness, subgrade k-value, and subbase thickness and stiffness). The effective ℓ -value increases with a higher effective thickness of concrete pavement, which can be calculated using Equations 30 and 31 (assuming unbonded layers).

$$h_e = \sqrt[3]{h_c^{\,3} + \frac{E_b}{E_c} h_b^{\,3}} \tag{30}$$

where:

h_e = effective thickness of combined slab (inch)
h_c = thickness of concrete slab (inch)
h_b = thickness of base (inch)
E_c = elastic modulus of concrete (psi)
E_b = elastic modulus of base (psi)

$$\ell_e = \sqrt[4]{\frac{Eh_e^{\,3}}{12(1-\nu^2)k}} \tag{31}$$

where:

ℓ_e = effective radius of relative stiffness (inch)

E = elastic modulus of the PCC layer (psi)

h_e = effective thickness of PCC slab (inch)

ν = Poisson's ratio

k = modulus of subgrade reaction

A thicker and stiffer subbase results in increasing effective slab thickness and the effective ℓ-value causing a lower composite deflection. On the other hand, reducing subbase thickness or the subbase modulus causes a greater composite deflection. Therefore, subbase thickness and modulus can be adjusted to meet design deflection criteria.

Traffic

Traffic is a key factor in pavement design for erosion considerations, and a higher level of traffic requires a more durable subbase system in order to protect the subbase and the subgrade. Traffic in the wheel path interfaces has the largest effect on the development of erosion. Lane distribution factors (LDF) and equivalent erosion ratios (EER) are used to properly account for traffic effects on erosion.

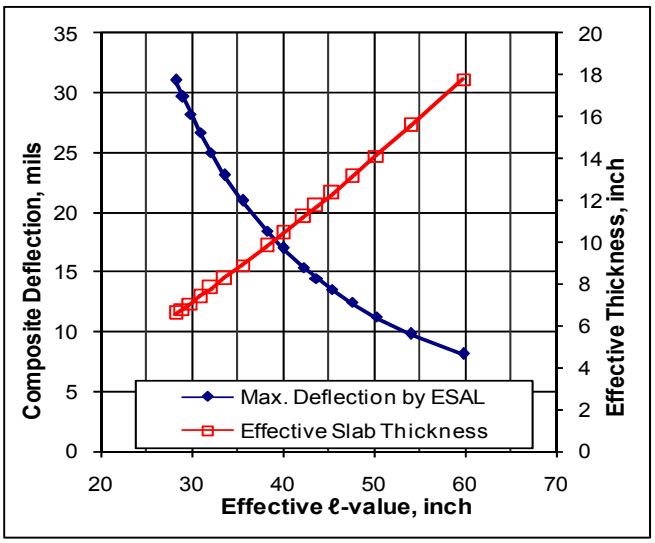

Figure 42 Deflection-Based Subbase Thickness and Modulus Design Chart.

Table 27 shows the adjustment of erosion rate by EER. EER converts traffic due to the lateral distribution across the wheel path into the traffic in the wheel path contributing to erosion. A normal distribution is often assumed for the lateral distribution of traffic, and the traffic wandering range would be increased with a wider lane width.

Table 27 Erosion Rate Adjustment Factor by Equivalent Erosion Ratio.

Design Lane Width, ft	EER Coefficient
11 or less	0.9
12	0.8
13	0.7
14 or more	0.6

Sustainability Factors

These factors are key to long-term pavement performance and should be determined relative to their role or function in affecting capabilities to conduct long-term repair. The inability to make future repair short of total reconstruction is tantamount to non-sustainability.

Load Transfer Efficiency

As the stiffness of the joint or crack decreases, slab deflection increases creating greater frictional stress at the slab interface causing greater distorted damage in the surface material. The accumulation of damaged material creates a greater degree of susceptibility to pumping action leading to the growth of a void under the slab that induces more deflection and further damage and loss of joint stiffness. This sequence could also accelerate subbase deterioration by interacting effects. However, load transfer devices or PCC shoulder effects could delay subbase damage with less deflection at a joint or crack. Deflection criteria accounts for the effect of LTE on the subbase design indirectly, and Table 28 shows the adjustment factor for erosion rate.

Table 28 Erosion Rate Adjustment Factor by Load Transfer Systems.

Load Transfer Devices at Transverse Joints or Cracks, or Dowels at Joints	**Tied PCC Shoulders, Curb and Gutter, or Greater than Two Lanes in One Direction**	
	Yes	No
Yes	0.7	0.8
No	0.9	1.0

Constructability

The subbase used under concrete pavement needs to have adequate structural capacity to support construction equipment and operations, otherwise the subbase can become damaged and need costly repairs. The current department requirements for subbases (4 inch ACP or 1 inch ACP over 6 inch CSB) have historically performed well under construction operations. The department did allow the use of 2 inch ACP over 8 inch LTS in the past on projects in the Fort Worth area; however, TxDOT personnel found that such thin ACP layers were susceptible to damage from construction traffic. In addition, researchers found from field coring operations that there appeared to be very little bond between ACP and lime-treated subgrade materials; such low bond can result in damage to thin ACP layers over LTS.

In areas where stabilized subgrade materials are needed to facilitate construction and reduce the effect of expansive soils on pavement roughness, the researchers recommend that pavement designers follow the TxDOT document titled, “Guidelines for Modification and Stabilization of Soils and Base for Use in Pavement Structures” that can be found at

ftp://ftp.dot.state.tx.us/pub/txdot-info/cmd/tech/stabilization.pdf. Stabilized subbases need to have the proper stabilizer type and content to perform properly and have adequate structural capacity for construction operations.

In addition, researchers recommend that designers address areas where significant moisture intrusion into subgrade soils can occur; this is of special concern for construction projects involving curb and gutter sections. Researchers observed isolated areas on one project where it appeared that significant moisture intrusion into the subgrade resulted in construction equipment damaging the subbase.

If TxDOT personnel are concerned about the structural capacity of a recently constructed subbase on a project, researchers suggest using a falling weight deflectometer to assess the structural capacity. TTI Research Report 409-3F contains a recommended simple interpretation scheme that relates the FWD surface curvature index (SCI) to the structural adequacy of thin pavement structures commonly used for low volume roads. The surface curvature index is simply the deflection underneath the FWD load plate (W1) minus the deflection 12 inches away from the load (W2), or W1-W2. According to the report, if the SCI at a 9,000 lb load level is less than 20 mils, the pavement has a good base; if it is between 20 and 40 mils, the base is marginal; and if it is greater than 40 mils, the base is weak or soft. The researchers suggest that this simple interpretation scheme can be used by TxDOT personnel to assess the structural capacity of subbase. A minimum of 30 FWD data points along the subbase section of interest should be obtained in order to adequately characterize the section (*29*).

Drainability

Pumping is a major cause of subbase voiding since eroded fine materials are transported under the slab to and through joints or cracks by water movement under pressure. When the subbase interface is not saturated, pumping action cannot transport or liquefy eroded fines significantly reducing the rate of erosion. The effect of precipitation on the number of wet weather days should be applied to adjust estimates of erosion.

Joint sealing appears to have an important effect on the incidence of interfacial saturation. Well-managed joint sealing could possibly minimize water and incompressible material infiltration into the joint and potential subgrade erosion or spalling of the joint. The longitudinal

joint sealing is particularly important since extensive amounts of surface water can enter through the lane/shoulder joints.

In design, the erosion rate should be weighted over dry and wet performance periods based on calibration for local conditions. Table 29 shows the adjustment factor of erosion rate according to annual wet days and joint sealing maintenance condition. Good joint sealing with low precipitation reduces erosion significantly and vice versa. The rate of erosion under dry conditions is approximately 25 percent of the wet condition rate of erosion.

Drainage conditions may also affect the effective number of wet weather days that the interfacial area is saturated. A good drainage system would remove water faster and reduce hydraulic erosion significantly. Therefore, surface drainage measures (along with regular resealing) and ditches should be provided to minimize the infiltration of water to subsurface, particularly through the longitudinally oriented joints or cracks.

Table 29 Erosion Rate Adjustment Factor Based on Annual Wet Days and Joint Seal Maintenance Condition.

Wet Days (day/year)	Joint Seal Maintenance Condition		
	Good	Moderate	Poor
>250	0.7	0.8	0.9
200–250	0.6	0.7	0.8
150–200	0.5	0.6	0.7
100–150	0.4	0.5	0.6
50–100	0.3	0.4	0.5
<50	0.2	0.3	0.4

BASE/SUBBASE DESIGN EXAMPLE USING THE DESIGN GUIDE SHEET

The base/subbase design guide sheet serves as a tool in the decision-making process regarding the selection of the base/subbase material type, thickness, and modulus relative to traffic level and environmental factors. An example of the base/subbase design process is explained as follows with input values in Figure 43.

Step 1: Input General Design Factors into the Design Guide Sheet

General input factors such as design period, overall material properties of PCC, and environmental factors in the design guide sheet are required and explained in Table 30.

Table 30 Input Factors of Design Guide Sheet − General.

Term	Description	Value in Example
Design period, *Y*	Years for traffic and erosion analysis that need to be decided reasonably to achieve economical layer thickness and material type	30 yr
PCC slab thickness	Design PCC layer thickness in inches	12 inches
Lane width	Design PCC layer width in feet	12 ft
Joint or crack spacing	Joint spacing of a JC pavement in feet or mean crack spacing of a CRC pavement in feet	6 ft (CRCP crack spacing)
PCC modulus	Elastic modulus of PCC. Default value is 4,000,000 psi	4,000,000 psi
PCC Poisson's ratio	Poisson's ratio of PCC. Default value is 0.15	0.15
PCC unit weight	Unit weight of PCC. Default value is 160 pcf	160 pcf
Compressive strength	Compressive strength of PCC obtained from unconfined compressive strength test. Default value is 6,000 psi	6,000 psi
Tensile strength	Tensile strength of PCC obtained from indirect tensile strength test. Default value is 600 psi	600 psi
CoTE of PCC	Coefficient of thermal expansion of PCC mainly governed by coarse aggregate type. Default value is 4×10^{-6} /°F for the PCC using limestone aggregate. CoTE for the PCC using gravel is 6×10^{-6} /°F	4×10^{-6} /°F

Table 30 Input factors of Design Guide Sheet – General (Continued).

Term	Description	Value in Example
PCC set temperature	Temperature of PCC during setting stage after paving. PCC will have zero volume change and stress at the set temperature. Volumetric change will occur by the gap between the set temperature and the current temperature of PCC, which results in curling and shrinkage stresses	90°F
Max. PCC top temperature	Maximum temperature on top of PCC during the curing period (earlier than 28 days), which can induce the early cracking by curling	105°F
Min. PCC top temperature	Minimum temperature on top of PCC during the curing period, which can induce the early cracking by shrinkage	60°F
PCC bottom temperature	Average temperature on bottom of PCC during the curing period	80°F
Wet days per year	Number of days for which precipitation was greater than 0.5 inch (12.7 mm) for the year. Data can be retrieved from long-term pavement performance (LTPP) data as the field name of "INTENSE_PRECIP_DAYS_YR" from the table of "CLM_VWS_PRECIP_ANNUAL"	100 day (dry area)
Max. ambient temperature	Highest air temperature during the curing period (earlier than 28 days), which can induce the early cracking by curling	100°F
Min. ambient temperature	Lowest air temperature during the curing period which can induce the early cracking by curling and shrinkage	55°F
Ambient relative humidity	Relative humidity of ambient during the curing period, which affects shrinkage and warping behaviors	50%
Equivalent damage ratio	Ratio converts lateral distribution across the wheel path into the traffic in the wheel path. A normal distribution is often assumed for the lateral distribution of traffic, and the traffic wandering range would be increased with wider lane width. Default is 0.7	0.7

BASE/SUBBASE DESIGN GUIDE SHEET

Input Design Factors

Traffic

Design period (yr)	ADT (two ways)	Percentage of Trucks (%)	Truck factor	Directional distribution factor	Lane Distribution Factor	Annual growth rate (%)	Vehicle speed (mph)
30	50,000	15	1.62	0.5	0.7	5	70

PCC layer

PCC slab thickness (inch)	Lane width (ft)	Joint or crack spacing (ft)	PCC modulus (psi)	PCC Poisson's ratio	PCC unit weight (pcf)	Compressive strength (psi)	Tensile strength (psi)
12	12	6	4,000,000	0.15	160	6,000	600

CoTE of PCC (inch/inch/°F)	PCC set temperature (°F)	Max. PCC top temperature (°F)	Min. PCC top temperature (°F)	PCC bottom temperature (°F)	Transverse load transfer devices	Longitudinal load transfer	Joint seal maintenance
0.000004	90	105	60	80	CRCP	Multi-lane	> 10yr (poo

Base layer

Base material type	Base thickness (inch)	Base modulus (psi)	Base Poisson's ratio	Base unit weight (pcf)	Base UCCS (psi)	Base friction coefficient	Base erodibility
AC	1.0	350,000	0.3	140	2,000	7.5	10

Subbase layer

Subbase material type	Subbase thickness (inch)	Subbase modulus (psi)	Subbase Poisson's ratio	Subbase unit weight (pcf)	Subbase UCCS (psi)	Subbase friction coefficient	Subbase erodibility
CTB-Limest	4.0	2,000,000	0.2	135	1,500	9	30

Subgrade layer

Subgrade material type	Subgrade k-value (psi/inch)	Subgrade modulus (psi)	Subgrade Poisson's ratio	Subgrade unit weight (pcf)	Subgrade UCCS (psi)	Subgrade friction coefficient	Subgrade erodibility
Sandy soil	150	6,000	0.35	130	20	1.1	500

Environmental factors and others

Wet days per year (day)	Max. ambient temperature (°F)	Min. ambient temperature (°F)	Ambient relative humidity (%)	Equivalent damage ratio	Drainage condition	Constructability	Cost analysis
100	100	55	50	0.7	Fair	Moderate	Moderate

Output Design Factors

Total ESAL in design lane	Effective ESAL in design lane	Max. deflection by loading (mils)	Effective thickness (inch)	Effective k-value (psi/inch)	Max. curling stress (psi)	Early cracking potential (%)	Max. subbase erosion during design life (%)
103,123,888	11,890,693	9.5	12.17	300	161.5	27	39

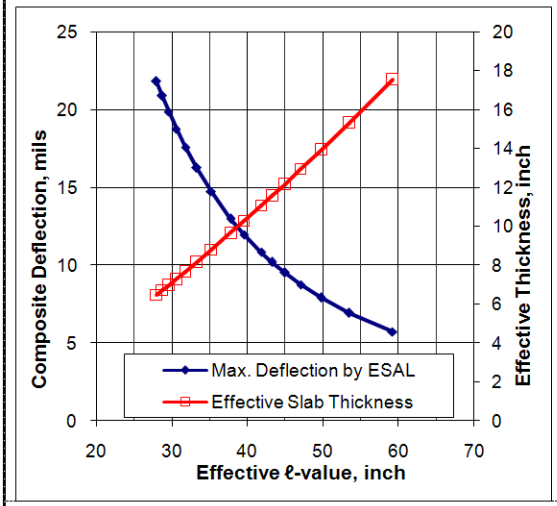

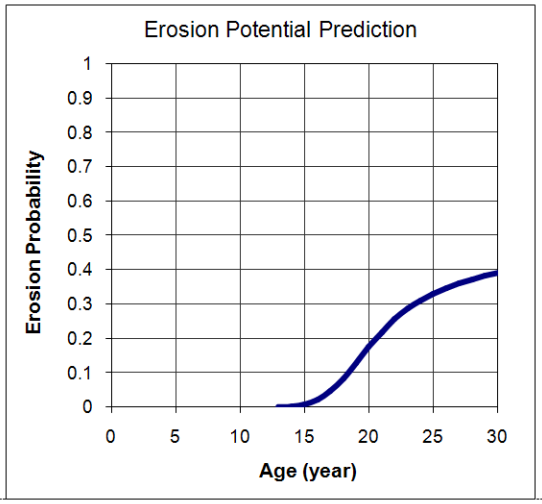

Figure 43 Screen shot of Base/Subbase Design Guide Sheet for Concrete Pavement.

Step 2: Estimate Traffic Data Based on Historical Data

Estimated traffic information such as ADT, percentage of truck, truck factor, directional and lane distribution factors, and annual growth rate is required in this step. Required traffic inputs for the design guide sheet are explained in Table 31.

Table 31 Input Factors of Design Guide Sheet − Traffic.

<table>
<tr><th>Term</th><th>Description</th><th>Value in Example</th></tr>
<tr><td>ADT (two way)</td><td>Average daily traffic in two directions at the start of the design period</td><td>50,000</td></tr>
<tr><td>Percentage of trucks, T</td><td>Percentage of trucks in the ADT</td><td>15%</td></tr>
<tr><td>Truck factor, T_f</td><td>Truck factor can be calculated by following equation (2):
$$T_f = \left(\sum_{i=1}^{m} p_i F_i\right) A$$
where, p_i is the percentage of total repetitions for the ith load group, F_i is the equivalent axle load factor (EALF) for the ith load group,
m is the number of load groups, and A is the average number of axles per truck</td><td>1.62</td></tr>
<tr><td>Directional distribution factor, D</td><td>Ratio of ADT in design direction usually assumed to be 0.5 unless the traffic in two directions is different</td><td>0.5</td></tr>
<tr><td>Lane distribution factor, L</td><td>Ratio of ADT in design lane which varies with the volume of traffic and the number of lanes. AASHTO guide recommended the following values (15):
<table><tr><th>No. of lanes in each direction</th><th>Percentage of 18-kip ESAL in design lane</th><th>Typical lane distribution factor</th></tr><tr><td>1</td><td>100</td><td>1.0</td></tr><tr><td>2</td><td>80–100</td><td>0.9</td></tr><tr><td>3</td><td>60–80</td><td>0.7</td></tr><tr><td>4</td><td>50–75</td><td>0.6</td></tr></table></td><td>0.7</td></tr>
<tr><td>Annual growth rate, r</td><td>Growth factor, G can be calculated by following equation recommended by AASHTO guide (15):
$$G = \frac{(1+r)^Y - 1}{r \cdot Y}$$</td><td>5%</td></tr>
</table>

Step 3: Select Base/Subbase Material Type

Material related design inputs are listed in Table 32 relative to: subbase type, thickness, modulus, Poison's ratio, unit weight, and unconfined compressive strength as a function of site-specific project conditions and subgrade characteristics. Other parameters of interest may be transport and stockpile related costs. A stabilizer may also be employed if needed (elaborated below) but a check of budgetary and Item 247 "Flexible Base" criteria should be made as part of this determination; otherwise, use an alternative material type. In the example (Figure 43), a 4 inch cement-treated (4 percent cement) limestone aggregate subbase and 1 inch AC base are used.

Table 32 Input Factors of Design Guide Sheet - Base, Subbase, and Subgrade.

<table>
<tr><th>Term</th><th>Description</th><th>Value in Example</th></tr>
<tr><td>Material type</td><td>Base: Select one among AC, bond-break layer, and No base
Subbase: Select one among untreated (flex) base, AC, and CTB-aggregate types (limestone, gravel, RC, and RAP), and No subbase
Subgrade: Input any soil type directly</td><td>Base: AC,
Subbase: 4% CTB - limestone,
Subgrade: Sandy soil</td></tr>
<tr><td>Thickness</td><td>Design layer thickness in inch. TxDOT design guide suggests using one of two types of base layer combinations: 1) 4 inches of AC pavement or asphalt stabilized base or 2) a minimum 1 inch AC bond breaker over 6 inch of a cement stabilized base</td><td>Base: 1 inch,
Subbase: 4 inch</td></tr>
<tr><td>Modulus</td><td>Elastic modulus of each layer obtained from the resilient modulus test. Without test results, the following values are recommended by Hall et al. (30):
<table>
<tr><th>Base Type</th><th>Modulus of Elasticity (psi)</th></tr>
<tr><td>Fine-grained soils</td><td>3,000–40,000</td></tr>
<tr><td>Sand</td><td>10,000–25,000</td></tr>
<tr><td>Aggregate</td><td>15,000–45,000</td></tr>
<tr><td>Lime-stabilized clay</td><td>20,000–70,000</td></tr>
<tr><td>Asphalt-treated base</td><td>300,000–600,000</td></tr>
<tr><td>Cement-treated base</td><td>1000 × (500+compressive strength)</td></tr>
<tr><td>Lean concrete base</td><td>1000 × (500+compressive strength)</td></tr>
</table></td><td>Base: 350,000 psi,
Subbase: 2,000,000 psi,
Subgrade: 6,000 psi</td></tr>
</table>

Table 32 Input Factors of Design Guide Sheet − Base, Subbase, and Subgrade (Continued).

<table>
<tr><th>Term</th><th>Description</th><th>Value in Example</th></tr>
<tr><td>Poisson's ratio</td><td>Poisson's ratio of each layer. Following typical values are recommended for design by Huang (2)
<table><tr><th>Material</th><th>Range</th><th>Typical</th></tr><tr><td>Hot mix asphalt</td><td>0.30–0.40</td><td>0.35</td></tr><tr><td>Portland cement concrete</td><td>0.15–0.20</td><td>0.15</td></tr><tr><td>Untreated granular materials</td><td>0.30–0.40</td><td>0.35</td></tr><tr><td>Cement-treated granular materials</td><td>0.10–0.20</td><td>0.15</td></tr><tr><td>Cement-treated fine-grained soils</td><td>0.15–0.35</td><td>0.25</td></tr><tr><td>Lime-stabilized materials</td><td>0.10–0.25</td><td>0.20</td></tr><tr><td>Lime-fly ash mixtures</td><td>0.10–0.15</td><td>0.15</td></tr><tr><td>Loose sand or silty sand</td><td>0.20–0.40</td><td>0.30</td></tr><tr><td>Dense sand</td><td>0.30–0.45</td><td>0.35</td></tr><tr><td>Fine-grained soils</td><td>0.30–0.50</td><td>0.40</td></tr><tr><td>Saturated soft clays</td><td>0.40–0.50</td><td>0.45</td></tr></table></td><td>Base: 0.3,
Subbase: 0.2,
Subgrade: 0.35</td></tr>
<tr><td>Unit weight</td><td>Unit weight of each layer in pcf</td><td>Base: 140 pcf,
Subbase: 135 pcf,
Subgrade: 130 pcf</td></tr>
<tr><td>UCCS</td><td>Compressive strength of each layer obtained from the unconfined compressive strength test. Approximate UCCS for subgrade are suggested as following by ACI (31):
<table><tr><th>Classification</th><th>Approximate UCCS, psi</th></tr><tr><td>Stiff, fine-grained</td><td>33</td></tr><tr><td>Medium, fine-grained</td><td>23</td></tr><tr><td>Soft, fine-grained</td><td>13</td></tr><tr><td>Very soft, fine-grained</td><td>6</td></tr></table></td><td>Base: 2,000 psi,
Subbase: 1,500 psi,
Subgrade: 20 psi</td></tr>
</table>

Step 4: Determine Base/Subbase Stabilization

The amount of stabilizer is a function of 7-day and 28-day UCCS requirements as depicted in Item 276 "Cement Treatment." The potential for early cracking by curling and warping behavior can be limited by reducing the percentage of cement. In the example (Figure 43), strength of base (2,000 psi) and subbase (1,500 psi) satisfy Item 276 "Cement Treatment" and 28-day UCCS requirements.

Step 5: Modify Base/Subbase Stabilization or Material Type Based on Erosion Considerations

Determine the proper amount of stabilizer relative to the maximum allowable erodibility as predicted by the design guide user sheet. Increase the percentage of stabilizer or change material type if the probability of erosion is higher than 80 percent at the end of the design period. Erodibilities of selected stabilized materials are listed in Table 33 based on Hamburg wheel-tracking device testing. Figure 45 shows variation of the probability of erosion as a function of subbase material type and stabilization level. In the example (Figure 43), erodibility of the AC bond breaker (10) in combination with the subbase (30) satisfies a maximum of 40 percent probability of erosion over a 30-year design period.

Table 33 Erodibility of Stabilized Base/Subbase Materials Using HWTD Test.

Aggregate Type and Percent of Stabilizer	Erodibility Using HWTD Test, mm/10,000 load repetitions			
	Natural Gravel Base (Limestone and Soil)		Reclaimed Asphalt + Soil (1:2)	100% Recycled Concrete
Stabilizer type	Asphalt	Cement	Cement	Cement
0	1.5	1.5	2.0	2.5
2	0.5	1.0	1.5	2.0
4	0.2	0.3	0.5	0.8
6	0.1	0.2	0.4	0.5

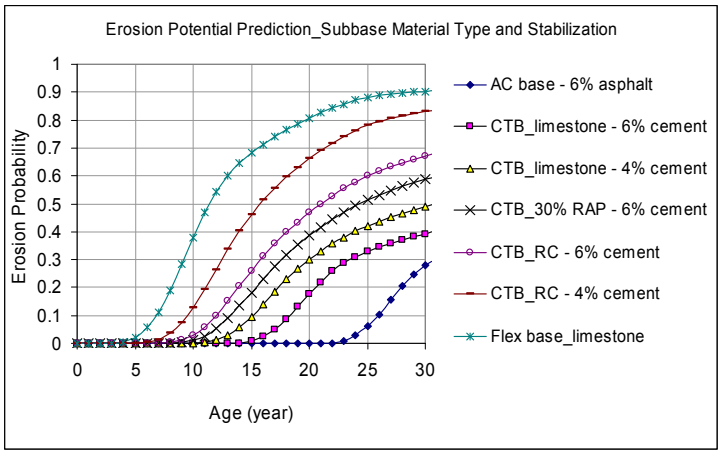

Figure 44 Erosion Potential versus Material Type and Stabilization Level.

Step 6: Adjust Base/Subbase Stabilization or Material Type Based on Subbase Friction

Friction between concrete and base/subbase should be limited to ensure crack-free construction. The coefficient of friction can be governed to some extent by choice of subbase material type or by use of an interlayer bond breaker. In the example (Figure 43), 1 inch AC layer is used as a bond breaker to provide a moderate level of friction. It may be possible to use a CTB without a bond breaker but provisions for increased steel contents for CRC design should be made to compensate for the additional change in cross-section. Friction coefficients listed in Table 34 are recommended by AASHTO (*15*). Coefficient greater than 20 may generate a high chance of bottom up reflection cracking. In the example (Figure 43), friction coefficient of base (7.5) and subbase (9.0) are employed.

Table 34 Typical Friction Coefficient of Stabilized Base/Subbase Materials.

Subbase/Base type	Friction Coefficient		
	Low	Mean	High
Fine grained soil	0.5	1.1	2
Sand	0.5	0.8	1
Aggregate	0.5	2.5	4
Lime-stabilized clay	3	4.1	5.3
ATB	2.5	7.5	15
CTB	3.5	8.9	13
Soil cement	6	7.9	23
LCB	3	8.5	20
LCB not cured	> 36 (higher than LCB cured)		

Step 7: Select Base/Subbase Thickness

Subbase thickness can be selected as a function of the expected deflection and the limiting level of faulting or erosion voiding (as would be predicted by the spreadsheet). In the example (Figure 43), maximum deflection is 9.5 mils, which is less than the design deflection criteria of 10 mils (can be defined by engineer relative to pavement type, subbase stiffness, traffic levels, etc.). Therefore, the 1 inch AC base and 4 inch CTB satisfied the design thickness design criteria.

Step 8: Check Load Transfer Efficiency

The change in deflection and the potential for erosion due to a change in LTE can be simulated using the design guide worksheet. The level of LTE is not directly related to the design of the base/subbase layer but does have a role in the potential for subbase erosion. Figure 45 shows how a variation of composite deflection affects the probability of erosion as a function of the load transfer conditions. In the example (Figure 43), deflection and erosion probabilities are controlled by the level of load transfer as a function of the transverse crack stiffness and the characteristics of the tie bars used in the longitudinal joint between the slab and the tied PCC shoulder.

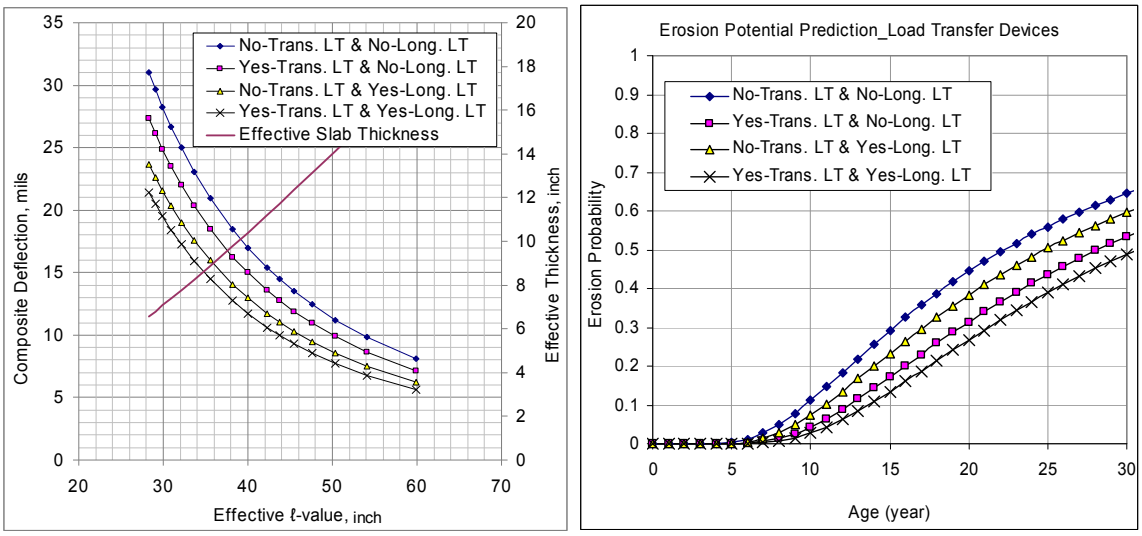

Figure 45 Erosion Potential versus Load Transfer Devices.

Step 9: Check the UCCS of Base/Subbase or SCI

A check of structural capacity of the subbase is made to ensure adequate support for construction equipment and operations. The levels of stabilization can be adjusted as required. Typically, if the opening UCCS is less than 350 psi or SCI is greater than 40, adjustments are necessary unless the deflection and erosion requirements are satisfied. Material cost, construction expenditure, and construction time should also be considered with the performance requirements to select a most economical design.

Step 10: Consider Precipitation and Drainage Conditions

The potential for moisture to reside below the slab affects the potential for erosion. The greater the potential to trap water the greater the amount of stabilization needed to resist the tendency for erosion and deterioration of the level of support. Better drainage and faster removal of water would also reduce hydraulic erosion significantly. The AASHTO guide suggests in Table 35 different drainage levels based on exit time (*15*). Figure 46 shows how erosion potential varies according to different drainage conditions (with poor joint seal condition) and joint seal condition (with very poor drainage conditions).

Table 35 Drainage Quality Based on the Time of Water Removing from Pavement.

Quality of Drainage	Water Removed Within
Excellent	2 hours
Good	1 day
Fair	1 week
Poor	1 month
Very poor	(water will not drain)

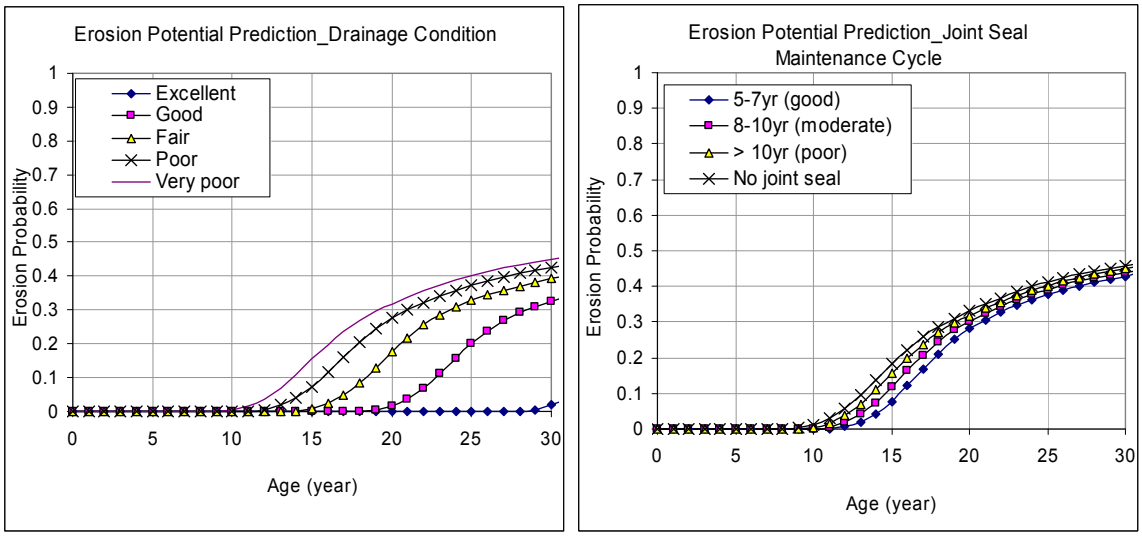

Figure 46 Erosion Potential versus Drainage and Joint Seal Maintenances.

Step 11: Cost-Effective Erosion-Resistant Design

Design process should consider other design factors affecting cost-effectiveness as listed in Table 36.

Table 36 Output Factors of Design Guide Sheet.

Term	Description	Value in Example
Total ESAL in design lane	Total equivalent single axle load during design period, ESAL can be calculated by following equation (*2*): $\text{ESAL} = Y \cdot 365 \cdot \text{ADT} \cdot T \cdot T_f \cdot D \cdot L \cdot G$	103,123,888
Effective ESAL in design lane	Equivalent number of ESAL under the most critical condition for erosion (sub-layers are saturated and all loading pass over wheel path only) matching with HWTD erosion test condition. It can be expressed simply as the following equation: $\text{Effective ESAL} = \text{Wet days}/365 \times \text{EDR} \times \text{ESAL}$	11,890,693
Max. deflection by loading	Maximum deflection by an 18-kip axle loading on the design pavement system	9.5×10^{-3} in (9.5 mils)

Table 36 Output Factors of Design Guide Sheet (Continued).

Term	Description	Value in Example
Effective thickness (unbonded conditions)	Composite thickness of PCC, base, and subbase layers to calculate the deflection by loading. It can be calculated using the following equation: $$h_e = \sqrt[3]{h_c^3 + \frac{E_b}{E_c} h_b^3}$$ h_e is the effective thickness of combined slab, h_c is the thickness of concrete slab, h_b is the thickness of base, E_c is the elastic modulus of concrete, and E_b is elastic modulus of base	12.17 inches
Effective k-value	Composite k-value of a single sub-layer converted from multi-layers (base, subbase, and subgrade) to calculate the deflection and stress of PCC by curling. It can be calculated by matching the curling deflection of the equivalent single layer with the curling deflection of the multi-layered system (tabulated by FE program analysis)	300 psi/in
Max. curling stress	Maximum tensile stress on PCC by curling. Curling occurs by the temperature difference between the top surface and bottom surface of PCC	161.5 psi
Early cracking potential	When the curling stress is higher than PCC tensile strength (this normally happens during the curing period), PCC would have a high chance of early cracking	27%
Max. subbase erosion during design life	Erosion of sub-layers would develop continuously during service period at the joint or crack locations. When the ultimate erosion depth is higher than design criteria, try more stabilizer or change material type to decrease erosion rate and erosion depth accordingly	39%

CHAPTER 6
SUMMARY AND CONCLUSIONS

The performances of subbases of selected pavement sections were investigated using a number of techniques including visual survey and nondestructive testing. Generally, untreated subbases have not performed well, particularly over moisture-sensitive subgrades while most CSB over sound subgrades have performed well.

Well maintained joint seals seem to be effective in blocking surface water from intruding the pavement section and helping reduce hydraulic pumping action. Loss of support seemed to be the primary reason for many of the early failures of pavement observed during this study; loss of support quickly led to insufficient stiffness of the associated joints. Accordingly, routine monitoring and timely sealing of joints and cracks could extend good support conditions cost effectively by minimizing the deterioration cycle.

Ideally, a subbase layer will consist of sufficient strength and erosion resistance, a moderate level of friction, some potential to chemically bond to the slab, and a conforming but uniform support. A subbase layer should be adequately flexible to minimize curling and warping-related stress but free of any tendencies to reflect cracking into the concrete slab. Additionally, a medium level of frictional restraint is desired to minimize the shear stress between the concrete and the base layer at an early slab age. Considering these characteristics in light of the objective of identifying alternative subbase types and materials, CTB, RAP, and the subbase materials using recycled concrete were selected as some of the most feasible candidate alternative subbase combinations.

Over the years, a bond breaker layer has been used to improve the effect of the reinforcing steel to achieve suitable cracking patterns in CRC pavement. Therefore, some measures are required to keep friction levels to tolerable limits in order to utilize a CTB and similar subbase materials.

Previous erosion test methods were reviewed and key points of each test method were summarized (details available in report 0-6037-1 [*1*]). According to these reviews, the paramount to formulating a new test procedure were featured such as the generation of an erodibility index and having applicability to field conditions. A new test method was formulated around using a rolling wheel erosion test device mainly due to the possibility of minimizing

many of the shortcomings of previous test methods such as long test times, no voiding, or difficult shear stress interpretation conditions.

Previous erosion models were reviewed and summarized (again, details available in technical report 0-6037-1). The mechanistic model by Jeong and Zollinger (*12*) was found to be the most suitable for improvement based on the ease of calibration through lab testing and field data. Lab test results using the new test method were applied for the model calibration process.

According to the review of previous subbase design guides, the NCHRP 1-37A MEPDG (*17*) presented some of the most comprehensive guidance with respect to erodibility classification determined based on dry condition brush test and strength test results. However, erosion since occurs mostly under saturated conditions; the new design guide employed for subbase erosion is based on wet condition test results relative to site-specific materials.

The NCHRP design guide provides general recommendations for subbase classification based on load transfer efficiency and traffic level but there is little guidance for other details such as layer thickness. For instance, high volume conditions may require high joint load transfer with an erosion-resistant base. Consequently, MEPDG design recommendation can be only roughly applied for material selection and stabilization level design.

The proposed test method is mechanical in nature using the HWTD, which qualifies a subbase tested under wet conditions relative to the magnitude of the shear stress creating the erosive action. This provides a significant advantage over other approaches in terms of the translation of laboratory derived erosion rates to performance in the field. This test method indicates subbase erosion under the contact of a concrete layer and even though void development occurs under wet conditions; erosion under dry conditions can be estimated from the wet condition test results. Moreover, this approach allows for testing of a core sample from the field as well as laboratory compacted samples in a relatively short period of time while providing a wide range of applicability to all types of subbase or subgrade materials.

Three types of materials (Flex, RC, and RAP) treated by various cement contents (0, 2, 4, 6 percent) were tested and evaluated under different stress levels and number of loads. As expected, more weight loss develops as shear stress and loading applications increase; however, the rate of weight loss drops off to some extent at higher stress levels and loading numbers. RC base materials show the highest erosion rate, and RAP base materials show the least erosion rate as long as the fine-size aggregate fraction is equivalent to other materials since the amount of

asphalt mastic increases shear strength. Up to 2 percent cement for Flex and RAP subbases, however, does not reduce the erosion rate significantly, but 4 percent cement reduces erosion remarkably when compared with unstabilized materials.

The HWTD test method can generate sufficient data in which to determine the model a and ρ parameter values, which are assumed to be applicable for assessing the erosion under both the wet and dry conditions. The weighting of the wet and dry conditions is a matter of calibration to local performance. A paired t-test analysis was conducted to validate proposed erosion model at a confidence level of 95 percent and there was statistically no difference between measured and fitted values.

Effects of friction between concrete slab and subbase and effects of the subbase support stiffness, which is expressed in terms of the subgrade k-value, were analyzed using ISLAB2000, CRCP-10, and MEPDG programs. CRCP-10 and MEPDG were used to verify friction effects; and ISLAB2000, CRCP-10, and MEPDG were used for the evaluation of subbase support stiffness effects. Crack spacing, crack width, steel stress, punchout, and roughness were determined as indicators to assess the long-term performance of concrete pavement system.

Also, on the basis of the FE analysis, the nighttime nonlinear temperature gradient condition led to the critical stress condition in the PCC slab. Because excessive stress conditions in the subbase layer could produce subbase distresses such as cracks, the stress responses in the subbase layer should be considered when selecting alternative subbase materials.

The decision process for the design and subbase material type selection is categorized into three areas of consideration or criteria: materials, design, and sustainability. The process begins with the selection of material factors such as type, strength, and erodibility requirements. Design factors include friction/bond characteristics, layer thickness, and traffic considerations. Finally, the design engineer considers the sustainability the subbase layer affords the overall pavement design. Load transfer, constructability, and drainability as well as precipitation and joint sealing maintenances should be considered in the design process in order to fully account for erosion damage. Accordingly, following this decision process, the design engineer should evaluate the key factors associated with a given subbase configuration.

The guidelines, design sheet, and material specifications are provided to assist the economical and sustainable design of a concrete pavement subbase layer. Many design factors that affect the performance of the subbase are recommended based on many references; however,

the service history of existing pavements on similar layer properties and environmental conditions should be considered first if available

REFERENCES

1. Jung, Y., D.G. Zollinger, M. Won, and A.J. Wimsatt. "Subbase and Subgrade Performance Investigation for Concrete Pavement," Research Report 0-6037-1. Texas Transportation Institute, The Texas A&M University System, College Station, Texas, May 2009.

2. Huang, Y.H. *Pavement Analysis and Design 2nd Edition*. Pearson Prentice Hall, Upper Saddle River, New Jersey, 2004.

3. Phu, N.C., and M. Ray. "The Erodibility of Concrete Pavement Subbase and Improved Subgrade Materials." Bulletin de Liaison des Laboratoires des Ponts et Chaussees, France, Special Issue 8, July 1979, pp. 32-45.

4. "Pavement – Soil Cement." Portland Cement Association, Skokie, Illinois, http://www.cement.org/pavements/pv_sc.asp, updated: 2008. Accessed: October 1, 2008.

5. "Reclaimed Asphalt Pavement-User Guideline-Asphalt Concrete." Turner-Fairbank Highway Research Center, McLean, Virginia, http://www.fhwa.dot.gov/publications/research/infrastructure/structures/97148/rap132.cfm. Accessed: October 1, 2008.

6. Guthrie, W.S., S. Sebesta, and T.Scullion. "Selecting Optimum Cement Contents for Stabilized Aggregate Base Materials." Report 4920-2. Texas Transportation Institute, The Texas A&M University System, College Station, Texas, February 2002.

7. Van Wijk, A.J. "Rigid Pavement Pumping: (1) Subbase Erosion and (2) Economic Modeling." Joint Highway Research Project File 5-10. School of Civil Engineering, Purdue University, West Lafayette, Indiana, May 16, 1985.

8. de Beer, M. "Aspects of the Erodibility of Lightly Cementitious Materials." Research Report DPVT 39, Roads and Transport Technology, Council for Scientific and Industrial Research, Pretoria, South Africa.

9. Rauhut, J.B., R.L. Lytton, and M.I. Darter. "Pavement Damage Functions for Cost Allocation, Vol. 1, Damage Functions and Load Equivalency Factors." Report No. FHWA/RD-82/126, July 1982.

10. Markow, M.J., and B.D. Brademeyer. "EAROMAR Version 2." Final Technical Report, FHWA/RD-82/086, April 1984.

11. Larralde, J. "Structural Analysis of Ridge Pavements with Pumping." Ph.D. Thesis, Purdue University, West Lafayette, Indiana, December 1984.

12. Jeong, J., and D. Zollinger. "Characterization of Stiffness Parameters in Design of Continuously Reinforced and Jointed Pavements." Transportation Research Record 1778, TRB, National Research Council, Washington, D.C., 2001, pp. 54-63.

13. TxDOT Manual. "Pavement Design Guide," http://onlinemanuals.txdot.gov/txdotmanuals/pdm/reocmmended_input_design_values.htm. Updated: November 1, 2008; accessed: October 1, 2009.

14. TxDOT Standard Specifications Item 276. "Cement Treatment (Plant-Mixed)." http://www.txdot.gov/txdot_library/consultants_contractors/publications/specifications.htm. Updated: June 1, 2004; accessed: October 1, 2009.

15. "AASHTO Guide for Design of Pavement Structures." American Association of State Highway and Transportation Officials, Washington, D.C., 1986.

16. Packard, R.G. "Thickness Design for Concrete Highway and Street Pavements." Portland Cement Association, Skokie, Illinois, 1984.

17. NCHRP, *Guide for Mechanistic-Empirical Design of New and Rehabilitated Pavement Structures, Final Report*. "Part 2. Design Inputs, Chapter 2. Material Characterization." National Cooperative Highway Research Program, http://www.trb.org/mepdg/guide.htm. Updated: August 2003; accessed: October 1, 2009.

18. NCHRP, *Guide for Mechanistic-Empirical Design of New and Rehabilitated Pavement Structures, Final Report*. "Part 3. Design Analysis, Chapter 4. Design of New and Reconstructed Rigid Pavements." National Cooperative Highway Research Program, http://www.trb.org/mepdg/guide.htm. Updated: August 2003; accessed: October 1, 2009.

19. NCHRP, *Guide for Mechanistic-Empirical Design of New and Rehabilitated Pavement Structures, Final Document*. "Appendix JJ: Transverse Joint Faulting Model." National Cooperative Highway Research Program, http://www.trb.org/mepdg/guide.htm. Updated: August 2003; accessed: October 1, 2009.

20. Phu, N.C., and M. Ray. "The Hydraulics of Pumping of Concrete Pavements." Bulletin de Liaison des Laboratoires des Ponts et Chaussees, Special Issue 8, France, July 1979, pp. 15-31.

21. Westergaard, H.M. "Analysis of Stresses in Concrete Pavements Due to Variations of Temperature." *Proceeding.*, *Highway Research Board*, Vol. 6, Washington, D.C., pp. 201-215, 1926.

22. Bradbury, R.D. *Reinforced Concrete Pavement*. Wire Reinforcement Institute, Washington, D.C., 1938.

23. Jang, SeHoon. "Automated Crack Control Analysis for Concrete Pavement Construction." Master's Thesis, Texas A&M University, College Station, Texas, August 2005.

24. Huang, Y.H. *Pavement Analysis and Design.* Prentice Hall, Inc., Englewood Cliffs, New Jersey, 1993.

25. Khazanovich, L., H.T. Tu, S. Rao, K. Galasova, E. Shats, and R. Jones. "ISLAB2000 – Finite Element Analysis Program for Rigid and Composite Pavements." ERES International, Champaign, Illinois, 2000.

26. Lim, S., D. Kestner, D.G. Zollinger, and D.W. Fowler. "Characterization of Crushed Concrete Materials for Paving and Non-paving Applications." Report 4954-1. Texas Transportation Institute, The Texas A&M University System, College Station, Texas, January 2003.

27. "Summary of Texas Recycled Concrete Aggregate Review." United States Department of Transportation—Federal Highway Administration, http://www.fhwa.dot.gov/pavement/recycling/rcatx.cfm. Modified: July 18, 2006; accessed: October 1, 2008.

28. Hall, J.W., J. Mallela, and K.L. Smith. "Report IPRF-01-G-002-021(G) Stabilized and Drainable Base for Rigid Pavement: A Design and Construction Guide." JP010P, American Concrete Pavement Association, Skokie, Illinois, October 2005.

29. Scullion, T. "Incorporating a Structural Strength Index into the Texas Pavement Evaluation System." TTI Research Report 409-3F. Texas Transportation Institute, The Texas A&M University System, College Station, Texas, April 1988.

30. Hall, K.T., M.I. Darter, T.E. Hoerner, and L. Khazanovich. "LTPP DATA ANALYSIS Phase I: Validation of Guidelines for k-Value Selection and Concrete Pavement Performance Prediction." Research Report No. FHWA-RD-96-198, ERES Consultants, Inc., Champaign, Illinois, January 1997.

31. ACI Committee 325. "Guide for Design of Jointed Concrete Pavements for Streets and Local Roads." ACI Committee Report 325. 12R-02, American Concrete Institute, 2002.

32. Kim, S., M.C. Won, and B.F. McCullough. "Three-Dimensional Nonlinear Finite Element Analysis of Continuously Reinforced Concrete Pavements." University of Texas at Austin, Center for Transportation Research, February 2000.

APPENDIX A:
SUPPLEMENTAL ANALYSIS OF RESPONSE OF PCC SLABS

The effectiveness of various subbase combinations (relative to the range of conditions represented in the alternative materials proposed for subbase use) on PCC pavement performance was assessed over a range of subbase stiffness values to analyze the effect on PCC pavement performance. To this end, finite element analysis was performed using the ABAQUS 6.7 computer program.

FE Model

The finite element configuration adopted for this analysis is shown in Figure 47. A two-dimensional (2-D) plain strain element type was selected where the subbase and subgrade support was modeled by Winkler foundation. The slab thickness of 10 inches and length of 10 ft was assumed for this analysis. Based on symmetry, half of the slab has been modeled with appropriate boundary conditions. The developed FE model has a 1 inch mesh size in all directions.

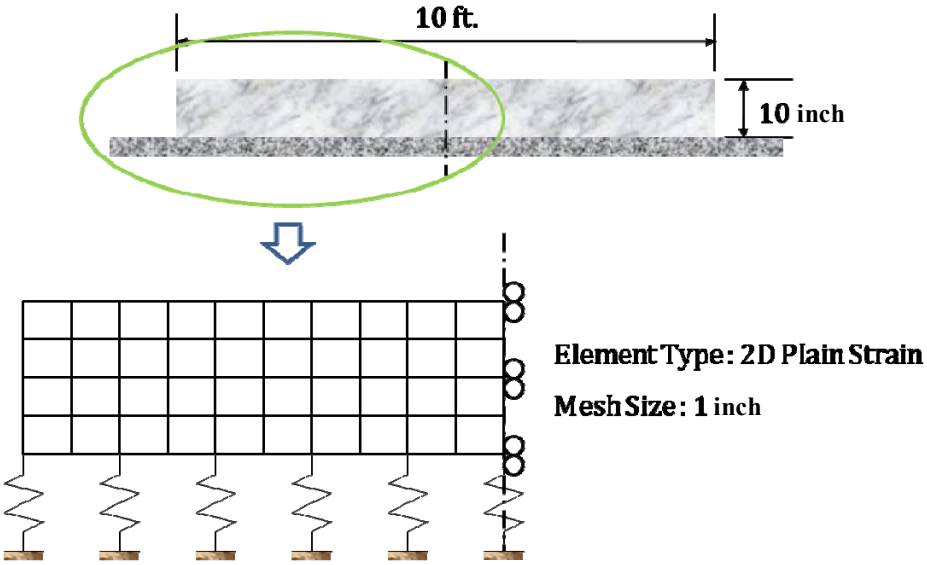

Figure 47 Finite Element Configuration.

Input Values and Analysis Cases

Selected concrete material and subbase properties are shown in Table 37 and Table 38. The subbase modulus of subgrade reaction value (k-value) was varied from 100 pci to 1,500 pci.

Table 37 Concrete Property.

Concrete Property	Value
Elastic Modulus	4.5×10^6 psi
Poisson's Ratio	0.15
Concrete Density	150 lb/ft^3
Coefficient of Thermal Expansion	6×10^{-6}/F

Table 38 Subbase Property.

Subbase Property	Value (pci)
Modulus of Subgrade Reaction (k-value)	100 300 500 800 1,000 1,500

Figure 48 shows the temperature gradients, which were varied from linear to 2nd and 3rd order for this analysis where the temperature variation between top and bottom was 30°F. Also, to compare daytime and nighttime temperature conditions, a positive temperature gradient (daytime condition) and a negative temperature gradient (nighttime condition) were designated in the analysis input.

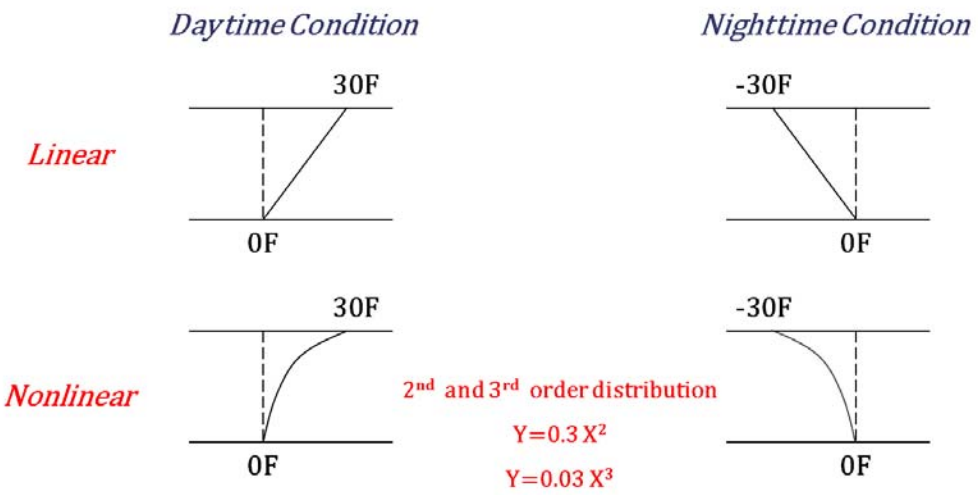

Figure 48 Temperature Gradients for Analysis Input.

To evaluate stresses due to the described temperature loading, analysis cases shown in Table 39 were performed. In these case studies, the effects of k-value on stress and deflection (under both linear and nonlinear temperature distribution) were determined. The stresses on top and bottom surfaces of the PCC slab have not only been compared but also stress at slab center through the slab depth has been noted. Moreover, deflections of the PCC slab were compared for all analysis cases. To verify stresses due to wheel loading, Westergaard's interior loading condition was considered where the PCC slab thickness of 8, 10, and 13 inches were varied along with k-values ranging from 100 psi/inch to 1,000 psi/inch in 100 psi/inch increments.

Table 39 Analysis Cases.

Temperature Condition	k-value (psi/inch)	Output
Linear	100 300 500 800 1,000 1,500	Top Stress Bottom Stress Stress at Slab Center Vertical Movement
2nd Order Nonlinear		
3rd Order Nonlinear		

Results

Figure 49 illustrates the stress distributions under daytime temperature gradient conditions. Red colored zones in the figure represent the tensile stressed area, and the green color presents the compressive stressed area. Nonlinear temperature gradient generates a larger red color zone than a linear temperature gradient condition does. Therefore, considering nonlinear temperature gradient conditions appears to be more critical for assessment of subbase or other pavement design-related effects.

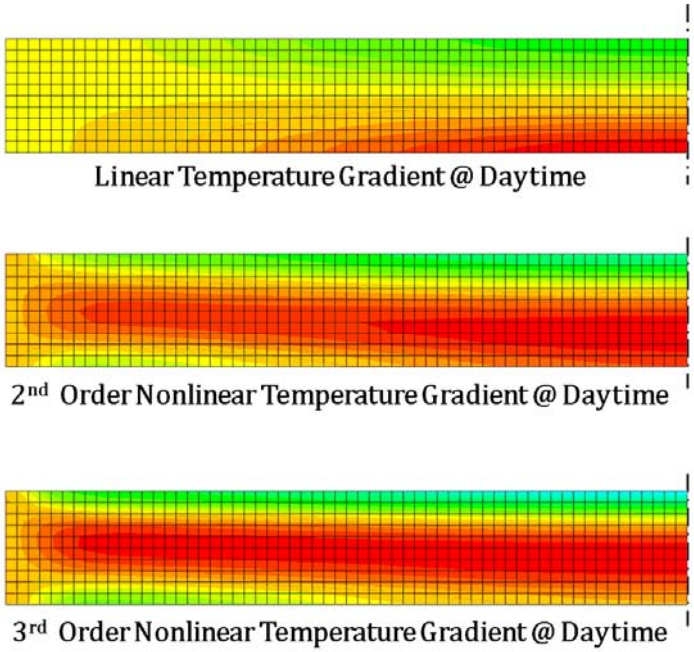

Figure 49 Stress Distributions at Daytime Temperature Condition.

Figure 50 presents daytime, mid-slab stresses at the top and bottom. Although tensile stress at the bottom surface of the slab increases with the modulus of subgrade reaction under both linear and nonlinear temperature gradient conditions, compared with the linear temperature gradient condition, nonlinear temperature gradients induce less tensile stress. These results tend to suggest that daytime temperature conditions are not as critical as other conditions may be.

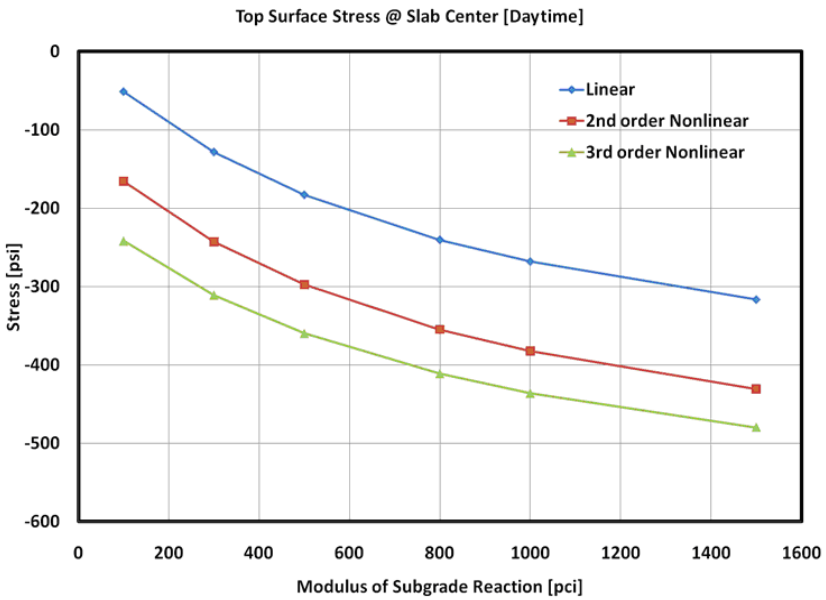

(a) Top Surface

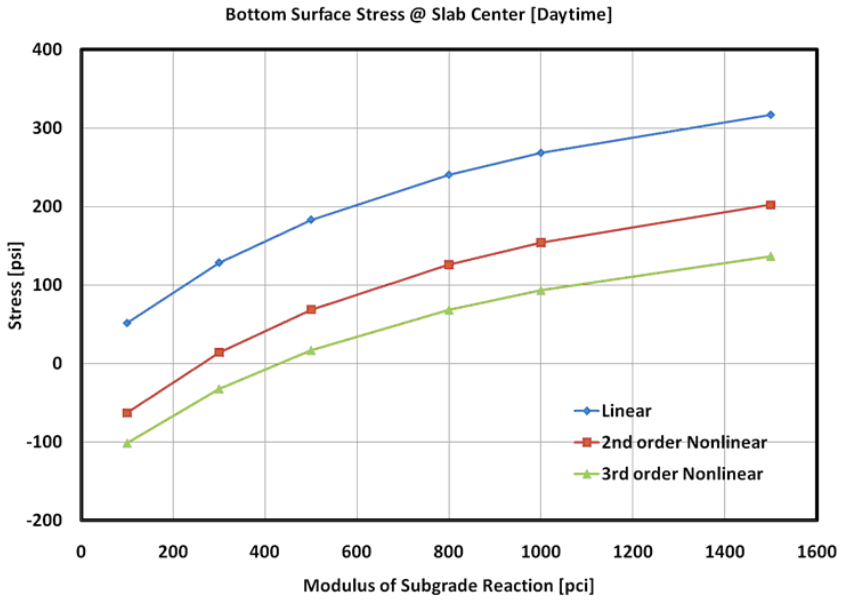

(b) Bottom Surface

Figure 50 Stress at Slab Center on Daytime Temperature Gradient Condition.

Figure 51 shows daytime mid-slab stress distributions along the PCC slab depth. Although maximum tensile stress is generated at the slab bottom surface under a linear temperature condition, the maximum tensile stress occurs away from the PCC slab surface under a nonlinear temperature gradient.

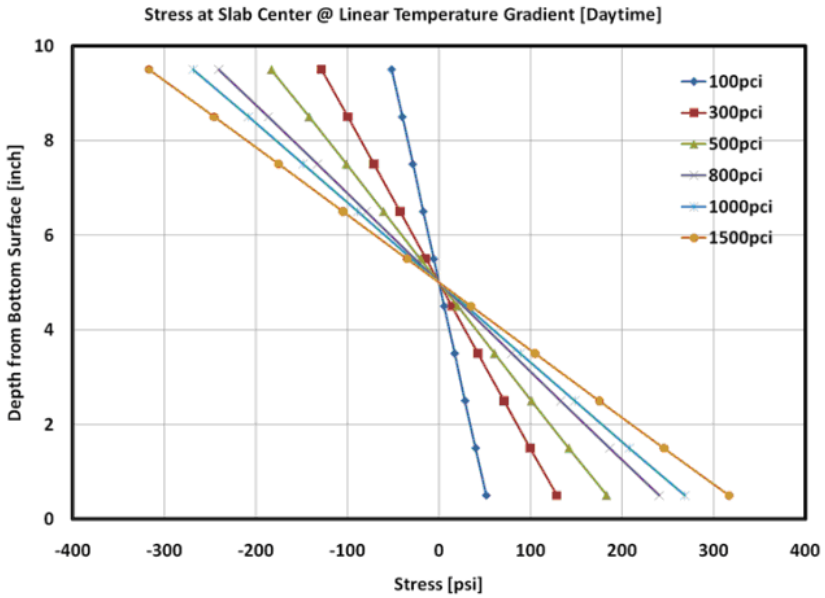

Linear Temperature Gradient

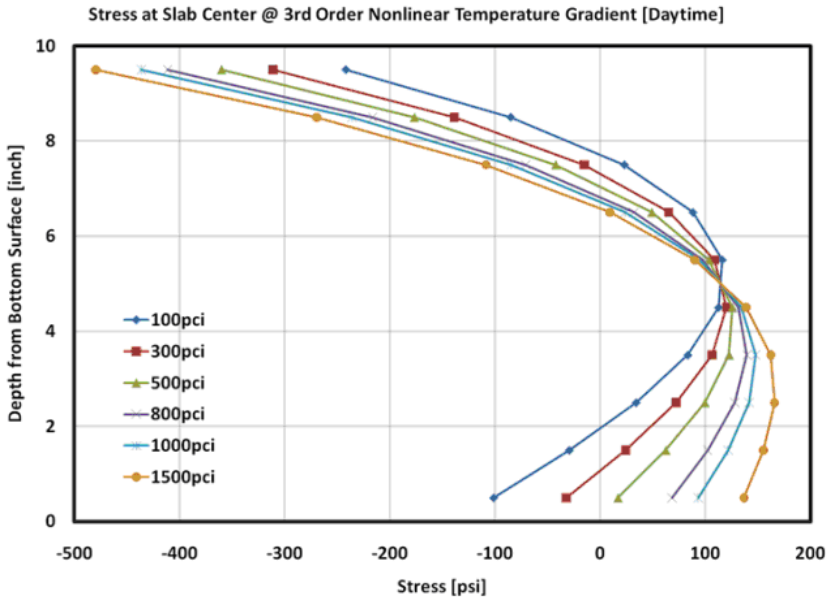

3rd order Nonlinear Temperature Gradient

Figure 51 Stress Distributions at Slab Center along Slab Depth on Daytime Condition.

Figure 52 illustrates the nighttime stress distributions. Red colored zones in the figure represent the tensile stressed area, and the green color presents the compressive stressed area. Compared with daytime temperature conditions, the tensile stress at the top of the slab and compressive stress at the bottom of the slab in both of linear and nonlinear temperature gradient conditions are shown. Also, a linear temperature gradient generates a larger tensile stress zone than in the case of nonlinear temperature gradient condition.

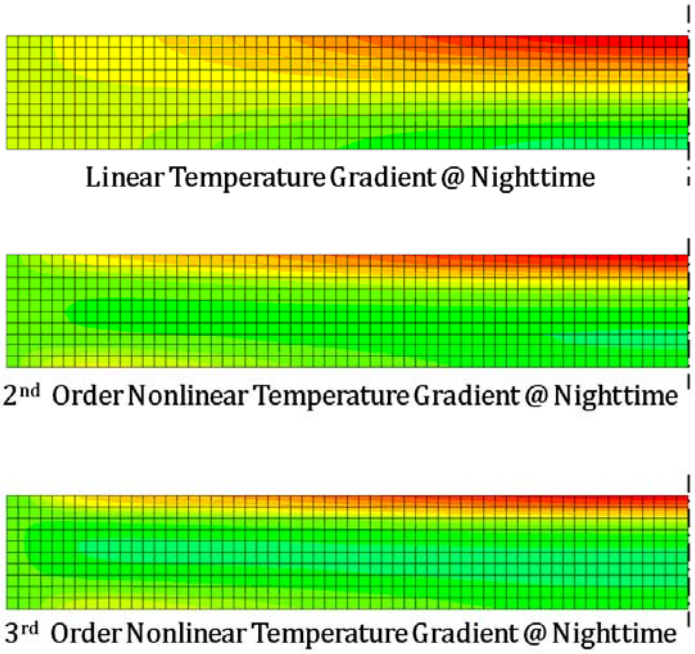

Figure 52 Stress Distributions at Nighttime Temperature Condition.

Figure 53 presents nighttime mid-slab stresses at the top and bottom of the PCC slab. Tensile stress at the top surface of the slab increases with the modulus of subgrade reaction. Also, compared with linear temperature gradient condition, nonlinear temperature gradients induce higher tensile stress. These analysis results suggest that the nonlinear nighttime temperature condition is critical.

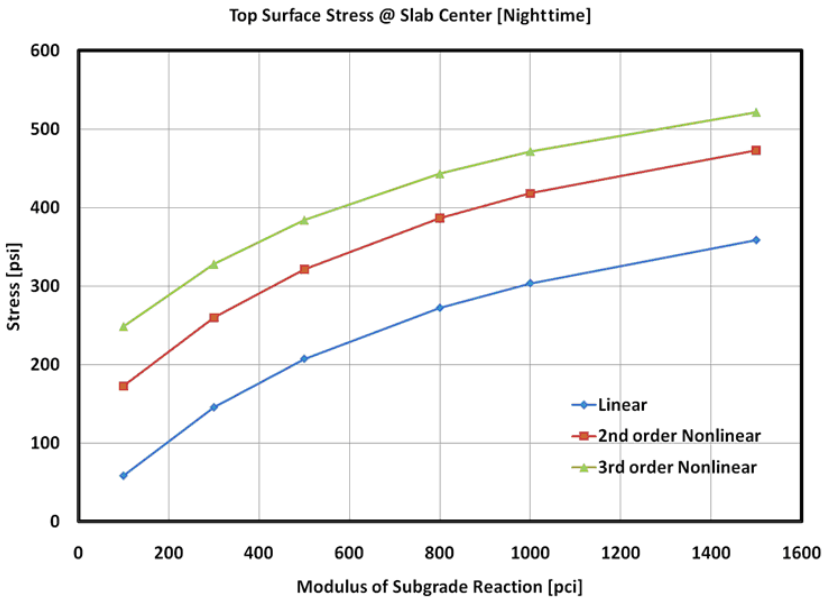

(a) Top Surface

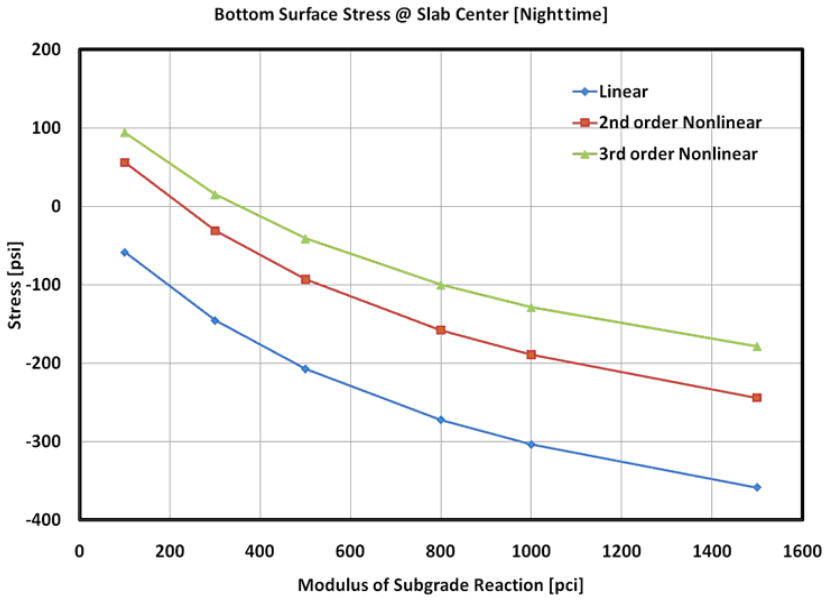

(b) Bottom Surface

Figure 53 Stress at Slab Center on Nighttime Temperature Gradient Condition.

Figure 54 shows nighttime, mid-slab stress distributions along the PCC slab depth. The maximum tensile stress generated at the slab surface under both linear and nonlinear temperature cases is shown. Based on these FE studies, the nonlinear nighttime temperature gradient condition is critical.

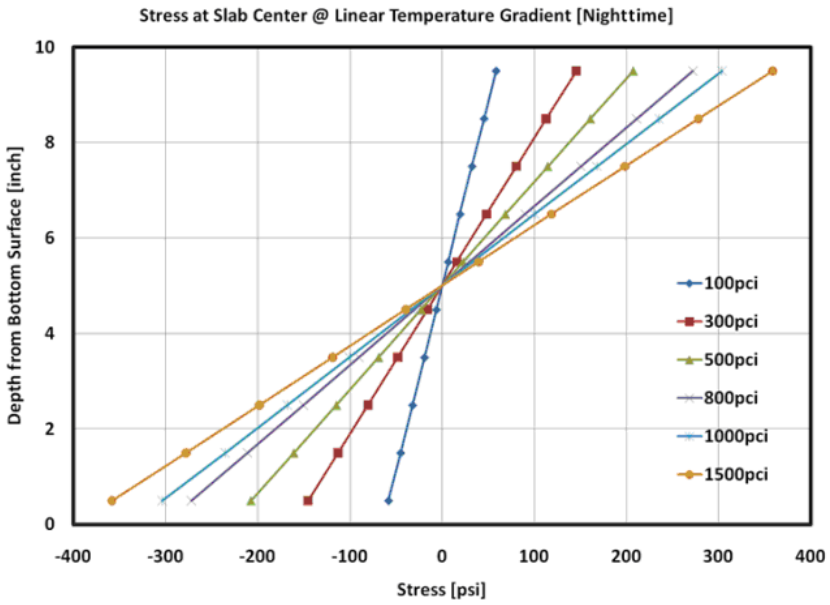

Linear Temperature Gradient

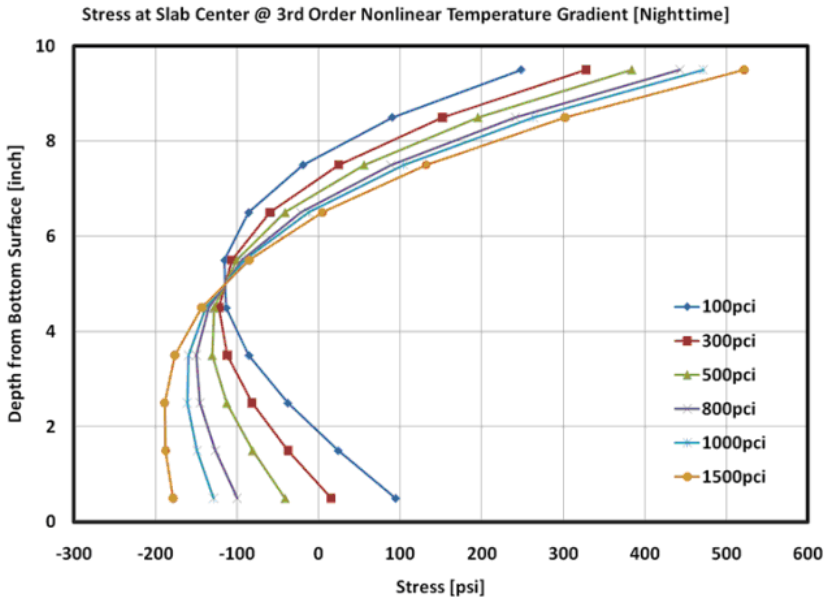

3rd order Nonlinear Temperature Gradient

Figure 54 Stress Distributions at Slab Center along Slab Depth on Nighttime Condition.

Alternatively, vertical movements of the PCC slab have been examined under a variety of temperature gradient conditions. Figure 55 and Figure 56 show the analysis results. Here, relative vertical movements between slab center and slab edge were determined to highlight the theoretical amount of slab curvature due to a change of modulus of subgrade reaction. As shown in Figure 55 and Figure 56, the relative vertical movements between slab center and edge decrease as k-value increases under both daytime and nighttime temperature gradients. However, there were no differences between the linear and nonlinear gradient conditions.

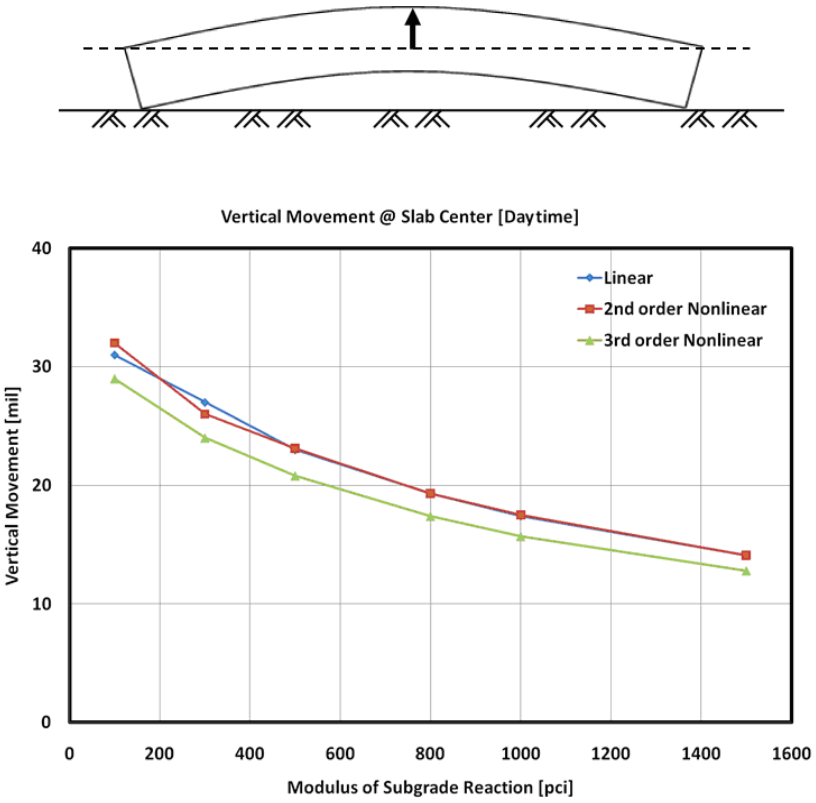

Figure 55 Daytime Relative Vertical Movements between Slab Center and Edge.

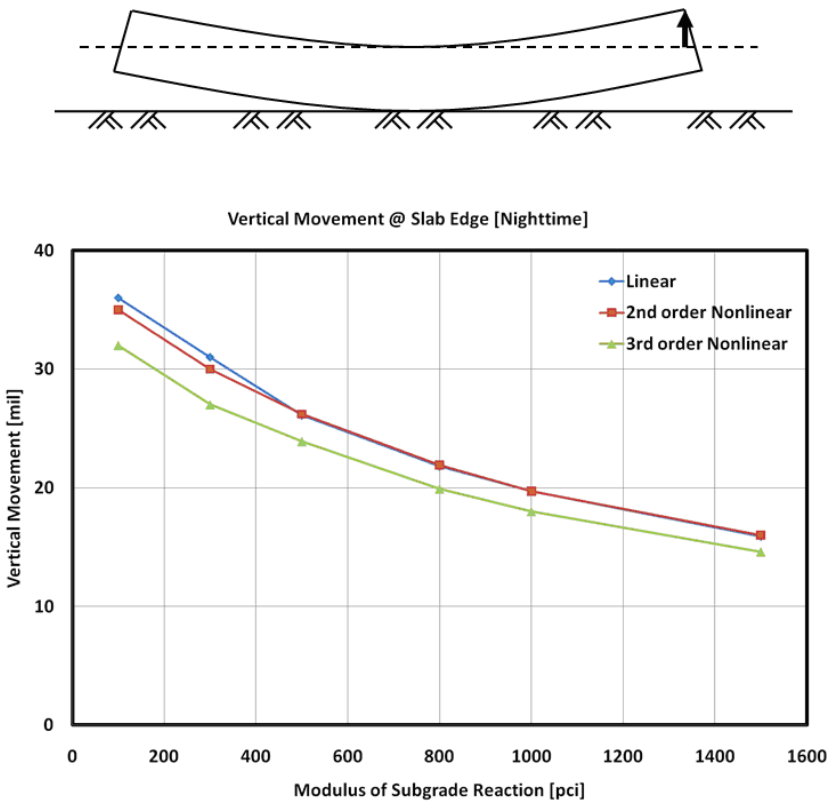

Figure 56 Nighttime Relative Vertical Movements between Slab Center and Edge.

Figure 57 presents the maximum stresses due to wheel loading. The maximum wheel load stress increases as slab thickness decreases. Also, the maximum wheel load stress tends to decrease as the subgrade modulus increases. However, the stress changes little at higher k-values, over 500 pci. For a 10 inch thickness, the maximum wheel load stresses are generally smaller than the stresses due to environmental loading.

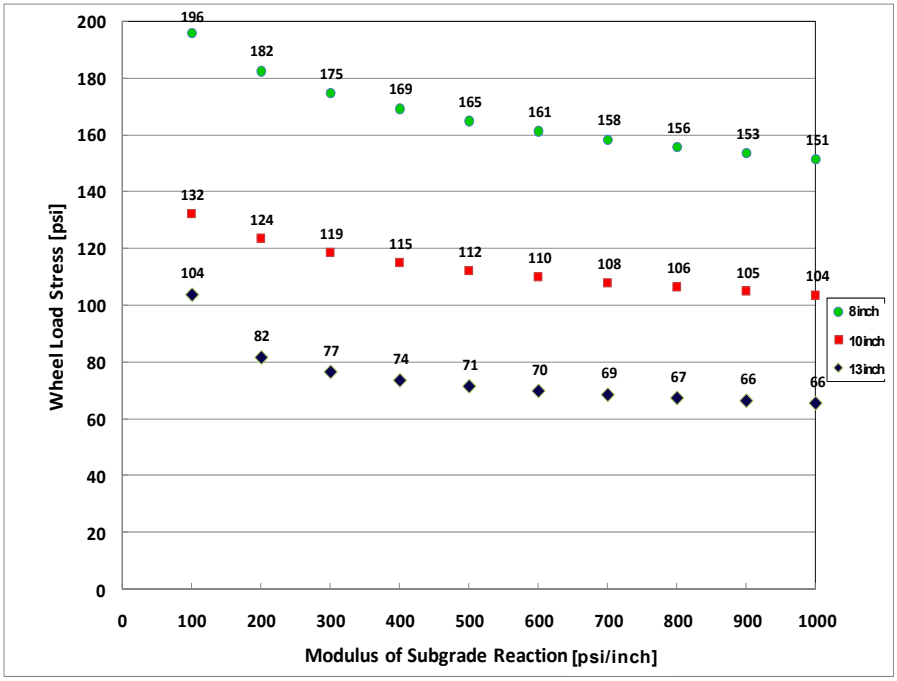

Figure 57 Stresses due to Wheel Loading.

FE ANALYSIS OF SUBBASE THICKNESS EFFECTS

Generally, supporting layers, including the subbase and subgrade, underlying a PCC slab have been simply modeled by a Winkler foundation using spring elements (*32*). In this study, however, the subbase layer was discretely modeled due to verify the responses of the subbase layer.

Modified FE Analysis

In this analysis, the subbase layer was considered as an independent layer separated from the PCC slab and subgrade. This approach was thought to be more effective in examining responses of the subbase layer. Therefore, in this study, the subbase layer was modeled as an elastic layer using two-dimensional plain strain elements shown in Figure 58. As shown in the figure, the right side is the center of the PCC slab and the left side the crack face. Also, the subbase layer is considered to be infinite in both horizontal directions. The subgrade layer under the subbase was modeled using spring elements. In this analysis, the subgrade reaction value, k-value refers to the vertical stiffness of the subgrade.

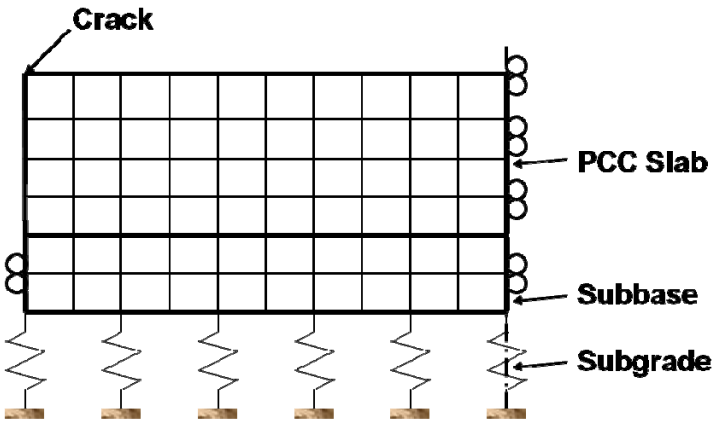

Figure 58 Modified FE Model.

Input Values and Analysis Cases

To verify the responses of the subbase, nonlinear temperature gradient conditions were employed. Figure 59 shows the temperature input conditions used. A reference temperature was selected and set at the middle of the PCC slab.

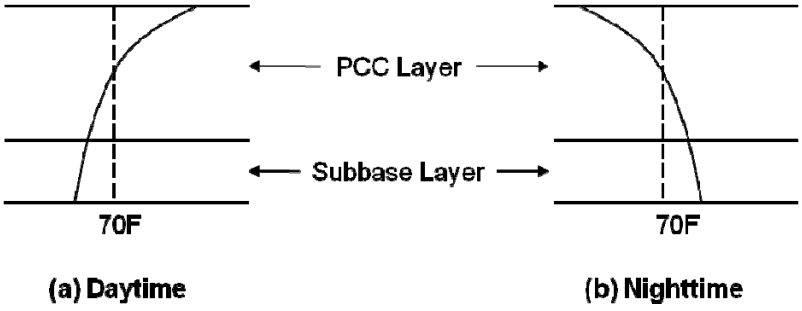

Figure 59 Temperature Gradients for Analysis Input.

Table 40 shows the geometry-related input values that were used in this analysis. An 8 ft long and 10 inch thick PCC slab was modeled. Also, the properties of subbase material were selected based on the properties of asphalt stabilized base material.

Table 40 Input Values.

Slab Thickness	10 inches
Slab Length	8 ft
Concrete Elastic Modulus	3.0×10^6 psi
Concrete Poisson's Ratio	0.15
Coefficient of Thermal Expansion of Concrete	6.0×10^{-6} /F
Concrete Unit Weight	150 pcf
Subbase Elastic Modulus	3.0×10^5 psi
Subbase Poisson's Ratio	0.35
Coefficient of Thermal Expansion of Subbases	1.2×10^{-5} /F
Unit Weight	150 pcf
Steel Size	#6

All analysis cases have been performed under daytime and nighttime temperature conditions. Also, to verify the response of the subbase layer, the longitudinal stresses at the top and bottom surfaces of the subbase were determined. Table 41 shows the input variable and values used in this FE analysis. The control values of each variable have been selected: k-value = 300 psi/inch, full bond between the slab and subbase, 150 psi/inch for the interfaced friction stiffness and 4 inch subbase thickness. The selected control values are listed in Table 41.

Table 41 Input Variables and Values.

Variables	Values
Temperature condition	3rd order daytime condition 3rd order nighttime condition
k-value (pci)	50; 100; 300; 500; 1,000; 1,500
Bonding condition	No bonding Partial bonding Perfect bonding
Friction (psi/in)	0; 50; 150; 500; 1,000; 5,000; 10,000
Subbase thickness (inch)	2, 4, 6, 8

Results

Figure 60 illustrates the modeled longitudinal stress distributions for daytime and nighttime temperature conditions. The blue color indicates compressive stress and the red color tensile stress. As shown in the figure, the longitudinal stresses have been concentrated at a spot in the subbase where the PCC slab crack is located. These stress responses might be caused by boundary condition of the subbase layer.

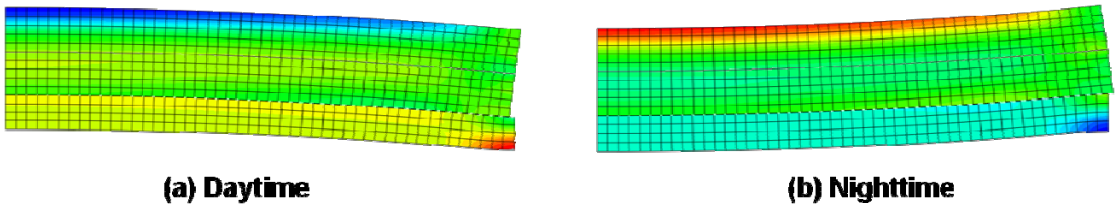

Figure 60 Stress Distributions at Daytime and Nighttime Temperature Conditions.

Effect of Subbase Thickness

To verify the effect of subbase thickness, thicknesses on performance were varied from 2 to 8 inches with 2 inch increments. Figure 61 shows the longitudinal stress distributions on the top surface and bottom surface of the subbase at daytime temperature gradient conditions. Figure 61 (a) illustrates that the maximum stress increases as the subbase thickness increases. However, in Figure 61 (b), the maximum tensile stresses corresponding to various subbase thicknesses show little difference in stress values.

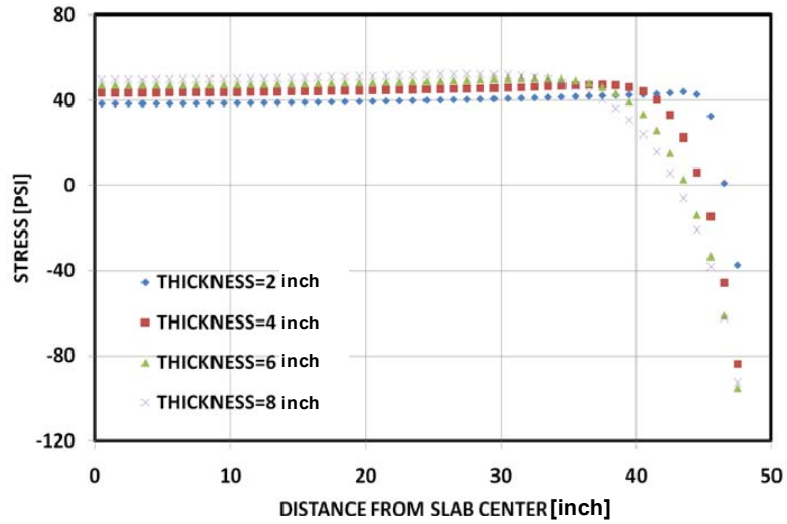

(a) Top

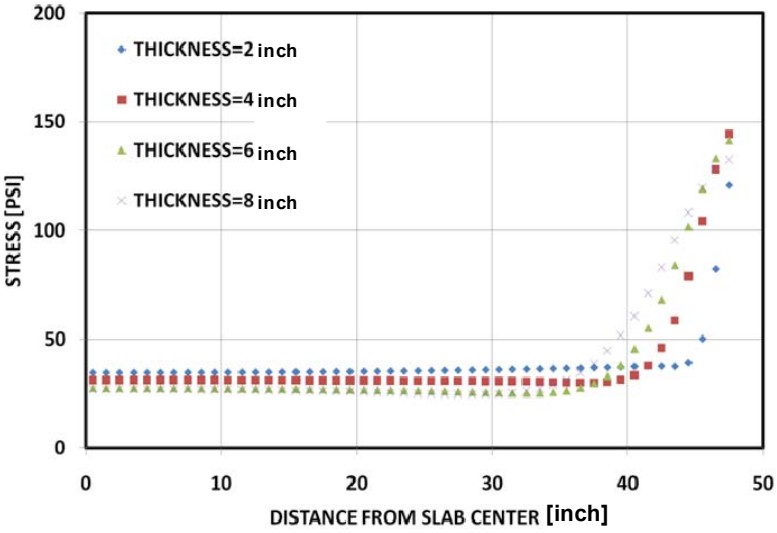

(b) Bottom

Figure 61 Effects of Subbase Thickness at Daytime.

Figure 62 presents the effects of subbase thickness at nighttime temperature conditions. The maximum tensile stress on the top of the subbase increases as the subbase thickness increases. A similar situation exists with daytime conditions; however, the amount of maximum stress change at the bottom of the subbase is smaller than the stress variation on the top of the subbase layer.

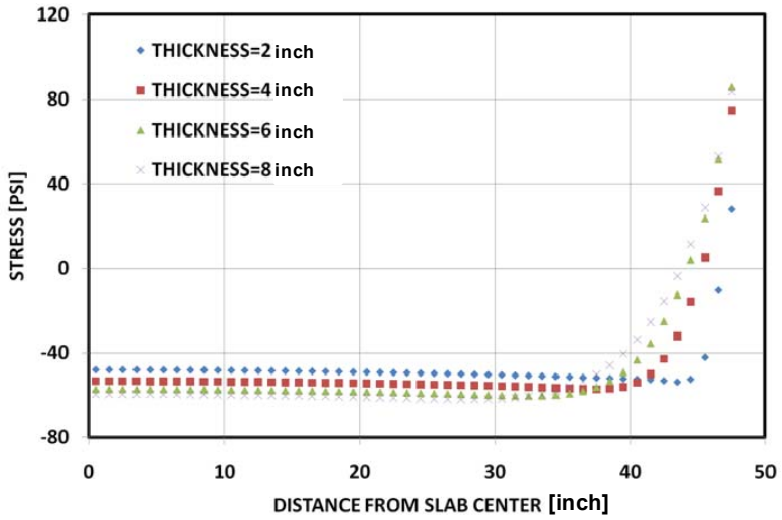

(a) Top

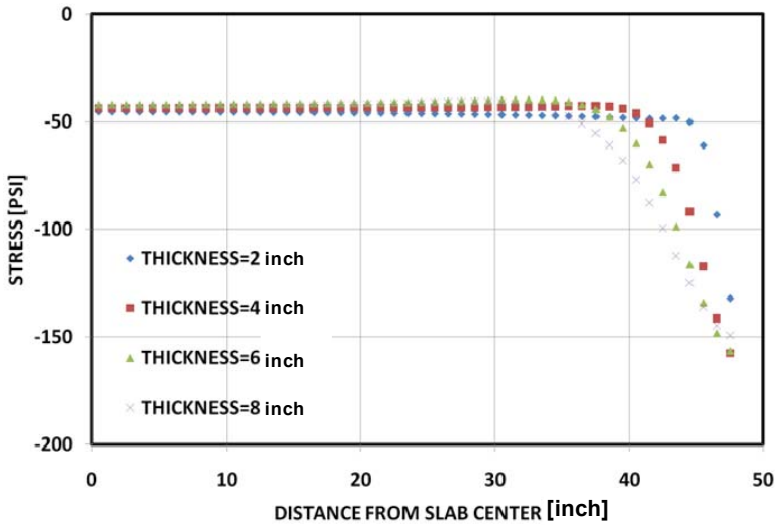

(b) Bottom

Figure 62 Effects of Subbase Thickness at Nighttime.

APPENDIX B: EROSION TEST PROCEDURE USING HAMBURG WHEEL-TRACKING DEVICE

1. **SCOPE**

1.1 Use this test method to determine the erosion susceptibility of subbase or subgrade materials due to mechanical and hydraulic shear on the layer interface generated by concrete slab movement under an applied moving wheel load. The configuration of the test device is the same as the one used for "Tex-242-F, Hamburg Wheel-Tracking Test," except for the shape of polyethylene mold. This test method measures the erosion depth versus number of passes.

1.2 The values given in parentheses (if provided) are not standard and may not be exact mathematical conversions. Use each system of units separately. Combining values from the two systems may result in nonconformance with the standard.

2. **APPARATUS**

2.1 *Wheel-Tracking Device,* an electrically powered device capable of moving a steel wheel with a diameter of 8 inches (203.6 mm) and width of 1.85 inches (47 mm) over a test specimen.

2.1.1 The load applied by the wheel is 158 ± 5 lb (705 ± 22 N).

2.1.2 The wheel must reciprocate over the test specimen, with the position varying sinusoidally over time.

2.1.3 The wheel must be capable of making 60 ± 2 passes across the test specimen per minute.

2.1.4 The maximum speed of the wheel must be approximately 1.1 ft/s (0.305 m/s) and will be reached at the midpoint of the slab.

2.2 *Temperature Control System,* a water bath capable of controlling the test temperature within ± 4°F (2°C) over a range of 77 to 158°F (25 to 70°C).

2.2.1 This water bath must have a mechanical circulating system to stabilize temperature within the specimen tank.

2.3 *Erosion Depth Measurement System,* a Linear Variable Differential Transducer (LVDT) device capable of measuring the erosion depth induced by the steel wheel within 0.0004 inches (0.01 mm), over a minimum range of 0.8 inches (20 mm).

2.3.1 The system should be mounted to measure the erosion depth at the midpoint of the wheels path on the slab.

2.3.2 Take erosion depth measurements at least every 100 passes of the wheel.

2.3.3 This system must be capable of measuring the erosion depth without stopping the wheel. Reference this measurement to the number of wheel passes.

2.3.4 Fully automated data acquisition and test control system (computer included).

2.4 *Wheel Pass Counter,* a non-contacting solenoid that counts each wheel pass over the test specimen.

2.4.1 Couple the signal from this counter to the erosion depth measurement, allowing the erosion depth to be expressed as a fraction of the wheel passes.

2.5 *Specimen Mounting System,* a stainless steel tray that can be mounted rigidly to the machine in the water bath.

2.5.1 This mounting must restrict shifting of the specimen during testing.

2.5.2 The system must suspend the specimen, allowing free circulation of the water bath on all sides.

2.5.3 The mounting system must provide a minimum of 0.79 inches (2 cm) of free circulating water on all sides of the sample.

3. MATERIALS

3.1 *Two high-density polyethylene molds,* shaped according to Figure 63, to secure circular, cylindrical test specimens.

3.2 *Two vibration absorbing neoprene pads*, 0.375 inch (9.5 mm) thick and 6 inch (152.5 mm) diameter, to simulate subgrade layers that support and prevent the compressive fracture of test specimens.

3.3 *Two jointed concrete capping blocks*, shaped according to Figure 64, to simulate the vertical movement of PCC slab under the wheel load on test specimens.

3.4 *Two rubber pads*, 0.125 inch thick (3.2 mm), 2.5 inch (63.5 mm) wide, and 6 inch (152.5 mm) length, to simulate tire contact and prevent the damage of concrete block surface by metal wheel edges during the test.

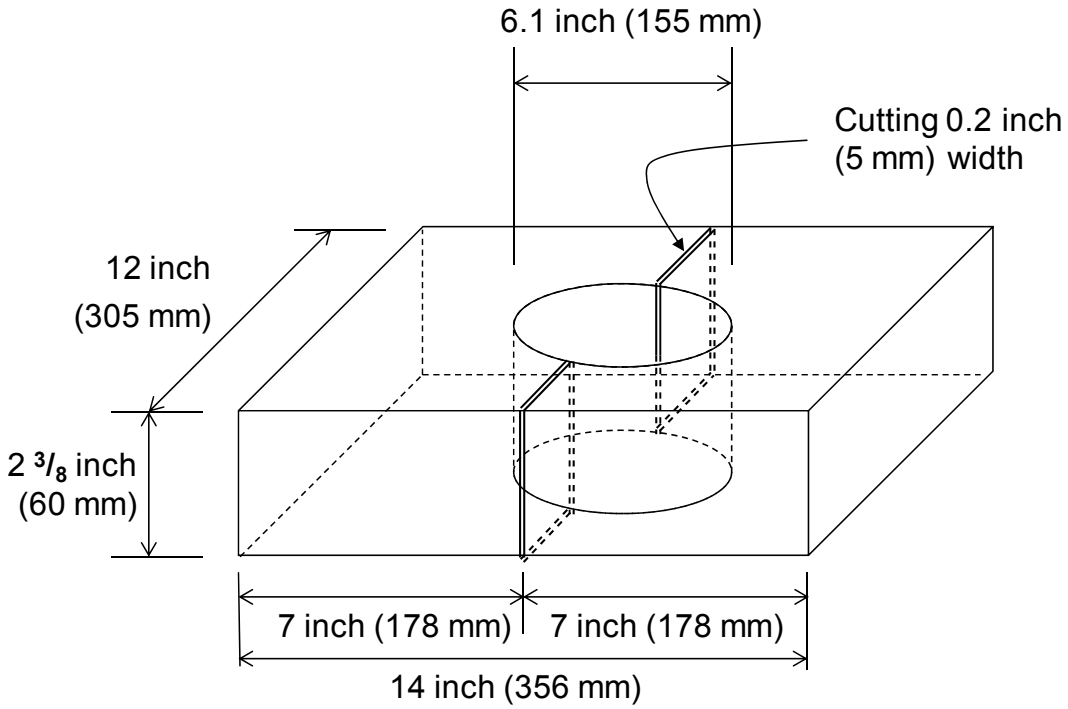

Figure 63 Configuration of High-Density Polyethylene Molds.

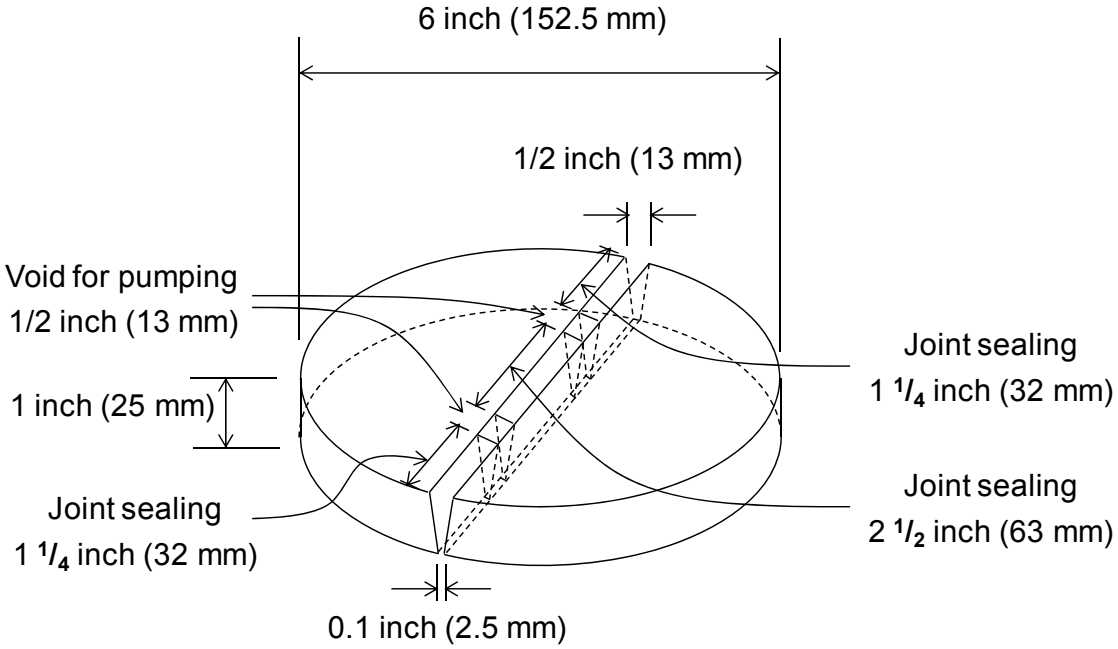

Figure 64 Configuration of Jointed Concrete Capping Blocks.

4. **SPECIMEN**

4.1 *Laboratory Molded Specimen*—Prepare specimens in accordance with Tex-101-E, Tex-110-E, Tex-113-E, and Tex-120-E. Specimen diameter must be 6 inches (152.5 mm), and specimen height must be 1 inch (25 mm).

4.1.1 Maximum aggregate size should be 0.4 inches (10 mm) and use the gradation under 0.4 inches (10 mm) to make specimens.

4.1.2 2.5 lb (1,100 g) of soil per sample is recommended and when a 6 inch (152.4 mm) height compaction mold is used, place a 5 inch (127 mm) thick disk in the mold to make a 1 inch (25.4 mm) thick sample.

4.1.3 Optimum moisture content for the compaction of specimens should be modified by the cement content rate according to Tex-120-E.

4.1.4 Specimens cured during 28 days in a moisture chamber are recommended to evaluate long-term erosion susceptibility.

Note 1 - When a test result is required in a short period, specimens cured during 7 days in a moisture chamber could be used instead of with an adjustment factor, which is defined by previous tests using the same material types.

4.1.5 Density of test specimens must be 93 ± 1%.

Note 2 - Weights for specimens prepared in the laboratory typically vary between 2 and 2.5 lb (900 and 1100 g) to achieve density due to different aggregate sources and mix types.

4.1.6 Use the bottom of the cured specimen as the top for erosion test. Seal other side (top while compacting) and side using plastic tape after surface water elimination.

4.2 *Core Specimen*—Specimen diameter must be 6 inches (150 mm) and needs to be cut with care to 1 inch (25 mm) height.

4.2.1 Use the dense and smooth cut surface of specimen as top and seal bottom and side using plastic tape after surface water elimination.

4.2.2 There is not a specific density requirement for core specimens.

5. **PROCEDURE**

5.1 Use two cylindrically molded specimens in accordance with Section 4.

5.2 Measure the sample weight.

5.3 Place a half of a high-density polyethylene mold into the mounting tray.

5.4 Place the vibration absorbing neoprene pads, specimens, jointed concrete capping blocks, and rubber pad (bond on to concrete blocks) in order into the molds.

5.5 Set the joints perpendicular to the wheel path.

5.6 Place the other half of the high-density polyethylene mold and secure into the mounting tray.

5.7 Fasten the mounting trays into the empty water bath.

5.8 Start the software, supplied with the machine, and enter the required test information into the computer (60 passes per minute and 5,000 or 10,000 load repetition).

5.9 Fill the water bath until the water temperature is at the desired test temperature (test temperature should be 77 ± 2°F (25 ± 1°C) for all specimens), and monitor the temperature of the water on the computer screen.

5.9.1 Saturate the test specimen in the water for an additional 30 minutes once reaching the desired water temperature.

5.10 Start the test after the test specimens have been in the water for 30 minutes at the desired test temperature. The testing device automatically stops the test when the device applies the number of desired passes or when reaching the maximum allowable erosion depth, 0.5 inches (13 mm).

6. REPORT

6.1 For each specimen, report the following items:

- the stabilizer content,
- the erosion depth versus number of passes at all 11 sensing locations,
- maximum erosion rate at the joint location,
- average erosion rate from the erosions of all 11 locations,
- weight of tested specimen after 24 hours oven dry, and
- gradation of tested specimen.

6.2 Erosion rate is the slope of linear regression line of test data.

APPENDIX C:
MODIFICATIONS OF SPECIFICATIONS

ITEM 247

FLEXIBLE BASE

247.1 Description. Construct a foundation course composed of flexible base.

247.2 Materials. Furnish uncontaminated materials of uniform quality that meet the requirements of the plans and specifications. Notify the Engineer of the proposed material sources and of changes to material sources. The Engineer may sample and test project materials at any time before compaction throughout the duration of the project to assure specification compliance. Use Tex-100-E material definitions.

A. Aggregate. Furnish aggregate of the type and grade shown on the plans and conforming to the requirements of Table 1. Each source must meet Table 1 requirements for liquid limit, plasticity index, and wet ball mill for the grade specified. Do not use additives such as but not limited to lime, cement, or fly ash to modify aggregates to meet the requirements of Table 1, unless shown on the plans.

Table 1 Material Requirements.

Property	Test Method	Grade 1	Grade 2	Grade 3	Grade 4
Master gradation sieve size (% retained)	Tex-110-E				As shown on the plans
2-1/2 inches		–	0	0	
1-3/4 inches		0	0–10	0–10	
7/8 inches		10–35	–	–	
3/8 inches		30–50	–	–	
No. 4		45–65	45–75	45–75	
No. 40		70–85	60–85	50–85	
Liquid limit, % max.1	Tex-104-E	35	40	40	As shown on the plans
Plasticity index, max.1	Tex-106-E	10	12	12	As shown on the plans
Plasticity index, min.1		As shown on the plans			
Wet ball mill, % max.2	Tex-116-E	40	45	–	As shown on the plans
Wet ball mill, % max. increase passing the No. 40 sieve		20	20	–	
Classification 3	Tex-117-E	1.0	1.1–2.3	–	As shown on the plans
Min. compressive strength 3, psi					As shown on the plans
lateral pressure 0 psi		45	35	–	
lateral pressure 15 psi		175	175	–	

1. Determine plastic index in accordance with Tex-107-E (linear shrinkage) when liquid limit is unattainable as defined in Tex-104-E.

2. When a soundness value is required by the plans, test material in accordance with Tex-411-A.

3. Meet both the classification and the minimum compressive strength, unless otherwise shown on the plans.

1. **Material Tolerances.** The Engineer may accept material if no more than 1 of the 5 most recent gradation tests has an individual sieve outside the specified limits of the gradation.

   When target grading is required by the plans, no single failing test may exceed the master grading by more than 5 percentage points on sieves No. 4 and larger or 3 percentage points on sieves smaller than No. 4.

   The Engineer may accept material if no more than 1 of the 5 most recent plasticity index tests is outside the specified limit. No single failing test may exceed the allowable limit by more than 2 points.

2. **Material Types.** Do not use fillers or binders unless approved. Furnish the type specified on the plans in accordance with the following.

   a. **Type A.** Crushed stone produced and graded from oversize quarried aggregate that originates from a single, naturally occurring source. Do not use gravel or multiple sources.

   b. **Type B.** Crushed or uncrushed gravel. Blending of 2 or more sources is allowed.

   c. **Type C.** Crushed gravel with a minimum of 60 percent of the particles retained on a No. 4 sieve with 2 or more crushed faces as determined by Tex-460-A, Part I. Blending of 2 or more sources is allowed.

   d. **Type D.** Type A material or crushed concrete. Crushed concrete containing gravel will be considered Type D material. Crushed concrete must meet the requirements in Section 247.2.A.3.b, "Recycled Material (Including Crushed Concrete) Requirements," and be managed in a way to provide for uniform quality. The Engineer may require separate dedicated stockpiles in order to verify compliance.

   e. **Type E.** As shown on the plans.

3. **Recycled Material.** Recycled asphalt pavement (RAP) and other recycled materials may be used when shown on the plans. Request approval to blend 2 or more sources of recycled materials.

   a. **Limits on Percentage.** When RAP is allowed, do not exceed 20 percent RAP by weight unless otherwise shown on the plans. The percentage limitations for other recycled materials will be as shown on the plans. When RAP and other recycled materials are applied as the aggregates for Item 276 "Cement Treatment," more than 20 percent RAP by weight and other percentage limitations are allowed only if the strength and erosion requirements in Item 276 "Cement Treatment" are satisfied.

   b. **Recycled Material (Including Crushed Concrete) Requirements.**

      (1) **Contractor Furnished Recycled Materials.** When the Contractor furnishes the recycled materials, including crushed concrete, the final product will be subject to the requirements of Table 1 for the grade specified. Certify compliance with DMS-11000, "Evaluating and Using Nonhazardous Recyclable Materials Guidelines," for Contractor furnished recycled materials. In addition, recycled materials must be free from reinforcing steel and other objectionable material and have at most 1.5 percent deleterious material when

tested in accordance with Tex-413-A. For RAP, do not exceed a maximum percent loss from decantation of 5.0 percent when tested in accordance with Tex-406-A. Test RAP without removing the asphalt.

(2) Department Furnished Required Recycled Materials. When the Department furnishes and requires the use of recycled materials, unless otherwise shown on the plans:

- Department required recycled material will not be subject to the requirements in Table 1;
- Contractor furnished materials are subject to the requirements in Table 1 and this Item;
- final product, blended, will be subject to the requirements in Table 1; and
- final product, unblended (100 percent Department furnished required recycled material), the liquid limit, plasticity index, wet ball mill, classification, and compressive strength is waived.

Crush Department-furnished RAP so that 100 percent passes the 2 inch sieve. The Contractor is responsible for uniformly blending to meet the percentage required.

(3) Department Furnished and Allowed Recycled Materials. When the Department furnishes and allows the use of recycled materials or allows the Contractor to furnish recycled materials, the final blended product is subject to the requirements of Table 1 and the plans.

c. Recycled Material Sources. Department-owned recycled material is available to the Contractor only when shown on the plans. Return unused Department-owned recycled materials to the Department stockpile location designated by the Engineer unless otherwise shown on the plans.

The use of Contractor-owned recycled materials is allowed when shown on the plans. Contractor-owned surplus recycled materials remain the property of the Contractor. Remove Contractor-owned recycled materials from the project and dispose of them in accordance with federal, state, and local regulations before project acceptance. Do not intermingle Contractor-owned recycled material with Department-owned recycled material unless approved by the Engineer.

B. Water. Furnish water free of industrial wastes and other objectionable matter.

C. Material Sources. When non-commercial sources are used, expose the vertical faces of all strata of material proposed for use. Secure and process the material by successive vertical cuts extending through all exposed strata, when directed.

247.3 Equipment. Provide machinery, tools, and equipment necessary for proper execution of the work. Provide rollers in accordance with Item 210, "Rolling." Provide proof rollers in accordance with Item 216, "Proof Rolling," when required.

247.4 Construction. Construct each layer uniformly, free of loose or segregated areas, and with the required density and moisture content. Provide a smooth surface that conforms to the typical sections, lines, and grades shown on the plans or as directed.

Stockpile base material temporarily at an approved location before delivery to the roadway. Build stockpiles in layers no greater than 2 ft thick. Stockpiles must have a total height between 10 and 16 ft unless otherwise shown on the plans. After construction and acceptance of the stockpile, loading from the stockpile for delivery is allowed. Load by making successive vertical cuts through the entire depth of the stockpile.

Do not add or remove material from temporary stockpiles that require sampling and testing before delivery unless otherwise approved. Charges for additional sampling and testing required as a result of adding or removing material will be deducted from the Contractor's estimates.

Haul approved flexible base in clean trucks. Deliver the required quantity to each 100 ft station or designated stockpile site as shown on the plans. Prepare stockpile sites as directed. When delivery is to the 100 ft station, manipulate in accordance with the applicable Items.

A. Preparation of Subgrade or Existing Base. Remove or scarify existing asphalt concrete pavement in accordance with Item 105, "Removing Stabilized Base and Asphalt Pavement," when shown on the plans or as directed. Shape the subgrade or existing base to conform to the typical sections shown on the plans or as directed.

When new base is required to be mixed with existing base, deliver, place, and spread the new flexible base in the required amount per station. Manipulate and thoroughly mix the new base with existing material to provide a uniform mixture to the specified depth before shaping.

When shown on the plans or directed, proof roll the roadbed in accordance with Item 216, "Proof Rolling," before pulverizing or scarifying. Correct soft spots as directed.

B. Placing. Spread and shape flexible base into a uniform layer with an approved spreader the same day as delivered unless otherwise approved. Construct layers to the thickness shown on the plans. Maintain the shape of the course. Control dust by sprinkling, as directed. Correct or replace segregated areas as directed, at no additional expense to the Department.

Place successive base courses and finish courses using the same construction methods required for the first course.

C. Compaction. Compact using density control unless otherwise shown on the plans. Multiple lifts are permitted when shown on the plans or approved. Bring each layer to the moisture content directed. When necessary, sprinkle the material in accordance with Item 204, "Sprinkling."

Begin rolling longitudinally at the sides and proceed toward the center, overlapping on successive trips by at least 1/2 the width of the roller unit. On superelevated curves, begin rolling at the low side and progress toward the high side. Offset alternate trips of the roller. Operate rollers at a speed between 2 and 6 mph as directed.

Rework, recompact, and refinish material that fails to meet or that loses required moisture, density, stability, or finish before the next course is placed or the project is accepted. Continue work until specification requirements are met. Perform the work at no additional expense to the Department.

1. **Ordinary Compaction.** Roll with approved compaction equipment as directed. Correct irregularities, depressions, and weak spots immediately by scarifying the areas affected, adding or removing approved material as required, reshaping, and recompacting.

2. **Density Control.** Compact to at least 100 percent of the maximum density determined by Tex-113-E unless otherwise shown on the plans. Determine the moisture content of the material at the beginning and during compaction in accordance with Tex-103-E.

   The Engineer will determine roadway density of completed sections in accordance with Tex-115-E. The Engineer may accept the section if no more than 1 of the 5 most recent density tests is below the specified density and the failing test is no more than 3 pcf below the specified density.

D. Finishing. After completing compaction, clip, skin, or tight-blade the surface with a maintainer or subgrade trimmer to a depth of approximately 1/4 inches, remove loosened material and dispose of it at an approved location. Seal the clipped surface immediately by rolling with a pneumatic tire roller until a smooth surface is attained. Add small increments of water as needed during rolling. Shape and maintain the course and surface in conformity with the typical sections, lines, and grades as shown on the plans or as directed.

In areas where surfacing is to be placed, correct grade deviations greater than 1/4 inches in 16 ft measured longitudinally or greater than 1/4 inches over the entire width of the cross-section. Correct by loosening, adding, or removing material. Reshape and recompact in accordance with Section 247.4.C, "Compaction."

E. Curing. Cure the finished section until the moisture content is at least 2 percentage points below optimum or as directed before applying the next successive course or prime coat.

247.5. Measurement. Flexible base will be measured as follows:

- **Flexible Base (Complete In Place).** The ton, square yard, or any cubic yard method.
- **Flexible Base (Roadway Delivery).** The ton or cubic yard in vehicle.
- **Flexible Base (Stockpile Delivery).** The ton, cubic yard in vehicle, or cubic yard in stockpile.

Measurement by the cubic yard in final position and square yard is a plans quantity measurement. The quantity to be paid for is the quantity shown in the proposal unless modified by Article 9.2, "Plans Quantity Measurement." Additional measurements or calculations will be made if adjustments of quantities are required.

Measurement is further defined for payment as follows.

A. Cubic Yard in Vehicle. By the cubic yard in vehicles of uniform capacity at the point of delivery.

B. Cubic Yard in Stockpile. By the cubic yard in the final stockpile position by the method of average end areas.

C. Cubic Yard in Final Position. By the cubic yard in the completed and accepted final position. The volume of base course is computed in place by the method of average end areas between the original subgrade or existing base surfaces and the lines, grades, and slopes of the accepted base course as shown on the plans.

D. Square Yard. By the square yard of surface area in the completed and accepted final position. The surface area of the base course is based on the width of flexible base as shown on the plans.

E. Ton. By the ton of dry weight in vehicles as delivered. The dry weight is determined by deducting the weight of the moisture in the material at the time of weighing from the gross weight of the material. The Engineer will determine the moisture content in the material in accordance with Tex-103-E from samples taken at the time of weighing.

When material is measured in trucks, the weight of the material will be determined on certified scales, or the Contractor must provide a set of standard platform truck scales at a location approved by the Engineer. Scales must conform to the requirements of Item 520, "Weighing and Measuring Equipment."

247.6. Payment. The work performed and materials furnished in accordance with this Item and measured as provided under "Measurement" will be paid for at the unit price bid for the types of work shown below. No additional payment will be made for thickness or width exceeding that shown on the typical section or provided on the plans for cubic yard in the final position or square yard measurement.

Sprinkling and rolling, except proof rolling, will not be paid for directly but will be subsidiary to this Item unless otherwise shown on the plans. When proof rolling is shown on the plans or directed, it will be paid for in accordance with Item 216, "Proof Rolling."

Where subgrade is constructed under this Contract, correction of soft spots in the subgrade will be at the Contractor's expense. Where subgrade is not constructed under this project, correction of soft spots in the subgrade will be paid in accordance with pertinent Items or Article 4.2, "Changes in the Work."

A. Flexible Base (Complete In Place). Payment will be made for the type and grade specified. For cubic yard measurement, "In Vehicle," "In Stockpile," or "In Final Position" will be specified. For square yard measurement, a depth will be specified. This price is full compensation for furnishing materials, temporary stockpiling, assistance provided in stockpile sampling and operations to level stockpiles for measurement, loading, hauling, delivery of materials, spreading, blading, mixing, shaping, placing, compacting, reworking, finishing, correcting locations where thickness is deficient, curing, furnishing scales and labor for weighing and measuring, and equipment, labor, tools, and incidentals.

B. Flexible Base (Roadway Delivery). Payment will be made for the type and grade specified. For cubic yard measurement, "In Vehicle" will be specified. The unit price bid will not include processing at the roadway. This price is full compensation for furnishing materials, temporary stockpiling, assistance provided in stockpile sampling and operations to level stockpiles for measurement, loading, hauling, delivery of materials, furnishing scales and labor for weighing and measuring, and equipment, labor, tools, and incidentals.

C. Flexible Base (Stockpile Delivery). Payment will be made for the type and grade specified. For cubic yard measurement, "In Vehicle" or "In Stockpile" will be specified. The unit price bid will not include processing at the roadway. This price is full compensation for furnishing and disposing of materials, preparing the stockpile area, temporary or permanent stockpiling, assistance provided in stockpile sampling and operations to level stockpiles for measurement, loading, hauling, delivery of materials to the stockpile, furnishing scales and labor for weighing and measuring, and equipment, labor, tools, and incidentals.

ITEM 276

CEMENT TREATMENT (PLANT-MIXED)

276.1. Description. Construct a base course composed of flexible base, hydraulic cement, and water, mixed in an approved plant.

276.2. Materials. Furnish uncontaminated materials of uniform quality that meet the requirements of the plans and specifications. Notify the Engineer of proposed sources of materials and of changes in material sources. The Engineer will verify that the specification requirements are met before the sources can be used. The Engineer may sample and test project materials at any time before compaction. Use Tex-100-E for material definitions.

A. Cement. Furnish hydraulic cement that meets the requirements of DMS-4600, "Hydraulic Cement," and the Department's Hydraulic Cement Quality Monitoring Program (HCQMP). Sources not on the HCQMP will require testing and approval before use.

B. Flexible Base. Furnish base material that meets the requirements of Item 247, "Flexible Base," for the type and grade shown on the plans, before the addition of cement.

C. Water. Furnish water that is free of industrial waste and other objectionable material.

D. Asphalt. When permitted for curing purposes, furnish asphalt or emulsion that meets the requirements of Item 300, "Asphalts, Oils, and Emulsions," as shown on the plans or as directed.

E. Mix Design. Using the materials proposed for the project, the Engineer will determine the target cement content and optimum moisture content necessary to produce a stabilized mixture meeting the strength and erosion requirements shown in Tables 1 and 2 for the class specified on the plans. The mix will be designed in accordance with Tex-120-E. The Contractor may propose a mix design developed in accordance with Tex-120-E. The Engineer will use Tex-120-E to verify the Contractor's proposed mix design before acceptance. The Engineer may use project materials sampled from the plant or the quarry, and sampled by the Engineer or the Contractor, as determined by the Engineer. Limit the amount of asphalt concrete pavement to no more than 50 percent of the mix unless otherwise shown on the plans or directed.

Table 1 Strength Requirements.

Class	7-Day Unconfined Compressive Strength, Min. psi
K	500
L	300
M	175
N	As shown on the plans

Table 2 Erosion Requirements.

Environment and Drainage	28-Day Erodibility Using Hamburg Wheel-Tracking Device Test, Max. mm/10,000 load repetitions	
	With Subsurface Drainage	Without Subsurface Drainage
Rainfall less than or equal 10 inch/yr	0.75	0.25
Rainfall greater than 10 inch/yr	0.5	0.13

276.3. Equipment. Provide machinery, tools, and equipment necessary for proper execution of the work. Provide rollers in accordance with Item 210, "Rolling." Provide proof rollers in accordance with Item 216, "Proof Rolling," when required.

A. Cement Storage Facility. Store cement in closed, weatherproof containers.

B. Mixing Plant. Provide a stationary pugmill, weigh-batch, or continuous mixing plant as approved. Equip plants with automatic proportioning and metering devices that produce a uniform mixture of base material, cement, and water in the specified proportions.

C. Spreader Equipment. When shown on the plans, provide equipment that will spread the cement-treated mixture in a uniform layer in 1 pass. When shown on the plans, equip spreaders with electronic grade controls.

276.4. Construction. Construct each layer uniformly, free of loose or segregated areas and with the required density and moisture content. Provide a smooth surface that conforms to the typical sections, lines, and grades shown on the plans or established by the Engineer. Start placement operations only when the air temperature is at least 35°F and rising or is at least 40°F. The temperature will be taken in the shade and away from artificial heat. Suspend operations when the Engineer determines that weather conditions are unsuitable.

A. Mixing. Thoroughly mix materials in the proportions designated on the mix design, in a mixing plant that meets the requirements of Section 276.3.B, "Mixing Plant." Mix at optimum moisture content, unless otherwise directed, until a homogeneous mixture is obtained. Do not add water to the mixture after mixing is completed unless directed.

B. Placing. Place the cement-treated base on a subgrade or base prepared in accordance with details shown on the plans. Bring the prepared roadway to the moisture content directed. Haul cement-treated base to the roadway in clean trucks and begin placement immediately. Place cement-treated base only on an area where compacting and finishing can be completed during the same working day. Spread and shape in a uniform layer with an approved spreader. Construct individual layers to the thickness shown on the plans. Maintain the shape of the course by blading. Correct or replace segregated areas as directed, at no additional expense to the Department.

Construct vertical joints between new cement-treated base and cement-treated base that has been in place 4 hours or longer. The vertical face may be created by using a header or by cutting back the face to approximately vertical. Place successive base courses using the same methods as the first course. Offset construction joints by at least 6 inches.

C. Compaction. Compact each layer immediately after placing. Complete compaction within 2 hours after plant-mixing water with dry material. When multiple lifts are permitted, complete compaction of the final lift within 5 hours after adding water to the treated base used in the first lift.

Moisture content in the mixture at the plant may be adjusted so that during compaction it is within 2.0 percentage points of optimum as determined by Tex-120-E. Determine the moisture content in the mixture at the beginning of and during compaction in accordance with Tex-103-E. Maintain uniform moisture content by sprinkling the treated material in accordance with Item 204, "Sprinkling."

Begin rolling longitudinally at the sides and proceed toward the center, overlapping on successive trips by at least 0.5 the width of the roller unit. On superelevated curves, begin rolling at the low side and progress toward the high side. Offset alternate trips of the roller. Operate rollers at a speed between 2 and 6 mph, as directed.

Compact to at least 95 percent of maximum density as determined in accordance with Tex-120-E. The Engineer will determine roadway density in accordance with Tex-115-E and will verify strength in accordance with Tex-120-E. Remove material that does not meet density requirements. Remove areas that lose required stability, compaction, or finish. Replace with cement-treated mixture and compact and test in accordance with density control methods.

The Engineer may accept the section if no more than 1 of the 5 most recent density tests is below the specified density and the failing test is no more than 3 pcf below the specified density.

D. Finishing. Immediately after completing compaction, clip, skin, or tight blade the surface of the cement-treated material with a maintainer or subgrade trimmer to a depth of approximately 1/4 inches. Remove loosened material and dispose of at an approved location. Roll the clipped surface immediately with a pneumatic tire roller until a smooth surface is attained. Add small increments of water as needed during rolling. Shape and maintain the course and surface in conformity with the typical sections, lines, and grades shown on the plans or as directed.

In areas where surfacing is to be placed, trim grade deviations greater than 1/4 inches in 16 ft measured longitudinally or greater than 0.25 inches over the entire width of the cross-section. Remove excess material, reshape, and then roll with a pneumatic tire roller. If material is more than 0.25 inches low, correct as directed. Do not surface patch.

E. Curing. Cure for at least 3 days by sprinkling in accordance with Item 204, "Sprinkling," or by applying an asphalt material at the rate of 0.05 to 0.20 gallons per square yard, as shown on the plans or as directed. Maintain the moisture content during curing at no lower than 2 percentage points below optimum. Do not allow equipment on the finished course during curing except as required for sprinkling, unless otherwise approved. Continue curing until placing another course or opening the finished section to traffic.

276.5. Measurement. Cement-treated base will be measured by the ton, cubic yard, or square yard as a composite mixture of cement, flexible base, and recycled materials.

Measurement by the cubic yard in final position and square yard is a plans quantity measurement. The quantity to be paid for is the quantity shown in the proposal unless modified by Article 9.2, "Plans Quantity Measurement." Additional measurements or calculations will be made if adjustments of quantities are required.

Measurement is further defined for payment as follows:

A. Cubic Yard in Vehicles. Cement-treated base will be measured by the cubic yard in vehicles as delivered on the road.

B. Cubic Yard in Final Position. Cement-treated base will be measured by the cubic yard in its completed and accepted final position. The volume of each course will be computed in-place between the original subgrade surfaces and the lines, grades, and slopes of the accepted base course as shown on the plans, and calculated by the method of average end areas.

C. Square Yard. Cement-treated base will be measured by the square yard of surface area. The dimensions for determining the surface area are established by the dimensions shown on the plans.

D. Ton. Cement-treated base will be measured by the ton (dry weight) in vehicles as delivered on the road. The dry weight is determined by deducting the weight of the moisture in the material at the time of weighing from the gross weight of the material. The Engineer will determine the moisture content in the material in accordance with Tex-103-E from samples taken at the time of weighing.

When material is measured in trucks, the weight of the material will be determined on certified scales, or the Contractor must provide a set of standard platform truck scales at a location approved by the Engineer. Scales must conform to the requirements of Item 520, "Weighing and Measuring Equipment."

276.6. Payment. The work performed and materials furnished in accordance with this Item and measured as provided under "Measurement" will be paid for at the unit price bid for "Cement Treatment (Plant Mix)" of the class (strength), flexible base type, grade, and thickness (for square yard measurement) specified. For cubic yard measurement, "In Vehicle" or "In Final Position" will be specified. This price is full compensation for furnishing and disposing of materials (including cement and base); storing, mixing, hauling, placing, sprinkling, compacting, finishing, curing, and maintaining and reworking treated base; and equipment, labor, tools, and incidentals.

Sprinkling and rolling, except proof rolling, will not be paid for directly but will be subsidiary to this Item, unless otherwise shown on the plans. When proof rolling is shown on the plans or directed by the Engineer, it will be paid for in accordance with Item 216, "Proof Rolling."

Where subgrade or base courses are constructed under this Contract, correction of soft spots will be at the Contractor's expense. Where subgrade or base is not constructed under this Contract, correction of soft spots will be paid for in accordance with pertinent Items and Article 4.2, "Changes in the Work."

Asphalt used solely for curing will not be paid for directly but will be subsidiary to this Item. Asphalt placed for curing and priming will be paid for under Item 310, "Prime Coat."

Removal and disposal of existing asphalt concrete pavement will be paid for in accordance with pertinent Items or Article 4.2, "Changes in the Work."

A. Thickness Measurement for Cubic Yard in Final Position and Square Yard Payment Adjustment. Before final acceptance, the Engineer will select the locations of tests within each unit and measure the treated base depths in accordance with Tex-140-E.

1. Units for Payment Adjustment.

a. Roadways and Shoulders. Units for applying a payment adjustment for thickness to roadways and shoulders are defined as 1,000 linear ft of treated base in each placement width. The last unit in each placement width will be 1,000 ft plus the fractional part of 1,000 ft remaining. Placement width is the width between longitudinal construction joints. For widening, the placement width is the average width placed of the widened section that is deficient in thickness.

b. Ramps and Other Areas. Units are defined as 2,000 sq. yd. or fraction thereof for establishing an adjusted unit price for ramps, intersections, irregular sections, crossovers, entrances, partially completed units, transitions to ramps, and other areas designated by the Engineer.

2. Price Adjustments of Deficient Areas.

a. Thickness Deficiency ≤ 1.0 inch. Table 3 will govern the price adjustment for each unit with deficient areas ≤ 1.0 inch.

Table 3 Measurements and Price Adjustment for Each Unit.

Thickness Deficiency	Additional Measurements	Average Thickness Deficiency of 3 Measurements		Price Adjustment
≤ 0.5 inches	None	N/A		Full Payment
> 0.5 inches	2	≤ 0.5 inches		Full Payment
		> 0.5 inches	≤ 0.8 inches	75% Payment
		> 0.8 inches	≤ 1.0 inches	50% Payment
		> 1.0 inch		In accordance with Section 276.6.A.2.b.

b. Thickness Deficiency ≥ 1.0 inch. Remove and replace areas of treated base found deficient in thickness by more than 1.0 inch, unless otherwise approved. Take exploratory measurements at 50 ft intervals parallel to the centerline in each direction from the deficient measurement until a measurement is not deficient by more than 1.0 inch. The minimum limit of non-pay will be 100 ft.

B. Excess Thickness and Width. For cubic yard in final position and square yard measurement, no additional payment will be made for thickness or width exceeding that shown on the plans.